How Blocking Lipopolysaccharide Synthesis and Transport Affects Cell Survival

How blocking lipopolysaccharide synthesis and transport affects cell survival

A dissertation presented

by

Emily Nagy

to

The Department of Molecular and Cellular Biology

In partial fulfillment of the requirements

for the degree of

Doctor of Philosophy

In the subject of

Biochemistry

Harvard University

Cambridge, Massachusetts

April 2019

Dissertation Advisors: Professors Daniel Kahne and Richard Losick Emily Nagy

How blocking lipopolysaccharide synthesis and transport affects cell survival

Abstract

Gram-negative bacteria are defined by their asymmetric second membrane. The outer leaflet, exposed to the cell surface, is composed of lipopolysaccharide (LPS), a large glycolipid. Conserved structural features of this molecule allow it to create a strong permeability barrier that blocks entry to many compounds, including antibiotics, making Gram-negative infections particularly difficult to treat in the clinic. LPS synthesis and transport to the cell surface is essential in most Gram-negative species, making it an attractive target for antimicrobial development, though no known clinically used antibiotics currently target either of these pathways. There are currently a small number of Gram-negative species, such as *Acinetobacter baumannii*, that can survive in the absence of LPS; however, what allows them, and not others, to do so is not well understood.

This work establishes that polymyxin B (PMB), a critical antibiotic of last resort, targets LPS transport to the cell surface as its mechanism of killing. PMB is known to bind LPS at the cell surface, which permeablizes the cell, but the understanding of its mechanism of action has been vague and nonspecific. Through a biochemical reconstitution of LPS transport, *in vivo* crosslinking experiments, and imaging studies, we provide evidence that PMB binds LPS at the inner membrane and prevents entry into LptFG, which are components of the Lpt machine that extract LPS from the inner membrane and transport and insert it into the outer membrane. This causes

a specific build-up of LPS in the inner membrane which leads to cell death. This dissertation also characterizes the phenotypes associated with LPS loss in *A. baumannii* and defines conditions in which growth and morphological defects are minimal. Using detailed growth analysis in a variety of conditions we develop a hypothesis about why LPS loss is tolerated in *A. baumannii*, but not other species such as *Escherichia coli*. We propose a model for how an outer membrane must be built without LPS and explain why we believe this to be rate limiting for growth. If our hypothesis is correct, we believe we can find conditions that will enable us to engineer an *E. coli* strain that can survive without LPS.

Table of Contents

List of Figures

Acknowledgements

Graduate school has been a journey filled with numerous ups and downs and I wouldn't be in this position today without the support and encouragement of many different people. I would like to express my appreciation to both of my advisors, Dan Kahne and Rich Losick, for all of their support and assistance over the past six years. They have given me space to explore and discover what interests me and to develop my projects without the fear of failure. While I have had great freedom to direct my projects, there have always been encouraging conversations waiting at just the right moment. They have also enabled me to pursue my other passion, teaching, and I cannot overstate how much I appreciate the support.

I have been fortunate to have had an extremely supportive committee over the course of this project. Andrew Murray, Vlad Denic, Karine Gibbs and, more recently, Cassandra Extavour have all provided valuable advice at my yearly meetings and I appreciate that they took the time to read my reports and think about my projects. I am particularly indebted to Andrew and Cassandra who have both taken time out of their busy schedules to listen and help with some complicated situations during my time here.

I also would like to acknowledge Natacha Ruiz and her student Blake Bertani. They involved me in an interesting project and I greatly enjoyed working with them. Both have answered numerous questions I've had about bacterial genetics and have helped me troubleshoot problems long distance which I know is never easy.

While being a joint student sometimes presents challenges, I have the benefit of two wonderful lab communities. I've been fortunate to work with many amazing people in both the

Losick and Kahne labs. In particular, I would like to thank Eileen Moison from the Kahne lab for her unwavering support over the years. She patiently helped me integrate into the lab and generously let me pick up a project that she had initiated. She was always willing to talk through results and brainstorm ideas and her friendship and encouragement kept me sane. Katie Schaefer in the Kahne lab also spent many hours listening to me vent and helping me troubleshoot experiments for which I'm eternally grateful.

I also must mention the LS50 community. What started out simply as a class and teaching experience has quickly become a family. I've learned so much about teaching and myself from the faculty, other teaching fellows and especially the students. The six weeks I spent with the course every year were all-encompassing, but they reenergized me to tackle my lab work with renewed enthusiasm. Andrew Murray has presented me with many opportunities through teaching and I am forever indebted to him for that. Also, the last few years would not have been nearly as fun without Mariela Petkova, my teaching partner. We started out as a completely green set of teaching fellows and have developed into a dynamic team over the past four years. She's always been incredibly supportive, and I've learned so much both about science and life in general from her.

I want to finish by acknowledging my wonderful family. My parents especially have been extremely supportive and always let me pursue my dreams and interests. From a very early age they instilled in me a love of learning and a curiosity about the world that I believe has led me to where I am today. I would like to finish by thanking an unconventional friend, my dog Nali. When I got him as a puppy three years ago there were many people telling me they didn't think it was a great idea, that he would take up too much time. Well I can say with absolute

confidence that the last few years would not have been nearly as fulfilling or fun without him. He always makes me smile after a bad day and forces me to get out and enjoy life which in turn makes me a better scientist.

Chapter 1

The Role of the Outer Membrane and Lipopolysaccharide, Its Most Abundant Component

1.1 Abstract

The outer membrane is the defining feature of Gram-negative bacteria, and the Kahne lab has spent much of the past two decades investigating the assembly and function of this second membrane. This membrane, unlike the cytoplasmic membrane, is asymmetric with an outer leaflet filled with lipopolysaccharide (LPS) instead of phospholipids. In this work, we have attempted to untangle what aspects of LPS synthesis and assembly in the outer membrane make it essential in so many species. We have also sought to understand the role of LPS as it relates to the antimicrobial activity of polymyxin B, a clinically important antibiotic. This chapter outlines the biosynthesis of LPS and its subsequent transport to the cell surface. It also describes what is known about the regulation of LPS biosynthesis in *E. coli* and species in which it is not essential. Finally, it will discuss recent efforts to target LPS biosynthesis and transport for antibiotic development and how that might relate to the polymyxins.

1.2 Gram-negative bacteria outer membrane structure and function

Bacteria are broadly divided into two classes, Gram-positive and Gram-negative, based on the cell's ability to retain crystal violet stain. All bacterial cells have a cytoplasmic membrane composed of phospholipids encased by a cell wall consisting of rigid crosslinked peptidoglycan.[1] The thickness of the cell wall, however, varies significantly between Gram-positive and Gram-negative species. Gram-positive bacteria have a thick cell wall whereas Gram-negative bacteria have only a thin layer of peptidoglycan surrounded by a second membrane, which compensates for the reduced cell wall.[1] This outer membrane is the defining feature of Gram negative bacteria (Figure 1.1).

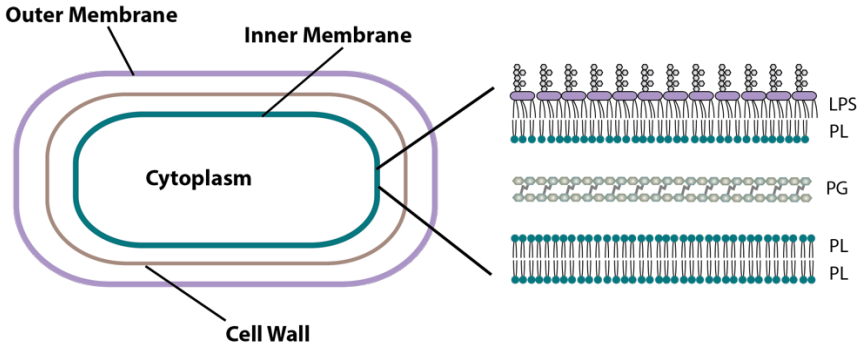

Figure 1.1. Gram-negative cellular structure. Gram negative bacteria consist of two compartments bounded by lipid bilayers. The cytoplasm is surrounded by the inner membrane which is composed entirely of phospholipids. Between the inner membrane and the second asymmetric outer membrane is the periplasm.

Unlike the inner membrane, which is composed entirely of phospholipids, the outer membrane is an asymmetric bilayer consisting of phospholipids on the inner leaflet and lipopolysaccharide (LPS) on the outer leaflet.[1,2] LPS is a large, complex molecule that has structural variation across species.[3-5] The lipid A core of the molecule, however, has several conserved features. It is composed of a glucosamine disaccharide bisphosphate to which

multiple acyl chains are attached. In addition to lipid A, LPS always has a core oligosaccharide, though the exact sugar composition can vary widely.[3,5] Many species also attach up to hundreds of additional sugars, called the O-antigen (Figure 1.2).

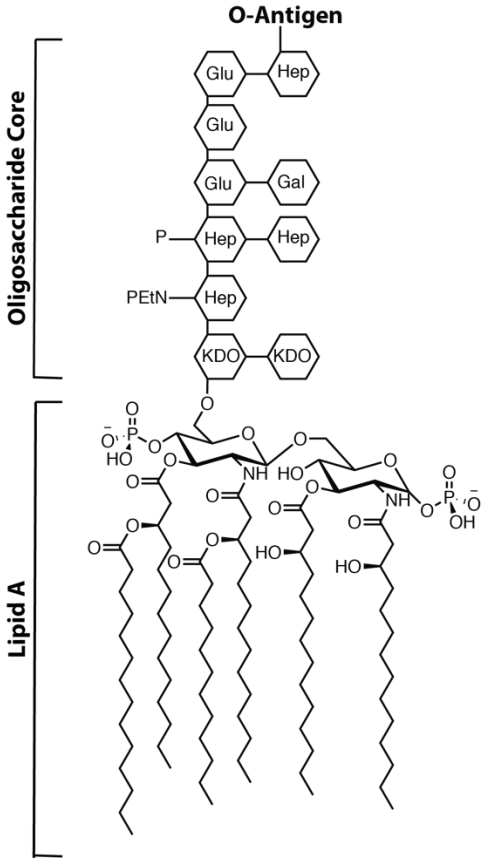

Figure 1.2 Structure of LPS. The structure of a typical *E. coli* molecule of LPS contains three primary components identified in bold. The lipid A core has six acyl chains attached to a disaccharide bisphosphate. The oligosaccharide core contains a variety of different sugar moieties and the O-antigen, if present, consists of up to hundreds of additional sugars. KDO = 3-deoxy-D-manno-octo-2-ulosonic acid, Hep = L-glycero-D-manno-heptose, Glu = D-glucose, Gal = D-galactose, PEtN = phosphoethanolamine, P = phosphate.

Because of the LPS component, the outer membrane serves as a protective barrier for the cell, preventing entry to most small molecules and hydrophobic compounds.[6,7] The core oligosaccharide and O-antigen, consisting of hydrophilic sugars, effectively blocks hydrophobic

compounds that might normally be able to cross a membrane. At the cell surface, the negatively charged phosphates of the lipid A core interact with divalent metal cations, forming an organized structure that can block most small molecules from diffusing across the membrane.[8] The combination of these structural features makes LPS an essential part of the protective aspect of this extra membrane.

Since the outer membrane is such an effective barrier, most of the molecules that enter the cell must be specifically imported through β-barrel porins, which provides the cell with the ability to control and regulate what molecules can enter.[7] As a result, Gram-negative bacteria are resistant to many different classes of antibiotics simply because these antibiotics cannot access the cytoplasm and thus their target. Multi-drug resistant strains are a significant problem in clinical settings, and four of the six ESKAPE pathogens, *Klebsiella pneumonia, Acinetobacter baumannii, Pseudomonas aeruginosa* and *Enterobacter*, are Gram-negative. These six pathogens are classified as highly resistant to most commonly used antibiotics, and finding new ways to treat these infections is of critical importance. Among the antibiotics classified as drugs of last resort for treatment of these infections is colistin, a small peptide that specifically binds LPS, allowing it to bypass the barrier.[9,10]

Because of the protective features, maintaining the integrity of the outer membrane, specifically the asymmetry, is important for a cell's survival. Since the inner leaflet of the membrane is composed of phospholipids, those phospholipids can flip spontaneously into the outer leaflet. The presence of phospholipids in this leaflet disrupts the electrostatic packing and makes the membrane leaky. Cells with high levels of phospholipids in the outer leaflet are more susceptible to antibiotics and other nonspecific toxins such as bile salts and detergents.[11] As a

result, there are dedicated systems for maintaining the asymmetry of the outer membrane. The *mla* pathway is composed of six proteins and spans from the inner to outer membrane (Figure 1.3).[11] There is a lipoprotein, MlaA, anchored in the outer membrane that extracts, through an unknown mechanism, phospholipids that are in the outer leaflet and passes them off to a soluble cytoplasmic protein, MlaC.[11] This shuttle protein transports the phospholipids back to the inner membrane where the other four proteins in the pathway are located. Although some believe the pathway can transport phospholipids bidirectionally and mechanistic details are still being elucidated, the pathway serves to ensure that phospholipids in the outer leaflet are recycled back to the inner membrane.[12-17] PldA is a β-barrel phospholipase in the outer membrane that degrades phospholipids in the outer leaflet, releasing fatty acids (Figure 1.3).[11,18,19] In addition to physically removing the phospholipids, recent evidence suggests that PldA, through the released fatty acids, signals to the cell that there is membrane stress.[14] In conjunction, these two pathways ensure that the proper barrier function of the outer membrane is maintained.[11,17,20,21]

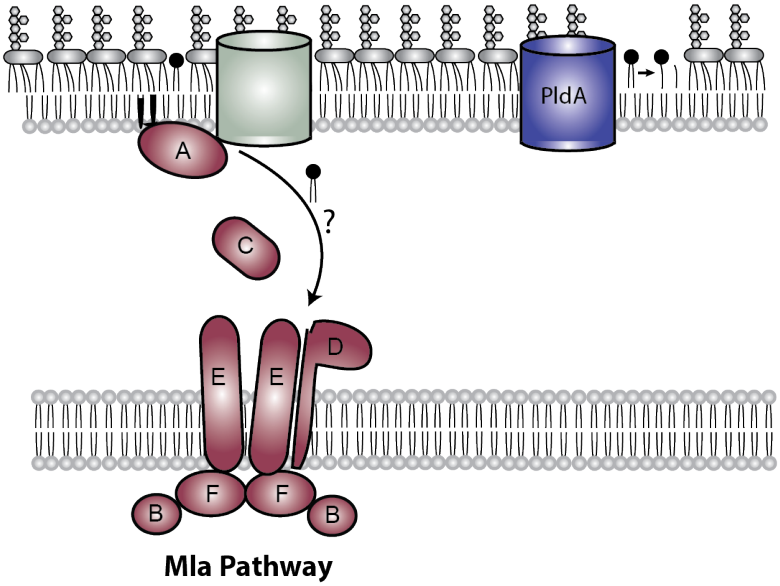

Figure 1.3. Lipid recycling pathways in *E. coli*. When phospholipids flip into the outer leaflet of the outer membrane, permeability increases. Cells have two primary systems in place to detect these phospholipids and remove them to maintain membrane asymmetry. The Mla pathway consists of six proteins and functions by removing the phospholipids and shuttling them back to the inner membrane. It is likely there are outer membrane proteins outside of Mla that assist with phospholipid removal from the membrane. PldA is a phospholipase embedded in the outer membrane. It destroys the phospholipids by cleaving off the fatty acids and serves as a sensor of LPS levels at the cell surface.

1.3 LPS biosynthesis and transport

LPS biogenesis is a complicated pathway that has been extensively studied over the past several decades. Synthesis begins in the cytoplasm via the Raetz pathway, which builds the lipid A molecule through a series of catalyzed steps (Figure 1.4 A).[3,22] After lipid A is inserted into the inner leaflet of the inner membrane, it is flipped across the membrane by MsbA.[23] At this stage, additional modifications such as attachment of the O-antigen or phosphate modifications are added, after which the molecule is ready for transport to the outer membrane.[24]

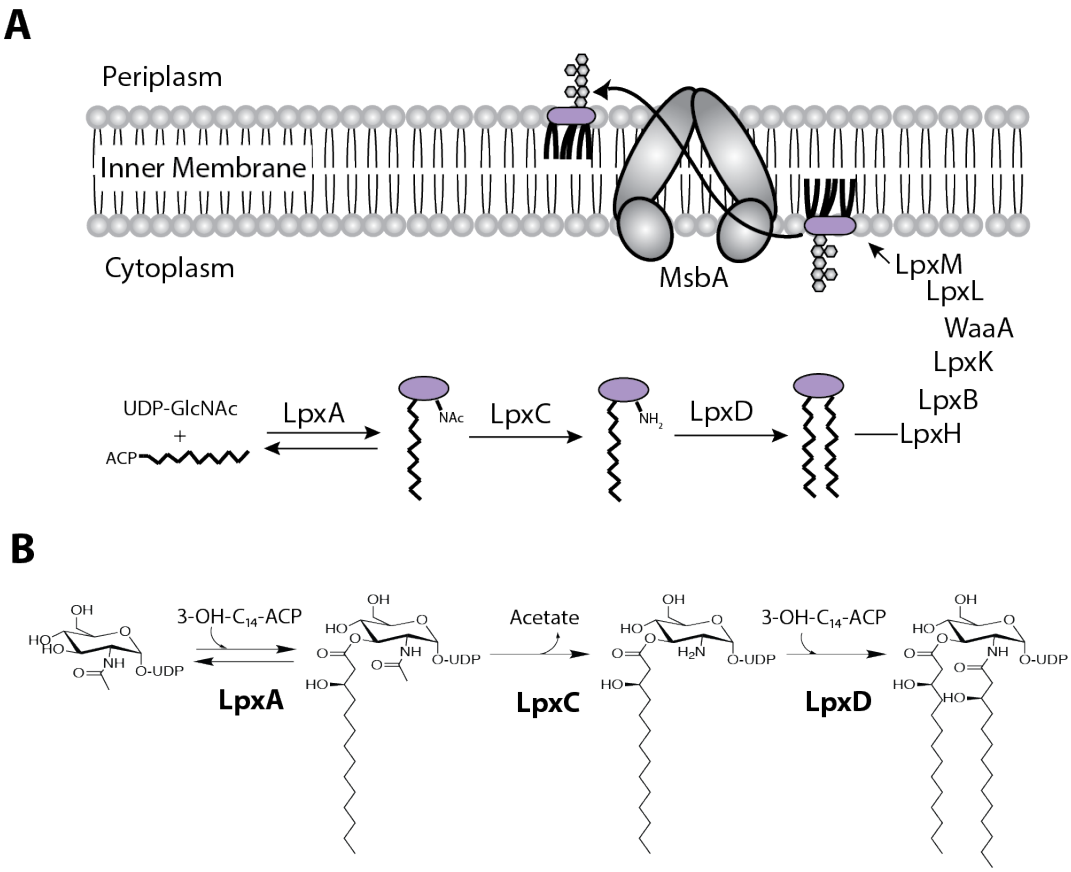

Figure 1.4 LPS biosynthesis pathway. (A) Cartoon representation of the biosynthetic pathway of LPS from acyl-ACP and UDP-GlcNAc precursors to insertion into the inner membrane. Synthesis and attachment of the O-antigen polymer and other phosphate modifications occur on the outer leaflet of the inner membrane. For the purposes of simplicity, none of the steps of this process are specifically depicted. (B) Chemical structures of intermediates for the first three steps in the pathway. ACP = acyl carrier protein

The first three steps in the biosynthetic pathway are catalyzed by the soluble cytoplasmic enzymes: LpxA, LpxC and LpxD. The first step, catalyzed by LpxA, attaches the acyl chain from (R)-3-hydroxymyristoyl-ACP to UDP-GlcNAc.[25] This reaction is reversible, so the first committed step in the pathway is the second, catalyzed by LpxC. LpxC deacetylates UDP-GlcNAc, which generates a free amine.[26-28] This step directly controls the levels of LPS synthesized since it is the first irreversible step and regulation occurs through proteolysis of LpxC as will be discussed further in a later section. LpxD then attaches a second acyl chain from another molecule of (R)-

3-hydroxymyristoyl-ACP.[29] Subsequent enzymes in the pathway are integral membrane proteins located on the inner leaflet of the inner membrane. These early steps are outlined in detail in Figure 1.4 B.

To make it to the outer membrane, the lipid A core and its hundreds of attached sugars must traverse two cellular compartments while passing through a rigid cell wall before being properly inserted into the outer membrane such that the asymmetry is maintained. This is an enormously complex process made even more complicated by the fact that there is no ATP in the periplasm, meaning the only energy source exists in the cytoplasm, two membranes and one compartment away from the final destination. To accomplish this process, the cell has a dedicated seven-protein machine (lipopolysaccharide transport pathway – Lpt) that creates a bridge spanning the periplasm, which has been extensively studied over the past decade[30-37] (Figure 1.5). At the inner membrane, $LptB_2FG$ comprise an ABC transporter that provides the energy for the entire transport process through ATP hydrolysis.[33,36] LptC is also an inner membrane protein, that in complex with $LptB_2FG$, selectively extracts LPS from the inner membrane and begins the transport process. LptC transfers LPS into LptA, a soluble periplasmic protein that can polymerize to form a bridge across the space.[37] At the outer membrane, LPS travels from LptA to LptDE, the outer membrane translocon.[31,32,38,39] The mechanism for insertion into the outer membrane is not fully understood. LptC, LptA, and the periplasmic part of LptD share a β-jellyroll structure that allows LPS to travel along the interior of these proteins.

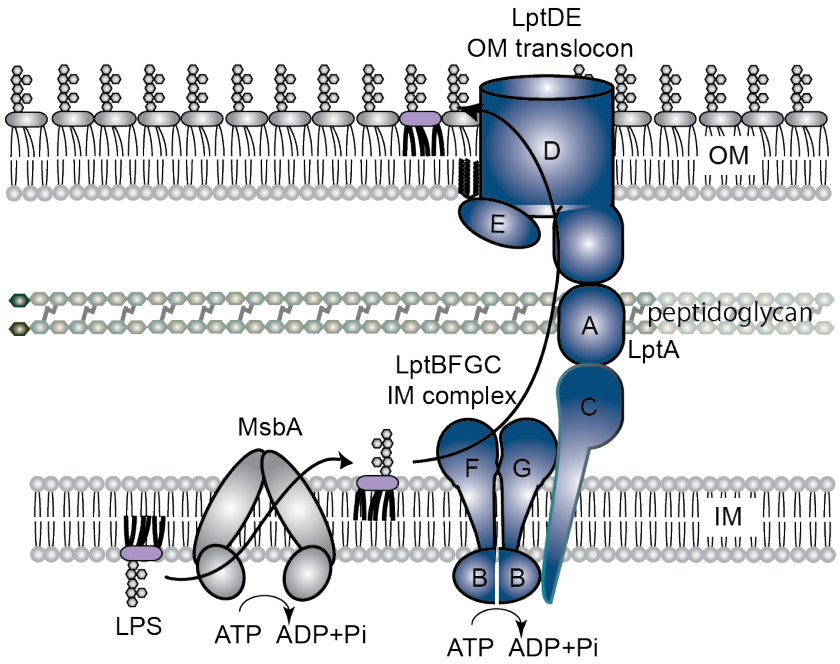

Figure 1.5 LPS transport pathway. LPS is flipped from the inner to the outer leaflet of the inner membrane by MsbA. It is then extracted from the membrane by $LptB_2FGC$ and transported across the periplasm by an LptA bridge. LptDE inserts LPS into the outer leaflet of the outer membrane.

1.4 LPS regulation

Cells need to maintain the asymmetry of the outer membrane for survival. To do this, cells must continuously ensure that there is a proper balance of phospholipid and LPS levels which requires a sensor as well as tight regulation of both biosynthetic pathways. The regulation of LPS synthesis is complex and only partially understood in *E. coli*, while even less is known for other Gram-negative organisms.[40] In *E. coli*, LPS levels in the membrane are controlled through post-translational regulation of LpxC levels.[41,42] Since this is the first committed step in the biosynthetic pathway, control at this step results in no build-up of lipid A intermediates. LpxC contains a C-terminal tag targeting it for proteolysis by FtsH, an integral membrane protease.[40,43] When cells are growing quickly, LpxC is highly stable and large amounts of LPS are synthesized; however, when growth slows and demand for LPS stalls, LpxC is quickly degraded by FtsH. The

exact mechanism of this change in stability is unknown, but it appears to be connected to ppGpp levels.[44]

Aside from needing to modulate LPS levels during growth, cells must also be able to respond to changes in LPS precursor levels, specifically fatty acid levels. Fatty acids are an important feedstock for LPS as six acyl chains must be added to each synthesized molecule, but they are also a critical resource for phospholipid synthesis. Cells have mechanisms to ensure that they maintain a proper balance between phospholipid and LPS synthesis. FabZ, an enzyme in the fatty acid biosynthesis pathway that directs fatty acids towards phospholipid synthesis, competes with LpxA for the (R)-3-hydroxymyristoyl-ACP substrate.[41,45] If FabZ is mutated in a way that increases its activity, LpxC is more stable, thus ensuring that LPS synthesis is also increased to balance phospholipid synthesis.[41] While the crosstalk between these two pathways is not well understood, it is important for cell survival.[46]

Recently it has been shown that cells can also respond to conditions of membrane stress by modulating LPS synthesis.[13] As was mentioned before, phospholipids in the outer leaflet of the membrane disrupt the LPS packing and increase permeability of the cell. In response, PldA activity increases resulting in degradation of phospholipids and release of fatty acids. These fatty acids are actively taken up by the cell and converted to acyl-CoA by FadD. This process results in a stabilization of LpxC and increased LPS synthesis. PldA appears to be acting as a sensor, relaying information about the outer membrane composition directly to LpxC.[14]

1.5 Essentiality of LPS

For decades, LPS was believed to be an essential component of the outer membrane. About twenty years ago, however, a strain of *Neisseria meningitidis* lacking *lpxA* was constructed in the

laboratory, showing that it was possible for cells to build a functional outer membrane composed solely of phospholipids.[47-49] More recently, strains of *Acinetobacter baumannii* lacking LPS, as a form of antibiotic resistance, have been isolated from patients treated with colistin.[50] These strains have loss of function mutations in either *lpxA* or *lpxC*, yet they are able to survive. The discovery of these strains has raised significant questions about why this conserved molecule, which defines Gram-negative bacteria, is essential in some species, such as *E. coli,* while being dispensable in others.

Even though *A. baumannii* can survive without LPS, the stage at which synthesis is blocked matters greatly. The three earliest steps in the pathway, *lpxA, lpxC* and *lpxD* are dispensable; however, removal of later steps is lethal.[51,52] This lethality is believed to be caused by toxicity of the synthetic intermediates that build up, though whether that is due to direct toxicity of the intermediate molecule or an overall drain on fatty acid resources, is unclear. Many of these later steps are only conditionally essential. If they are removed in conjunction with *lpxC*, they are no longer lethal, presumably because the cell is no longer making any intermediates.

Losing LPS does not come without a cost as *A. baumannii* cells lacking LPS exhibit a characteristic set of phenotypes. They grow more slowly than wild type cells in rich medium and have heterogeneous morphology.[53-56] Also, the outer membrane composed entirely of phospholipids does not provide the normal barrier function, so the cells are quite leaky.[57] As a result, they are significantly more susceptible to a wide variety of antibiotics.[50]

1.6 LPS synthesis and transport as a drug target

Since LPS is essential in all but a few instances, much work has been done to develop inhibitors of the biosynthesis, and more recently the transport, pathway. Several different groups have

created potent inhibitors of LpxC.[58-63] While there are many potential targets in LPS biosynthesis, LpxC is particularly appealing since it is the first committed step as well as the point of regulation for the entire pathway. Resistance to these inhibitors rarely occurs in *lpxC* itself, but rather in *fabZ*.[58,59,64] Mutations in *fabZ* downregulate its activity thus bringing phospholipid synthesis back into balance with the reduced LPS synthesis. While none of these inhibitors has made it to the clinic, they are a useful tool for studying the biosynthesis and transport of LPS.

While much of the focus has been on finding inhibitors of LpxC, blocking the pathway at later points may also prove effective. Our lab has worked to develop screens specifically for molecules that block later stages of synthesis and transport. Recently inhibitors of MsbA, the flippase that moves LPS from the inner to outer leaflet of the inner membrane, have been discovered.[65,66] These compounds are lethal to *A. baumannii* as well, presumably because of a build-up lipid A at the inner membrane. One could envision inhibitors of the Lpt transport pathway could also have the same effect and efforts are underway to find such compounds.

1.7 Polymyxin antibiotics

The polymyxins are a class of antibiotics first isolated in 1947.[67] They are cationic cyclic peptides naturally produced by a variety of *Bacillus* species with potent activity against Gram-negative bacteria.[68,69] Their clinical use was suspended in the early 1960s due to irreversible nephrotoxicity; however, with the rise of multi-drug resistant infections, they have become a drug of last resort for treatment of Gram-negative infections[9,10,70,71]. Both polymyxin B (PMB) and polymyxin E (colistin) are currently listed as critically important antibiotics.

PMB is a nonribosomally synthesized cyclic peptide composed of a heptapeptide macrocycle with a tripeptide chain and a fatty acid (Figure 1.6). There has been extensive investigation into

the structure-activity relationship (SAR) of PMB in an attempt to reduce the associated nephrotoxicity.[72,73] While the efforts have not yielded a less toxic compound of equal potency, much has been learned about the moieties important for activity. The five positively charged 2,4-diaminobutyric acid (Dab) residues are believed to be the source of the nephrotoxicity as they promote uptake by renal cells.[74] Removing more than one Dab residue, however, has serious effects on the activity.[75,76] It has also been shown that the fatty acyl tail is critical for activity.[72] Polyxyin B nonapeptide (PMBN), PMB with only a dipeptide chain and no fatty acid, is not antimicrobial[75-79]. The significance of these structural features becomes clearer when one looks at the mechanism of action.

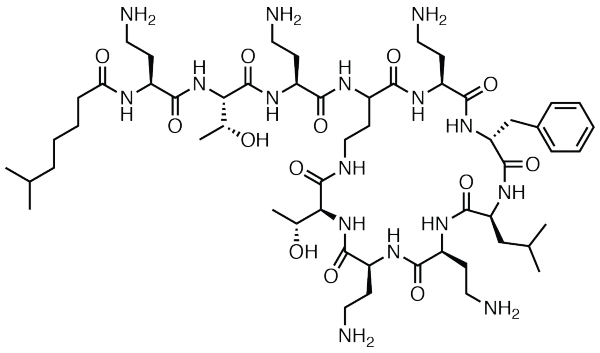

Figure 1.6 Structure of polymyxin B (PMB).

The reason PMB specifically targets Gram-negative bacteria is that it targets LPS. It is able to bind LPS in the outer membrane, disrupting the packing, which then promotes its own uptake across the membrane.[80-82] Many of the important structural features outlined above are important for LPS binding.[73] The positively charged Dab residues can interact with the negatively charged phosphates of lipid A, replacing the cations and disrupting the electrostatic interactions

that pack the molecules together. It is believed that the fatty acid tail can also intercalate with the acyl chains of LPS. In combination, these interactions allow PMB to cross the membrane and gain access to the periplasm. Details concerning the mechanism of killing beyond this point are vague.[81,83] Many believe PMB acts as a nonspecific detergent, permeabilizing the inner membrane to kill the cell.[84,85] However, experiments showing release of cytoplasmic contents do not necessarily correlate with the timeframe of killing.[82,86-88] Others have proposed cellular targets, but they present no *in* vivo evidence for a specific interaction. At the moment, there is very little direct evidence to support any of these as the sole mechanism of killing.

Resistance mechanisms to PMB killing primarily involve altering the structure of LPS to reduce PMB binding.[89-92] Most commonly, cells add phosphoethanolamine (PEtN) or aminoarabinose (L-Ara4N) to the phosphates of LPS, eliminating the charge.[24,93-95] This significantly reduces the binding affinity of PMB for LPS. While it is assumed this serves to reduce the amount of PMB entering the cell, this has not been specifically shown to be the mechanism of this resistance. In addition to modifications, organisms such as *A. baumannii* can remove LPS altogether as a form of resistance.[50,96] The literature suggests this is effective because there is no LPS on the surface to promote PMB's uptake. However, it is known that these cells are permeable to a wide variety of compounds, so it does not appear that this suggestion is true.[97] The fact that PMB cannot kill cells that lack LPS suggests that killing is not simply a matter of gaining entry to the cell via LPS in the outer membrane and then killing by a nonspecific target. If this were the case, cells lacking LPS should still be easily killed by this nonspecific mechanism. Beyond uptake, much of PMB's proposed mechanism of action is speculative with little direct evidence to support it.

1.8 Elucidating the mechanism of action for PMB and understanding the essentiality of LPS

The work in this dissertation has sought to better understand the roles of LPS, both as an essential aspect of cellular survival and as a component of PMB-mediated killing. By clarifying the mechanism of PMB, I believe we can enable more directed development of less toxic analogues for clinical use. In Chapter 2, we propose a hypothesis that PMB killing involves the blocking of LPS transport to the cell surface, creating a toxic build-up of LPS at the inner membrane. We use various biochemical tools developed by the lab to show that, both *in vitro* and *in vivo*, PMB treatment blocks LPS access to specific sites along the transport pathway. We have also developed a PMB probe with crosslinking abilities that could be used for future investigations into specific interactions between PMB and Lpt components. While studying PMB and its effects on LPS, we questioned why some species can survive without LPS while most others cannot. We wondered whether we could leverage *A. baumannii*'s survival to learn more about which pathways might be involved. In Chapter 3, we show that phenotypes of LPS deficiency are dependent on the rate at which cells are growing. We propose a model where outer membrane synthesis, and specifically phospholipid flipping, is rate limiting in these cells. We also attempt to elucidate why blocking synthesis at later steps, such as *lpxD*, is more toxic to the cell. Our investigation implies that slow growth, to enable proper membrane formation and prevent stress responses, might be the key to survival in the absence of LPS.

1.9 References

1 Silhavy, T. J., Kahne, D. & Walker, S. The bacterial cell envelope. *Cold Spring Harb Perspect Biol* **2**, a000414, doi:10.1101/cshperspect.a000414 (2010).

2 Funahara, Y. & Nikaido, H. Asymmetric localization of lipopolysaccharides on the outer membrane of Salmonella typhimurium. *J Bacteriol* **141**, 1463-1465 (1980).

3 Raetz, C. R. & Whitfield, C. Lipopolysaccharide endotoxins. *Annu Rev Biochem* **71**, 635-700, doi:10.1146/annurev.biochem.71.110601.135414 (2002).

4 Raetz, C. R. Biochemistry of endotoxins. *Annu Rev Biochem* **59**, 129-170, doi:10.1146/annurev.bi.59.070190.001021 (1990).

5 Caroff, M. & Karibian, D. Structure of bacterial lipopolysaccharides. *Carbohydr Res* **338**, 2431-2447 (2003).

6 Nikaido, H. Molecular basis of bacterial outer membrane permeability revisited. *Microbiol Mol Biol Rev* **67**, 593-656 (2003).

7 Delcour, A. H. Outer membrane permeability and antibiotic resistance. *Biochim Biophys Acta* **1794**, 808-816, doi:10.1016/j.bbapap.2008.11.005 (2009).

8 Nikaido, H. & Vaara, M. Molecular basis of bacterial outer membrane permeability. *Microbiol Rev* **49**, 1-32 (1985).

9 Falagas, M. E. & Kasiakou, S. K. Colistin: the revival of polymyxins for the management of multidrug-resistant gram-negative bacterial infections. *Clin Infect Dis* **40**, 1333-1341, doi:10.1086/429323 (2005).

10 Li, J. *et al.* Colistin: the re-emerging antibiotic for multidrug-resistant Gram-negative bacterial infections. *Lancet Infect Dis* **6**, 589-601, doi:10.1016/S1473-3099(06)70580-1 (2006).

11 Malinverni, J. C. & Silhavy, T. J. An ABC transport system that maintains lipid asymmetry in the gram-negative outer membrane. *Proc Natl Acad Sci U S A* **106**, 8009-8014, doi:10.1073/pnas.0903229106 (2009).

12 Thong, S. *et al.* Defining key roles for auxiliary proteins in an ABC transporter that maintains bacterial outer membrane lipid asymmetry. *Elife* **5**, doi:10.7554/eLife.19042 (2016).

13 Sutterlin, H. A. *et al.* Disruption of lipid homeostasis in the Gram-negative cell envelope activates a novel cell death pathway. *Proc Natl Acad Sci U S A* **113**, E1565-1574, doi:10.1073/pnas.1601375113 (2016).

14 May, K. L. & Silhavy, T. J. The Escherichia coli Phospholipase PldA Regulates Outer Membrane Homeostasis via Lipid Signaling. *MBio* **9**, doi:10.1128/mBio.00379-18 (2018).

15 Abellon-Ruiz, J. *et al.* Structural basis for maintenance of bacterial outer membrane lipid asymmetry. *Nat Microbiol* **2**, 1616-1623, doi:10.1038/s41564-017-0046-x (2017).

16 Ekiert, D. C. *et al.* Architectures of Lipid Transport Systems for the Bacterial Outer Membrane. *Cell* **169**, 273-285 e217, doi:10.1016/j.cell.2017.03.019 (2017).

17 Kamischke, C. *et al.* The Acinetobacter baumannii Mla system and glycerophospholipid transport to the outer membrane. *Elife* **8**, doi:10.7554/eLife.40171 (2019).

18 Istivan, T. S. & Coloe, P. J. Phospholipase A in Gram-negative bacteria and its role in pathogenesis. *Microbiology* **152**, 1263-1274, doi:10.1099/mic.0.28609-0 (2006).

19 Dekker, N. Outer-membrane phospholipase A: known structure, unknown biological function. *Mol Microbiol* **35**, 711-717 (2000).

20 Munguia, J. *et al.* The Mla pathway is critical for Pseudomonas aeruginosa resistance to outer membrane permeabilization and host innate immune clearance. *J Mol Med (Berl)* **95**, 1127-1136, doi:10.1007/s00109-017-1579-4 (2017).

21 Kerrinnes, T. *et al.* Phospholipase A1 modulates the cell envelope phospholipid content of Brucella melitensis, contributing to polymyxin resistance and pathogenicity. *Antimicrob Agents Chemother* **59**, 6717-6724, doi:10.1128/AAC.00792-15 (2015).

22 Whitfield, C. & Trent, M. S. Biosynthesis and export of bacterial lipopolysaccharides. *Annu Rev Biochem* **83**, 99-128, doi:10.1146/annurev-biochem-060713-035600 (2014).

23 Zhou, Z., White, K. A., Polissi, A., Georgopoulos, C. & Raetz, C. R. Function of Escherichia coli MsbA, an essential ABC family transporter, in lipid A and phospholipid biosynthesis. *J Biol Chem* **273**, 12466-12475 (1998).

24 Raetz, C. R., Reynolds, C. M., Trent, M. S. & Bishop, R. E. Lipid A modification systems in gram-negative bacteria. *Annu Rev Biochem* **76**, 295-329, doi:10.1146/annurev.biochem.76.010307.145803 (2007).

25 Anderson, M. S. & Raetz, C. R. Biosynthesis of lipid A precursors in Escherichia coli. A cytoplasmic acyltransferase that converts UDP-N-acetylglucosamine to UDP-3-O-(R-3-hydroxymyristoyl)-N-acetylglucosamine. *J Biol Chem* **262**, 5159-5169 (1987).

26 Anderson, M. S. *et al.* UDP-N-acetylglucosamine acyltransferase of Escherichia coli. The first step of endotoxin biosynthesis is thermodynamically unfavorable. *J Biol Chem* **268**, 19858-19865 (1993).

27 Anderson, M. S., Robertson, A. D., Macher, I. & Raetz, C. R. Biosynthesis of lipid A in Escherichia coli: identification of UDP-3-O-[(R)-3-hydroxymyristoyl]-alpha-D-glucosamine as a precursor of UDP-N2,O3-bis[(R)-3-hydroxymyristoyl]-alpha-D-glucosamine. *Biochemistry* **27**, 1908-1917 (1988).

28 Young, K. *et al.* The envA permeability/cell division gene of Escherichia coli encodes the second enzyme of lipid A biosynthesis. UDP-3-O-(R-3-hydroxymyristoyl)-N-acetylglucosamine deacetylase. *J Biol Chem* **270**, 30384-30391 (1995).

29 Kelly, T. M., Stachula, S. A., Raetz, C. R. & Anderson, M. S. The firA gene of Escherichia coli encodes UDP-3-O-(R-3-hydroxymyristoyl)-glucosamine N-acyltransferase. The third step of endotoxin biosynthesis. *J Biol Chem* **268**, 19866-19874 (1993).

30 Chimalakonda, G. *et al.* Lipoprotein LptE is required for the assembly of LptD by the beta-barrel assembly machine in the outer membrane of Escherichia coli. *Proc Natl Acad Sci U S A* **108**, 2492-2497, doi:10.1073/pnas.1019089108 (2011).

31 Chng, S. S., Ruiz, N., Chimalakonda, G., Silhavy, T. J. & Kahne, D. Characterization of the two-protein complex in Escherichia coli responsible for lipopolysaccharide assembly at the outer membrane. *Proc Natl Acad Sci U S A* **107**, 5363-5368, doi:10.1073/pnas.0912872107 (2010).

32 Freinkman, E., Chng, S. S. & Kahne, D. The complex that inserts lipopolysaccharide into the bacterial outer membrane forms a two-protein plug-and-barrel. *Proc Natl Acad Sci U S A* **108**, 2486-2491, doi:10.1073/pnas.1015617108 (2011).

33 Okuda, S., Freinkman, E. & Kahne, D. Cytoplasmic ATP hydrolysis powers transport of lipopolysaccharide across the periplasm in E. coli. *Science* **338**, 1214-1217, doi:10.1126/science.1228984 (2012).

34 Owens, T. W. *et al.* Structural basis of unidirectional export of lipopolysaccharide to the cell surface. *Nature* **567**, 550-553, doi:10.1038/s41586-019-1039-0 (2019).

35 Ruiz, N., Kahne, D. & Silhavy, T. J. Transport of lipopolysaccharide across the cell envelope: the long road of discovery. *Nat Rev Microbiol* **7**, 677-683, doi:10.1038/nrmicro2184 (2009).

36 Sherman, D. J. *et al.* Decoupling catalytic activity from biological function of the ATPase that powers lipopolysaccharide transport. *Proc Natl Acad Sci U S A* **111**, 4982-4987, doi:10.1073/pnas.1323516111 (2014).

37 Sherman, D. J. *et al.* Lipopolysaccharide is transported to the cell surface by a membrane-to-membrane protein bridge. *Science* **359**, 798-801, doi:10.1126/science.aar1886 (2018).

38 Bos, M. P., Tefsen, B., Geurtsen, J. & Tommassen, J. Identification of an outer membrane protein required for the transport of lipopolysaccharide to the bacterial cell surface. *Proc Natl Acad Sci U S A* **101**, 9417-9422, doi:10.1073/pnas.0402340101 (2004).

39 Wu, T. *et al.* Identification of a protein complex that assembles lipopolysaccharide in the outer membrane of Escherichia coli. *Proc Natl Acad Sci U S A* **103**, 11754-11759, doi:10.1073/pnas.0604744103 (2006).

40 Langklotz, S., Schakermann, M. & Narberhaus, F. Control of lipopolysaccharide biosynthesis by FtsH-mediated proteolysis of LpxC is conserved in enterobacteria but not

in all gram-negative bacteria. *J Bacteriol* **193**, 1090-1097, doi:10.1128/JB.01043-10 (2011).

41 Ogura, T. *et al.* Balanced biosynthesis of major membrane components through regulated degradation of the committed enzyme of lipid A biosynthesis by the AAA protease FtsH (HflB) in Escherichia coli. *Mol Microbiol* **31**, 833-844 (1999).

42 Sorensen, P. G. *et al.* Regulation of UDP-3-O-[R-3-hydroxymyristoyl]-N-acetylglucosamine deacetylase in Escherichia coli. The second enzymatic step of lipid a biosynthesis. *J Biol Chem* **271**, 25898-25905 (1996).

43 Fuhrer, F., Langklotz, S. & Narberhaus, F. The C-terminal end of LpxC is required for degradation by the FtsH protease. *Mol Microbiol* **59**, 1025-1036, doi:10.1111/j.1365-2958.2005.04994.x (2006).

44 Schakermann, M., Langklotz, S. & Narberhaus, F. FtsH-mediated coordination of lipopolysaccharide biosynthesis in Escherichia coli correlates with the growth rate and the alarmone (p)ppGpp. *J Bacteriol* **195**, 1912-1919, doi:10.1128/JB.02134-12 (2013).

45 Mohan, S., Kelly, T. M., Eveland, S. S., Raetz, C. R. & Anderson, M. S. An Escherichia coli gene (FabZ) encoding (3R)-hydroxymyristoyl acyl carrier protein dehydrase. Relation to fabA and suppression of mutations in lipid A biosynthesis. *J Biol Chem* **269**, 32896-32903 (1994).

46 Emiola, A., Andrews, S. S., Heller, C. & George, J. Crosstalk between the lipopolysaccharide and phospholipid pathways during outer membrane biogenesis in Escherichia coli. *Proc Natl Acad Sci U S A* **113**, 3108-3113, doi:10.1073/pnas.1521168113 (2016).

47 Steeghs, L. *et al.* Meningitis bacterium is viable without endotoxin. *Nature* **392**, 449-450, doi:10.1038/33046 (1998).

48 Peng, D., Hong, W., Choudhury, B. P., Carlson, R. W. & Gu, X. X. Moraxella catarrhalis bacterium without endotoxin, a potential vaccine candidate. *Infect Immun* **73**, 7569-7577, doi:10.1128/IAI.73.11.7569-7577.2005 (2005).

49 Steeghs, L. *et al.* Outer membrane composition of a lipopolysaccharide-deficient Neisseria meningitidis mutant. *EMBO J* **20**, 6937-6945, doi:10.1093/emboj/20.24.6937 (2001).

50 Moffatt, J. H. *et al.* Colistin resistance in Acinetobacter baumannii is mediated by complete loss of lipopolysaccharide production. *Antimicrob Agents Chemother* **54**, 4971-4977, doi:10.1128/AAC.00834-10 (2010).

51 Richie, D. L. *et al.* Toxic Accumulation of LPS Pathway Intermediates Underlies the Requirement of LpxH for Growth of Acinetobacter baumannii ATCC 19606. *PLoS One* **11**, e0160918, doi:10.1371/journal.pone.0160918 (2016).

52 Wei, J. R. *et al.* LpxK Is Essential for Growth of Acinetobacter baumannii ATCC 19606: Relationship to Toxic Accumulation of Lipid A Pathway Intermediates. *mSphere* **2**, doi:10.1128/mSphere.00199-17 (2017).

53 Mu, X. *et al.* The Effect of Colistin Resistance-Associated Mutations on the Fitness of Acinetobacter baumannii. *Front Microbiol* **7**, 1715, doi:10.3389/fmicb.2016.01715 (2016).

54 Beceiro, A. *et al.* Biological cost of different mechanisms of colistin resistance and their impact on virulence in Acinetobacter baumannii. *Antimicrob Agents Chemother* **58**, 518-526, doi:10.1128/AAC.01597-13 (2014).

55 Bojkovic, J. *et al.* Characterization of an Acinetobacter baumannii lptD Deletion Strain: Permeability Defects and Response to Inhibition of Lipopolysaccharide and Fatty Acid Biosynthesis. *J Bacteriol* **198**, 731-741, doi:10.1128/JB.00639-15 (2015).

56 Powers, M. J. & Trent, M. S. Phospholipid retention in the absence of asymmetry strengthens the outer membrane permeability barrier to last-resort antibiotics. *Proc Natl Acad Sci U S A* **115**, E8518-E8527, doi:10.1073/pnas.1806714115 (2018).

57 Garcia-Quintanilla, M. *et al.* Inhibition of LpxC Increases Antibiotic Susceptibility in Acinetobacter baumannii. *Antimicrob Agents Chemother* **60**, 5076-5079, doi:10.1128/AAC.00407-16 (2016).

58 Tomaras, A. P. *et al.* LpxC inhibitors as new antibacterial agents and tools for studying regulation of lipid A biosynthesis in Gram-negative pathogens. *MBio* **5**, e01551-01514, doi:10.1128/mBio.01551-14 (2014).

59 Clements, J. M. *et al.* Antibacterial activities and characterization of novel inhibitors of LpxC. *Antimicrob Agents Chemother* **46**, 1793-1799 (2002).

60 Barb, A. W. & Zhou, P. Mechanism and inhibition of LpxC: an essential zinc-dependent deacetylase of bacterial lipid A synthesis. *Curr Pharm Biotechnol* **9**, 9-15 (2008).

61 Mdluli, K. E. *et al.* Molecular validation of LpxC as an antibacterial drug target in Pseudomonas aeruginosa. *Antimicrob Agents Chemother* **50**, 2178-2184, doi:10.1128/AAC.00140-06 (2006).

62 Onishi, H. R. *et al.* Antibacterial agents that inhibit lipid A biosynthesis. *Science* **274**, 980-982 (1996).

63 Jackman, J. E. *et al.* Antibacterial agents that target lipid A biosynthesis in gram-negative bacteria. Inhibition of diverse UDP-3-O-(r-3-hydroxymyristoyl)-n-acetylglucosamine deacetylases by substrate analogs containing zinc binding motifs. *J Biol Chem* **275**, 11002-11009 (2000).

64 Zeng, D. *et al.* Mutants resistant to LpxC inhibitors by rebalancing cellular homeostasis. *J Biol Chem* **288**, 5475-5486, doi:10.1074/jbc.M112.447607 (2013).

65 Ho, H. *et al.* Structural basis for dual-mode inhibition of the ABC transporter MsbA. *Nature* **557**, 196-201, doi:10.1038/s41586-018-0083-5 (2018).

66 Zhang, G. *et al.* Cell-based screen for discovering lipopolysaccharide biogenesis inhibitors. *Proc Natl Acad Sci U S A* **115**, 6834-6839, doi:10.1073/pnas.1804670115 (2018).

67 Stansly, P. G., Shepherd, R. G. & White, H. J. Polymyxin: a new chemotherapeutic agent. *Bull Johns Hopkins Hosp* **81**, 43-54 (1947).

68 Choi, S. K. *et al.* Identification of a polymyxin synthetase gene cluster of Paenibacillus polymyxa and heterologous expression of the gene in Bacillus subtilis. *J Bacteriol* **191**, 3350-3358, doi:10.1128/JB.01728-08 (2009).

69 Stansly, P. G. & Schlosser, M. E. Studies on Polymyxin: Isolation and Identification of Bacillus polymyxa and Differentiation of Polymyxin from Certain Known Antibiotics. *J Bacteriol* **54**, 549-556 (1947).

70 Azad, M. A. *et al.* Polymyxin B Induces Apoptosis in Kidney Proximal Tubular Cells. *Antimicrob Agents Chemother* **57**, 4329-4335, doi:10.1128/AAC.02587-12 (2013).

71 Falagas, M. E. & Kasiakou, S. K. Toxicity of polymyxins: a systematic review of the evidence from old and recent studies. *Crit Care* **10**, R27, doi:10.1186/cc3995 (2006).

72 Nakajima, K. Structure-activity relationship of colistins. *Chem Pharm Bull (Tokyo)* **15**, 1219-1224 (1967).

73 Velkov, T., Thompson, P. E., Nation, R. L. & Li, J. Structure--activity relationships of polymyxin antibiotics. *J Med Chem* **53**, 1898-1916, doi:10.1021/jm900999h (2010).

74 Mingeot-Leclercq, M. P., Tulkens, P. M., Denamur, S., Vaara, T. & Vaara, M. Novel polymyxin derivatives are less cytotoxic than polymyxin B to renal proximal tubular cells. *Peptides* **35**, 248-252, doi:10.1016/j.peptides.2012.03.033 (2012).

75 Katsu, T., Nakagawa, H. & Yasuda, K. Interaction between polyamines and bacterial outer membranes as investigated with ion-selective electrodes. *Antimicrob Agents Chemother* **46**, 1073-1079 (2002).

76 Tsubery, H., Ofek, I., Cohen, S. & Fridkin, M. Structure-function studies of polymyxin B nonapeptide: implications to sensitization of gram-negative bacteria. *J Med Chem* **43**, 3085-3092 (2000).

77 Tsubery, H., Ofek, I., Cohen, S. & Fridkin, M. The functional association of polymyxin B with bacterial lipopolysaccharide is stereospecific: studies on polymyxin B nonapeptide. *Biochemistry* **39**, 11837-11844 (2000).

78 Vaara, M. & Vaara, T. Sensitization of Gram-negative bacteria to antibiotics and complement by a nontoxic oligopeptide. *Nature* **303**, 526-528 (1983).

79 Vaara, M. & Viljanen, P. Binding of polymyxin B nonapeptide to gram-negative bacteria. *Antimicrob Agents Chemother* **27**, 548-554 (1985).

80 Moore, R. A., Bates, N. C. & Hancock, R. E. Interaction of polycationic antibiotics with Pseudomonas aeruginosa lipopolysaccharide and lipid A studied by using dansyl-polymyxin. *Antimicrob Agents Chemother* **29**, 496-500 (1986).

81 Hancock, R. E. & Chapple, D. S. Peptide antibiotics. *Antimicrob Agents Chemother* **43**, 1317-1323 (1999).

82 Zhang, L., Dhillon, P., Yan, H., Farmer, S. & Hancock, R. E. Interactions of bacterial cationic peptide antibiotics with outer and cytoplasmic membranes of Pseudomonas aeruginosa. *Antimicrob Agents Chemother* **44**, 3317-3321 (2000).

83 Brogden, K. A. Antimicrobial peptides: pore formers or metabolic inhibitors in bacteria? *Nat Rev Microbiol* **3**, 238-250, doi:10.1038/nrmicro1098 (2005).

84 Deris, Z. Z. *et al.* Probing the penetration of antimicrobial polymyxin lipopeptides into gram-negative bacteria. *Bioconjug Chem* **25**, 750-760, doi:10.1021/bc500094d (2014).

85 Sampson, T. R. *et al.* Rapid killing of Acinetobacter baumannii by polymyxins is mediated by a hydroxyl radical death pathway. *Antimicrob Agents Chemother* **56**, 5642-5649, doi:10.1128/AAC.00756-12 (2012).

86 Daugelavicius, R., Bakiene, E. & Bamford, D. H. Stages of polymyxin B interaction with the Escherichia coli cell envelope. *Antimicrob Agents Chemother* **44**, 2969-2978 (2000).

87 Dixon, R. A. & Chopra, I. Leakage of periplasmic proteins from Escherichia coli mediated by polymyxin B nonapeptide. *Antimicrob Agents Chemother* **29**, 781-788 (1986).

88 Dixon, R. A. & Chopra, I. Polymyxin B and polymyxin B nonapeptide alter cytoplasmic membrane permeability in Escherichia coli. *J Antimicrob Chemother* **18**, 557-563 (1986).

89 Olaitan, A. O., Morand, S. & Rolain, J. M. Mechanisms of polymyxin resistance: acquired and intrinsic resistance in bacteria. *Front Microbiol* **5**, 643, doi:10.3389/fmicb.2014.00643 (2014).

90 Groisman, E. A., Kayser, J. & Soncini, F. C. Regulation of polymyxin resistance and adaptation to low-Mg2+ environments. *J Bacteriol* **179**, 7040-7045 (1997).

91 Arroyo, L. A. *et al.* The pmrCAB operon mediates polymyxin resistance in Acinetobacter baumannii ATCC 17978 and clinical isolates through phosphoethanolamine modification of lipid A. *Antimicrob Agents Chemother* **55**, 3743-3751, doi:10.1128/AAC.00256-11 (2011).

92 Trent, M. S., Ribeiro, A. A., Lin, S., Cotter, R. J. & Raetz, C. R. An inner membrane enzyme in Salmonella and Escherichia coli that transfers 4-amino-4-deoxy-L-arabinose to lipid A: induction on polymyxin-resistant mutants and role of a novel lipid-linked donor. *J Biol Chem* **276**, 43122-43131, doi:10.1074/jbc.M106961200 (2001).

93 Loutet, S. A. & Valvano, M. A. Extreme antimicrobial peptide and polymyxin B resistance in the genus Burkholderia. *Front Cell Infect Microbiol* **1**, 6, doi:10.3389/fcimb.2011.00006 (2011).

94 Trent, M. S. *et al.* Accumulation of a polyisoprene-linked amino sugar in polymyxin-resistant Salmonella typhimurium and Escherichia coli: structural characterization and transfer to lipid A in the periplasm. *J Biol Chem* **276**, 43132-43144, doi:10.1074/jbc.M106962200 (2001).

95 Nummila, K., Kilpelainen, I., Zahringer, U., Vaara, M. & Helander, I. M. Lipopolysaccharides of polymyxin B-resistant mutants of Escherichia coli are extensively substituted by 2-aminoethyl pyrophosphate and contain aminoarabinose in lipid A. *Mol Microbiol* **16**, 271-278 (1995).

96 Lim, T. P. *et al.* Multiple Genetic Mutations Associated with Polymyxin Resistance in Acinetobacter baumannii. *Antimicrob Agents Chemother* **59**, 7899-7902, doi:10.1128/AAC.01884-15 (2015).

97 Moffatt, J. H. *et al.* Lipopolysaccharide-deficient Acinetobacter baumannii shows altered signaling through host Toll-like receptors and increased susceptibility to the host antimicrobial peptide LL-37. *Infect Immun* **81**, 684-689, doi:10.1128/IAI.01362-12 (2013).

Chapter 2

Polymyxin B-Mediated Killing Involves Inhibition of LPS Transport at the Inner Membrane

---

All data in this chapter outside of the imaging studies (Figure 2.11, Eileen Moison) was generated by me unless otherwise noted. Much of this work was done in collaboration with Eileen Moison who performed the initial *in vitro* crosslinking experiments to LptA and also made significant contributions to the design of subsequent experiments.

Some of the work in this chapter is reproduced from:

Bertani, BR., Taylor R.J, **Nagy E**., Kahne D., Ruiz N. (2018). A cluster of residues in the lipopolysaccharide exporter that selects substrate variants for transport to the outer membrane. *Mol Microbiol* ***109****, 541-554.*

2.1 Abstract

This chapter describes the development of a new model for the mechanism of polymyxin B (PMB) mediated cell death. We utilized biochemical and imaging tools developed by the lab to show that treatment with PMB inhibits LPS transport at a specific step in the process. An *in vitro* reconstitution of transport reveals that PMB treatment blocks LPS interactions with residues (in LptC and LptA) later in the transport pathway. We confirm this result *in vivo* and show that inhibition occurs at concentrations relevant to the minimum inhibitory concentration (MIC). Using newly acquired crystallography data, we extend the investigation to include residues earlier in the transport pathway where PMB does not block crosslinking. Using these data, we propose a new mechanism for PMB that includes blocking transport, resulting in a build-up of LPS at the inner membrane. We also develop a new PMB probe that can be used for further studies into the specific mechanism of the interaction with the Lpt inner membrane components. Lastly, we describe work done in collaboration to elucidate an LPS binding site in LptG.

2.2 Background

Multi-drug resistant strains of bacteria present a tremendous challenge in the clinic today. Gram-negative species, in particular, are difficult to treat because of the already limited number of antibiotics that can effectively penetrate the outer membrane. Colistin (polymyxin E), a potent inhibitor of Gram-negative bacteria, is currently a drug of last resort, partially because it is so effective against infections that are difficult to trerat, but also because of associated nephrotoxicity.[1,2] Since the polymyxins are so important clinically, there has been much interest in developing compounds with improved potency and/or less toxicity. Thus far, efforts in this area have been unsuccessful in producing an improved pharmaceutical. We believe that some of the difficulty may be due to the vague understanding of polymyxin's mechanism of action.[3] Elucidating specifically how polymyxin kills cells would enable more directed development of analogues.

During a screen for compounds that interact with LpxC inhibitors, our lab discovered that these inhibitors strongly antagonize polymyxin B (PMB) activity (Figure 2.1 A, replicated from unpublished data from Ge Zhang, a former graduate student in the Kahne lab).[4,5] Treatment with increasing concentrations of an LpxC inhibitor rescued cells from killing by PMB in a checkerboard assay. This experiment was done with wild type strains of *A. baumannii*, since it can survive without LPS and thus can be treated with high concentrations of an LpxC inhibitor without cell death. To determine if rescue was simply a result of less LPS in the outer membrane to promote PMB uptake, cells were co-treated with PMB and an LpxC inhibitor, and viability was measured over a 30-minute period (Figure 2.1 B). This is about the length of one cell division, so surface LPS could not yet have been diluted through multiple divisions. The results showed that the LpxC

inhibitor can rescue cells from PMB even when there is still LPS present in the outer membrane. As was discussed in Chapter 1, we would expect that if PMB were killing cells by a nonspecific mechanism, these treated cells should be equally susceptible. Our interpretation of these data was that active LPS synthesis was required for PMB killing, and thus perhaps PMB could be targeting some aspect of LPS synthesis or transport.

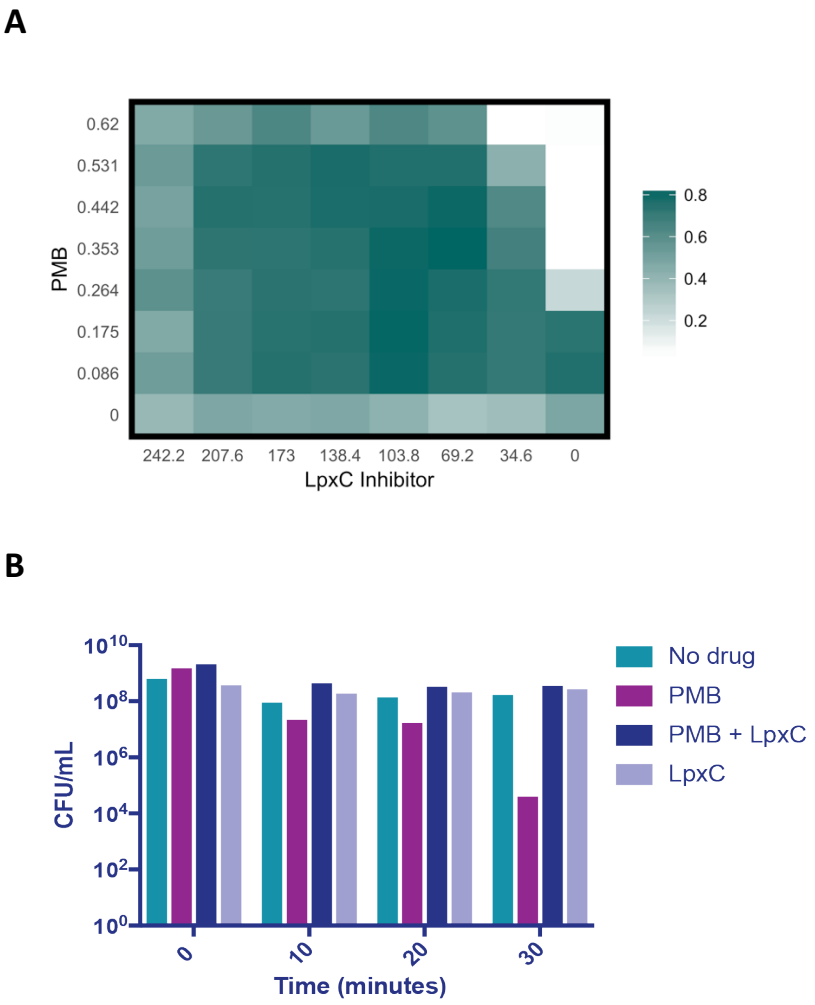

Figure 2.1 In *A. baumannnii* synthesis of LPS is required for PMB-mediated killing. A) An LpxC inhibitor (PF-5081090) antagonizes PMB based on two-dimensional minimal inhibitory concentration (MIC) measurements. PMB was added in a linear dilution up to 2x MIC (0.62 µM). Since the LpxC inhibitor does not kill *A. baumannii*, it was added to as high of concentration (242 µM) as was reasonable. (B) An LpxC inhibitor rescues cells from PMB-mediated lethality. A lethal concentration of PMB (10x MIC) with or without PF-5081090 (242 µM) was added to a culture of *A. baumannii*. Spot dilutions at each time point were made in order to determine the CFU/mL.

Over the past decade, our lab has developed tools to study LPS transport, both *in vitro* and *in vivo*.[6,7] One of these tools involves incorporating the inner membrane complex of the Lpt pathway ($LptB_2FGC$) into LPS-filled proteoliposomes and then adding soluble LptA to the mixture (Figure 2.2). Upon the addition of ATP, LPS can be transported from the liposome to LptA where it can be trapped via a UV-activatable crosslinking residue (*p*BPA). These LPS x LptA complexes can then be visualized by immunoblotting. Monitoring the accumulation of LPS on LptA through this *in vitro* reconstitution can be used as a proxy for LPS transport through the system.

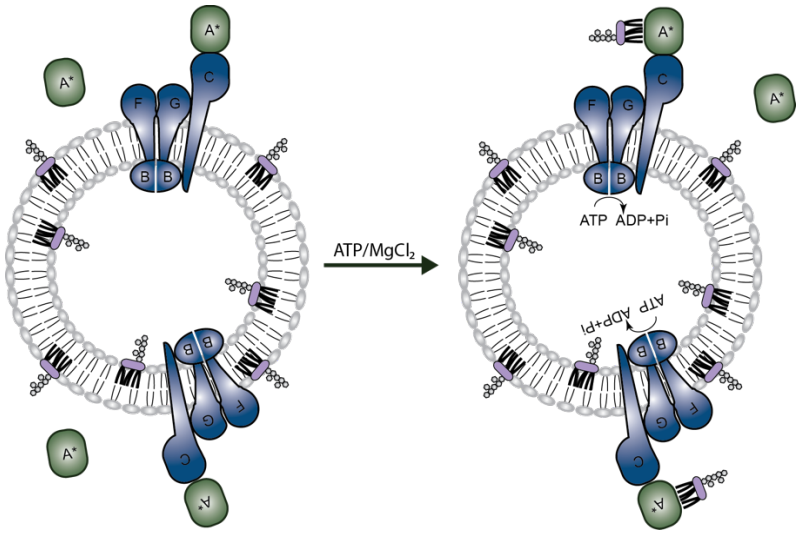

Figure 2.2 *In vitro* reconstitution of LPS transport. Proteoliposomes containing $LptB_2FGC$ and LPS were mixed with soluble LptA containing a crosslinking residue (*p*BPA) at position I36. Transport of LPS was initiated by the addition of ATP. Any LPS bound to LptA was crosslinked by exposure to UV for 5 minutes and then LPS x LptA crosslinks were detected by immunoblotting.

To investigate if PMB might be interfering with LPS transport to the cell surface, Eileen Moison, a graduate student in the Kahne lab, treated the proteoliposomes in this assay with increasing concentrations of PMB or PMBN (Figure 2.2). Treatment with PMB completely blocked

crosslinking of LPS to LptA in this system, while PMBN treatment had no dose dependent effect. Since PMBN is not antimicrobial yet still binds LPS, this supported the idea that the inhibition observed might be related to PMB's activity and not simply a result of LPS binding.[8,9]

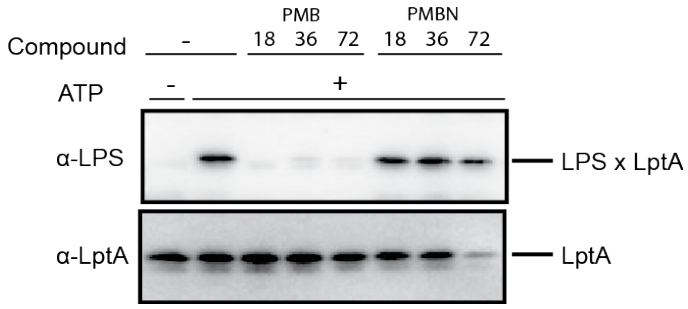

Figure 2.3 Treatment with PMB prevents crosslinking of LPS to LptA *in vitro*. Soluble LptA was added to proteoliposomes containing $LptB_2FGC$ and then the liposomes were incubated with PMB or PMBN (18, 36, or 72 μM) for 15 minutes before the addition of ATP to initiate transport. Samples were incubated with ATP for 60 minutes at 30°C before crosslinking by 5 minutes of UV exposure. LPS x LptA crosslinks were visualized by immunoblotting.

It is known that LPS accumulation at the inner membrane is toxic to cells.[10,11] Even in species that survive without LPS, it must be blocked either very early in synthesis or very late in transport to prevent the build-up of intermediates in the pathway.[12,13] We wondered if PMB might be blocking transport of LPS through the Lpt pathway, thus causing a build-up of LPS at the inner membrane and a lack of LPS at the cell surface. If this were the case, this process could be at least a component of PMB's mechanism of action. We used several different approaches to further investigate PMB's effect on LPS transport.

2.3 Development of a PMB probe for crosslinking studies

2.3.1 Introduction

A PMB probe with a crosslinking residue would be one way to identify any potential interactions between PMB and an Lpt pathway component. Cells could be treated with the probe and then upon UV exposure, the PMB probe would attach to any nearby proteins. These protein x PMB complexes could be visualized and identified through immunoblotting since the number of candidate proteins would be limited. Any positive hits could be further analyzed by mass spectrometry to determine the exact residues in the protein that are interacting, and this information could then be compared to known structural characterization for relevance to transport. We wanted to design and synthesize such a probe for future polymyxin studies.

2.3.2 Results

The primary consideration when designing the probe was to find a position and type of crosslinker that would have a minimal impact on antimicrobial activity. Any crosslinks obtained with a probe with comparable antimicrobial activity to PMB would be more likely to be relevant to that activity. The structure of PMB has not proven amenable to many changes, but it is known that removing the charge of a single Dab residue has a minimal impact on activity (Figure 2.4).[14] Since the fatty acyl tail on the tripeptide is required for killing and thus potentially involved in any mechanism, we chose to replace either Dab^1 (PMB*1) or Dab^3 (PMB*3) of the tripeptide with a crosslinking residue since these positions are closest to the acyl chain. A diazirine crosslinker was used since it is small and flexible, most closely mimicking the characteristics of Dab.

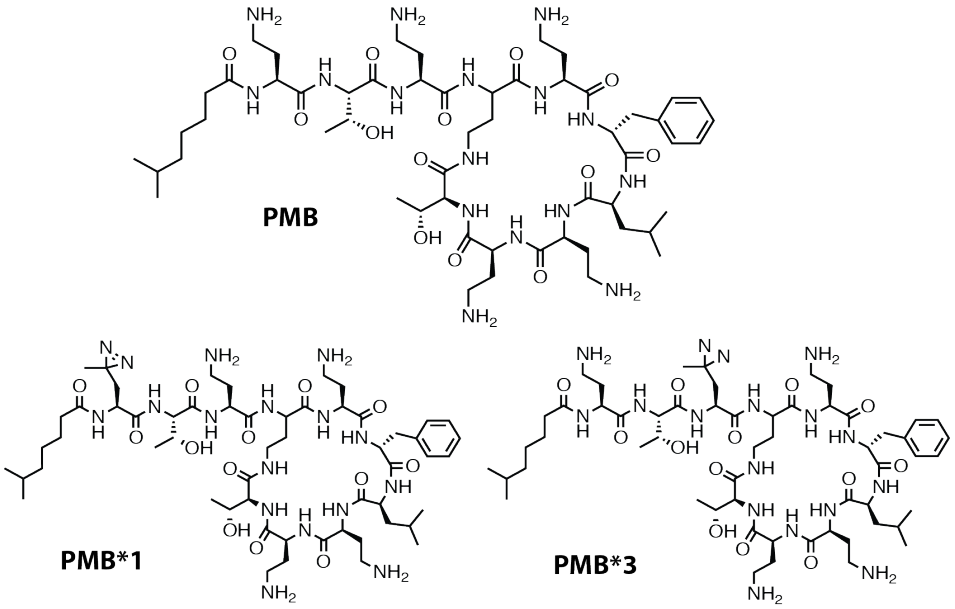

Figure 2.4 Structure of PMB and crosslinking probes. PMB is composed of a heptapeptide macrocycle with a tripeptide tail connected to a fatty acid. The residues are numbered from the N-terminal end. Two crosslinkers were designed, one with Dab^1 replaced by a diazirine residue (PMB*1) and the other with Dab^3 replaced (PMB*3).

To synthesize the probe, we used solid phase peptide synthesis to generate the linear peptide and then followed established protocols to cyclize (Figure 2.5).[15,16] The only deviation from the published route was the final deprotection reaction, since hydrogenation is not compatible with a diazirine residue. We synthesized PMB as well as the two probes (Figure 2.4). To gain adequate solubility, the formic acid salts of each compounded (post purification) had to be converted to sulfate salts.

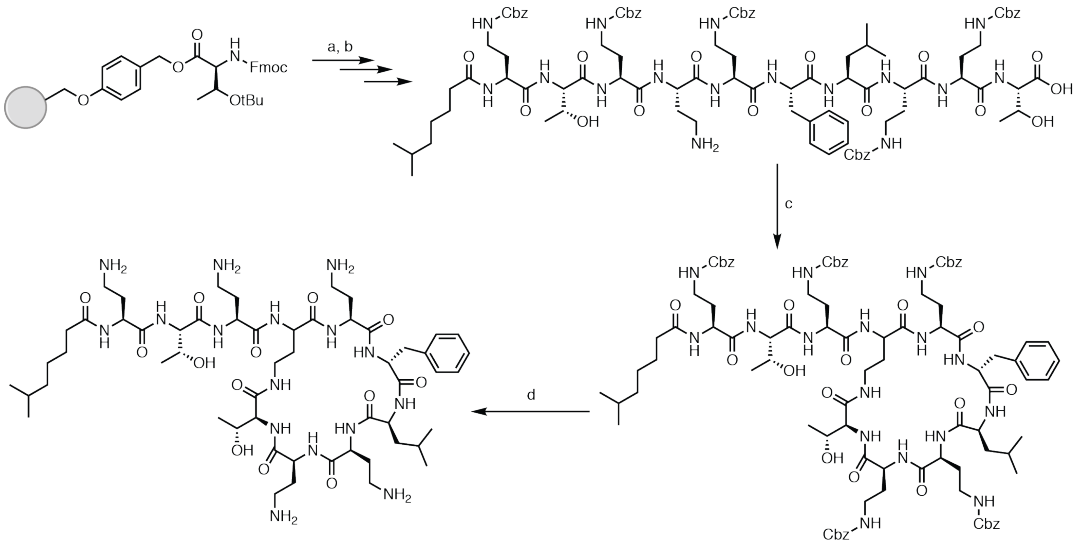

Figure 2.5 Synthesis scheme for polymyxin. a) Solid phase peptide synthesis using Wang resin preloaded with Fmoc-Thr(tBu). b) 95:5 TFA:H_2O, 2 hours, 0°C. c) PyBOP, HOBt, DIPEA in DMF, 4 hours, r.t. d) TFA, thioanisole in acetonitrile, 4 hours, r.t

We determined the antimicrobial activity of each probe by measuring the minimal inhibitory concentration (MIC) for strains of *E. coli* and *A. baumannii*. PMB*1 has significantly less activity than PMB in both species, whereas PMB*3 retains comparable activity (4-fold difference or less) (Table 2.1). There were also substantial differences in activity between *E. coli* and *A. baumannii,* which we attributed to differences in LPS structure and thus binding. For later experiments, we focused on PMB*3 since it has the most potent antimicrobial activity.

Table 2.1 MIC values of PMB, PMBN, and PMB probes. NR754 is an *E. coli* variant of MC4100 and 19606 is a strain of *A. baumannii.*

Strain	MIC (μM)			
	PMB	**PMBN**	**PMB*1**	**PMB*3**
NR754	0.28	>40	9.0	0.56
19606	0.56	>40	>36	2.26

To test the crosslinking ability of the probe, we incubated it with LPS in different ratios and then exposed the sample to UV. We observed LPS x PMB*3 crosslinks via immunoblotting with an LPS antibody as well as silver staining (Figure 2.6). To use the probe in the *in vitro* reconstitution of LPS transport, we needed to be able to visualize the probe separately from LPS. We planned to utilize a commercially available antibody to polymyxin, but the antibody was reactive to LPS and not PMB (data not shown). We considered trying to see PMB*3 x protein complexes via gel shift due to the change in mass but decided it would be impractical due to the small size of PMB. The probe needed to be redesigned to include a residue that could be detected by an antibody.

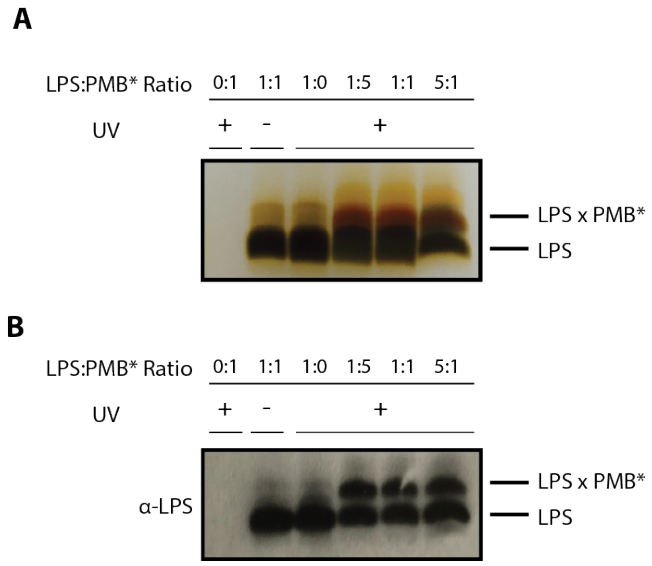

Figure 2.6 Crosslinking of PMB*3 to LPS. (A) Crosslinks visualized by silver stain of LPS. Samples of LPS and PMB*3 were mixed and then exposed to UV for 15 minutes. After irradiation, samples were separated on an SDS-PAGE gel and silver stained. Samples were normalized such that the same amount of LPS was loaded in each lane. (B) Crosslinks visualized by immunoblotting. Samples were run on the same SDS-PAGE gel but were then transferred to a PVDF membrane and probed with an α-LPS antibody.

A recent paper reported a PMB probe containing an alkyne incorporated into the fatty acyl chain.[17] A biotin molecule could then be attached to the alkyne through Click chemistry, enabling the probe to be visualized using a streptavidin antibody. Their probe still had antibiotic activity, so we were confident we could also incorporate an alkyne at the same position in our probe without too much effect. The synthetic route we had been using proved incompatible with the alkyne residue and after troubleshooting, we decided a new approach was necessary. We followed the protocol established in the recent publication, which used a different resin and protecting strategy, and were able to successfully make small quantities of the probe (Figure 2.7). Purification has proven to be difficult due to hydrophobicity and aggregation of the compound so scaling up to make large quantities of the probe would be difficult at this stage.

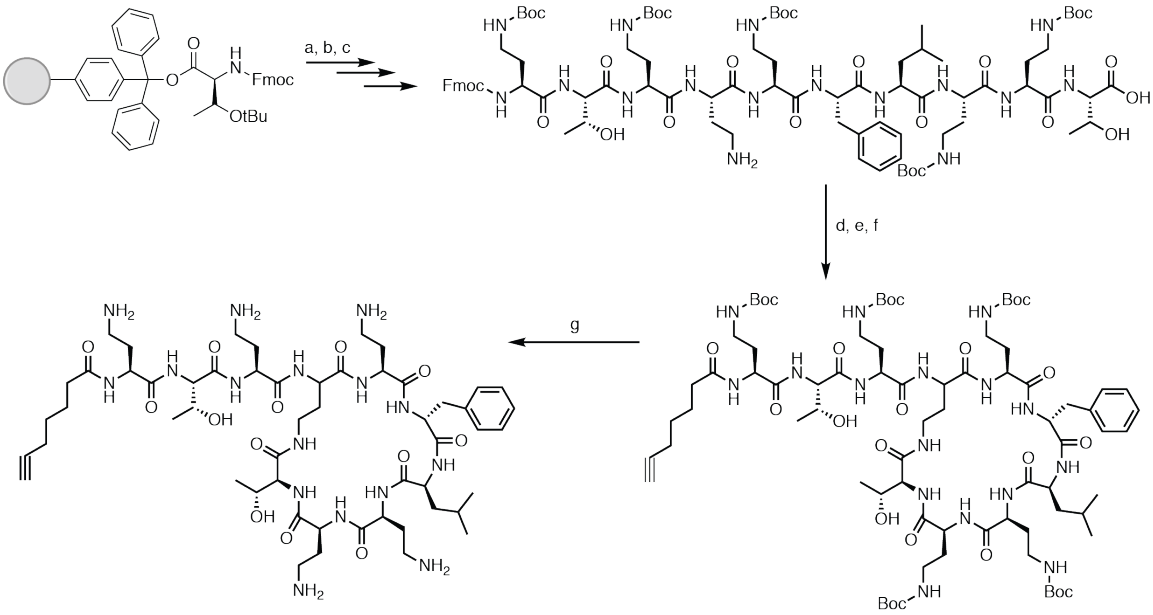

Figure 2.7 Redesigned synthesis scheme for polymyxin. a) Solid phase peptide synthesis using chlorotrityl chloride resin loaded with Fmoc-Thr(tBu). b) $Pd(PPh_3)_4$, Bu_3SnH, *p*-nitrophenol in DCM, 2 hours, r.t. c) 0.8% TFA in H_2O, 90 minutes., r.t. d) PyBOP, HOBt, DIPEA in DMF, 2 hours, (Continued) r.t. e) 20% piperidine in DMF, 20 minutes, r.t. f) 6-heptynoic acid, HATU, DIPEA in DMF, 1 hour, r.t. g) TFA:TIS:H_2O (95:2.5:2.5), 40 minutes, 0°C.

2.3.3 Discussion

We have created a probe that can be used to detect direct PMB interactions with proteins. While we envision those interactions being with components of the Lpt pathway, the probe could also be used for whole cell studies to look for unknown interacting partners. The probe has comparable antimicrobial activity to PMB and it can be visualized using readily available reagents. In the future, our lab may use the probe for mass spectrometry studies of PMB's interactions with the Lpt pathway, though sufficiently large quantities will need to be synthesized.

2.4 Investigation of PMB inhibition of LPS transport

2.4.1 Introduction

Since our lab has sophisticated biochemical tools to look at LPS transport, we wondered if we could utilize them to further understand the *in vitro* inhibition of LPS transport to LptA that we had observed upon treatment with PMB. We wondered if PMB would also abolish crosslinking to positions in LptC known to bind LPS. Since LptC represents an earlier step in the transport pathway, we could potentially determine if LPS was extracted from the inner membrane but getting stuck somewhere in the transporter or rather not extracted at all. We could also use *in vivo* crosslinking at many of the same positions to test the biological relevance of what we were observing *in vitro*. Finally, using a fluorescent polymyxin probe developed in the lab, we could observe LPS localization during PMB treatment (all microscopy experiments performed by Eileen Moison). Using all of these available tools in conjunction with recent structural data for the transporter, we have developed a model of how PMB might be interfering with the inner membrane complex of the Lpt transport pathway as a mechanism to kill cells.

2.4.2 Results

To test if earlier steps in the LPS transport pathway were inhibited, we set up the same *in vitro* reconstitution assay as before (Section 2.2) with the crosslinking residue at position T47 of LptC rather than in LptA. This residue is located in the β-jellyroll portion of LptC, meaning LPS has already been extracted from the membrane, but not yet transferred to LptA. We saw the same inhibition of crosslinking with PMB treatment that we had observed with LptA (Figure 2.8 A). In this case, there is still a faint LPS x LptC crosslink band because there is always a certain amount of LPS preloaded into the purified complex. We again noted that there was no dose dependent effect observed with treatment with PMBN.

The concentrations of PMB used in the reconstitution assay were quite high relative to the MIC for *E. coli*, and we always saw complete inhibition of crosslinking. We wanted to determine the lowest dose at which we could observe inhibition and find concentrations where there was a dose dependent response. Several lower concentrations of PMB were tested for inhibition of crosslinking to LptC (Figure 2.8 B). We could see a dose dependent inhibition of crosslinking at concentrations from 1 to 9uM and complete inhibition was observed at 18uM, the lowest concentration we had used in previous assays.

PMB inhibition of transport could be the result of PMB binding LPS and then affecting transport as part of a complex with LPS. A less likely possibility would have PMB directly interacting with the Lpt components in an LPS independent manner. One way to distinguish between these two possibilities is to make the proteoliposomes with mixtures of wild type and modified LPS. This modified LPS has ethanolamine modifications on the phosphates which reduces PMB's ability to bind. If PMB interference with transport is independent of binding, these modifications should have no effect. Increasing the amount of modified LPS in the

proteoliposomes resulted in a decrease in PMB inhibition of transport (Figure 2.8 C) though the effect is modest and only seen at higher concentrations. This result suggests LPS binding is required for the observed inhibition.

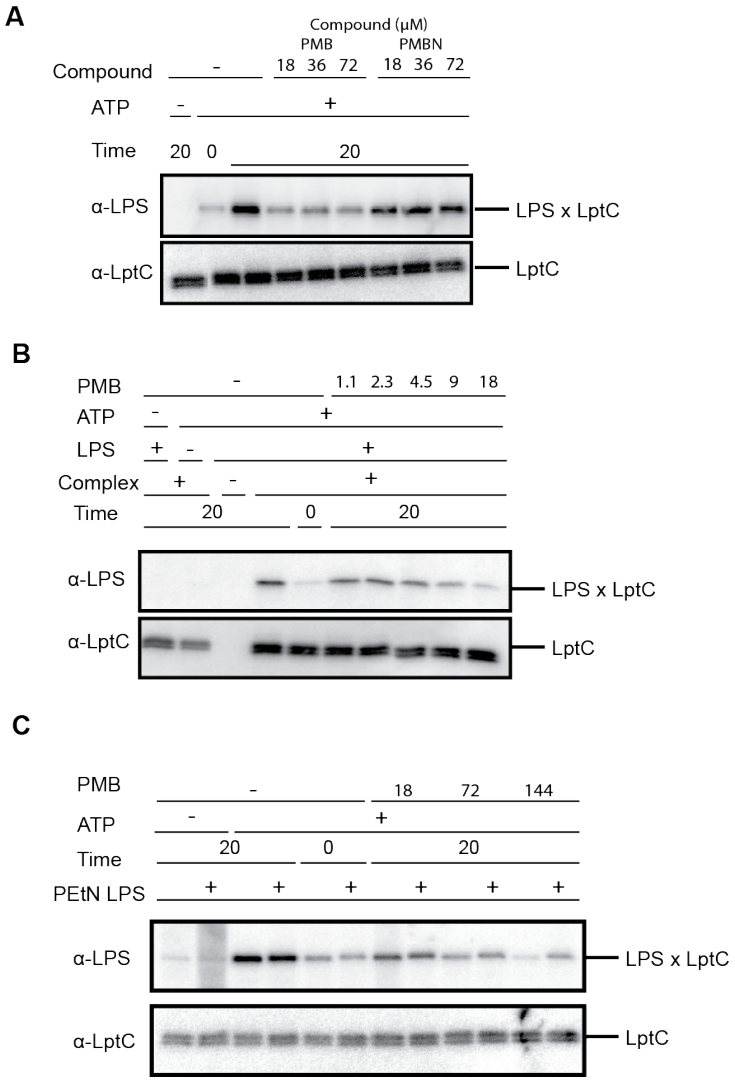

Figure 2.8 LPS release to LptC *in vitro.* A) Treatment with PMB prevents crosslinking of LPS to LptC *in vitro*. Proteoliposomes containing LptB_2FGC-T47*p*BPA were incubated with PMB or PMBN (18, 36, or 72 μM) for 15 minutes before the addition of ATP to initiate transport. For the 0-minute time points, samples were crosslinked for 3 minutes immediately after addition of ATP. All other samples were exposed to UV after 20 minutes of incubation. LPS x LptC crosslinks were visualized by immunoblotting. B) PMB inhibition is dose dependent. In the same experimental setup as above, varying doses of PMB (1.1 to 18 μM) were added 15. C) Proteoliposomes were prepared with either wild type LPS or LPS modified with phosphoethanolamine on the phosphates (PEtN LPS) and B_2FGC-T47*p*BPA. The experimental protocol was identical to (A).

While the biochemical results were encouraging, there are several reasons to be concerned that the proteoliposomes might not be a good representation of the effect in a biological system. The treatment concentrations of PMB required to see inhibition are more than 20-fold above the MIC, and there is only a single target (Lpt components) in the liposomes, whereas in the complex environment of the cell, there could be other more favorable interactions. Additionally, we could not rule out the possibility that PMB was affecting the proteoliposomes through detergent like activity. To address these concerns, we wanted to test PMB's effect on transport in living cells.

Our lab had established a protocol for monitoring LPS transport in living cells using the same T47 residue in LptC.[7] *E. coli* BL21(DE3) cells overexpressing the inner membrane $LptB_2FGC$ complex were grown and treated with concentrations of PMB below (0.5x) and above (10x) the MIC (1x) for 90 minutes (values shown in Table 2.2 in methods). With treatment above the MIC, LPS crosslinking to LptC was completely abolished (Figure 2.9 A), while sub inhibitory treatment resulted in a build-up of LPS at the T47 position. Treatment with PMBN did slightly inhibit crosslinking (similar to what had been observed *in vitro*), but it was not a dose dependent effect. We were encouraged that even in the complex system of the cell where PMB must cross the outer membrane into an environment with many potential targets, it was still blocking LPS transport. While we do not know for sure why LPS builds up at sub-inhibitory concentrations, we hypothesize that it is a result of disruption to the outer membrane triggering an increase in LPS transport.

To ensure that the observed results were not some artifact of overexpression of the inner membrane components, we repeated the assay in cells with leaky expression of $LptB_2FGC$ (Figure

2.9 B).[7] While the crosslinking levels are much lower, the same trend is observed. Treatment at concentrations above the MIC eliminates crosslinking.

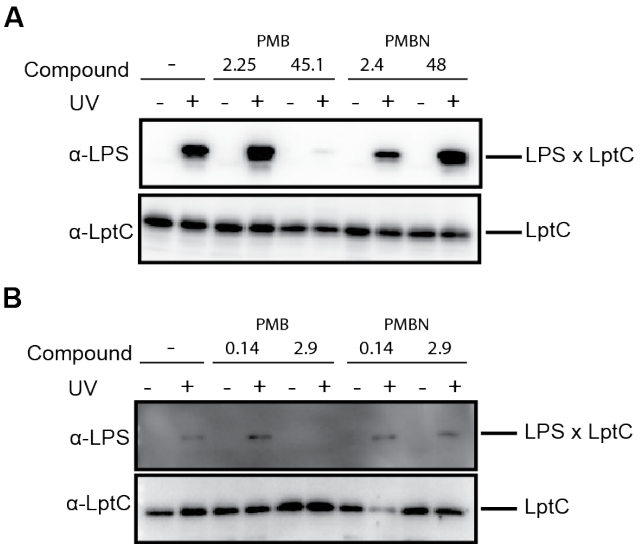

Figure 2.9 PMB treatment inhibits crosslinking of LPS to LptC *in vivo*. A) Cultures of BL21 (DE3) were induced to overexpress $LptB_2FGC$-T47*p*BPA and 30 minutes after induction were treated with PMB (0, 2.25 or 45.1 μM) or PMBN (2.4 or 48 μM). After 90 minutes of treatment, cells were harvested and exposed to UV for 5 minutes. LPS x LptC crosslinks were detected by immunoblotting. B) Cultures of MC4100 with leaky expression of LptC-T47*p*BPA were grown and treated with PMB (0, 0.14 or 2.9 μM) or PMBN (0.14 or 2.9 μM) for 90 minutes. Cells were exposed to UV for 5 minutes and LPS x LptC crosslinks were detect by immunoblotting.

More recently, a crystal structure of $LptB_2FGC$ from our lab led to the identification of positions in the LptC transmembrane helix that crosslink LPS.[18] This helix interacts with the helices of LptFG in the inner membrane. LPS diffuses into the lumen of LptFG at this interface, and subsequent ATP hydrolysis allows for extraction of the LPS into the β-jellyroll structure of LptC. While the T47 residue of LptC allows for monitoring of successful LPS extraction, the M19 and G21 residues in the helix of LptC report on a much earlier, energy independent, step of transport. We tested the effect of PMB treatment on crosslinking to these residues in the same overexpression strain

used earlier (Figure 2.10). Interestingly, PMB does not inhibit crosslinking to these residues in the same way as it does to T47. For G21, the crosslinking is quite weak and as a result, the data is not as consistent; however, PMB treatment does not inhibit crosslinking to any significant extent. At position M19, treatment with concentrations above the MIC actually results in a build-up of LPS. Based on the structure, G21 points inward into the lumen of LptFG, while M19 is on the exterior of the complex, in the membrane environment. It has been shown that abolishing the ATPase activity of LptB results in a build-up of LPS at both positions M19 and G21 suggesting that LPS is simply diffusing in and out of the machine. PMB treatment, however, only causes a build-up outside the machine indicating that LPS is specifically stalled at the entrance helices. This would prevent transport, thus causing an accumulation of LPS in the membrane at the outer surface of $LptB_2FGC$.

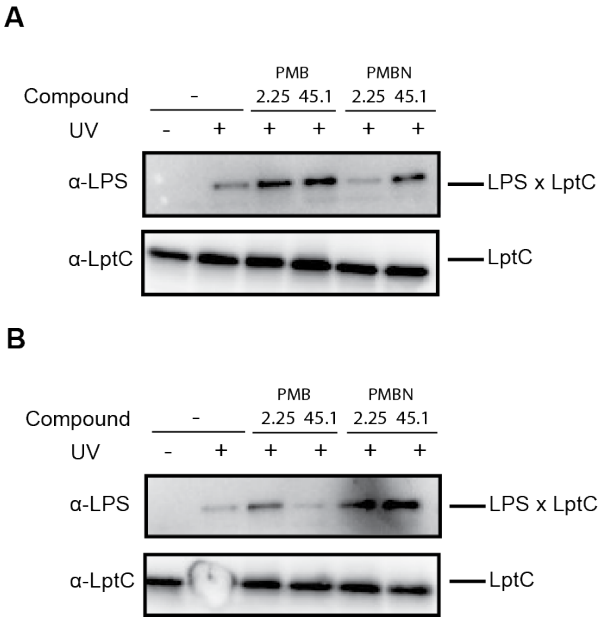

Figure 2.10 PMB treatment differentially affects crosslinking at positions earlier in the transport pathway. A) Cells overexpressing $LptB_2FGC$-M19*p*BPA were treated with PMB (0, 2.25 or 45.1 µM) or PMBN (2.25 or 45.1 µM) for 90 minutes. LPS x LptC crosslinks were detected by immunoblotting. B) Same as in part A except cells are overexpressing $LptB_2FGC$-G21*p*BPA.

Our lab had also developed a dansyl-polymyxin probe (dansyl-PMBN), that specifically binds LPS, for studying LPS localization in the cell.[16] Wild-type *E. coli* cells show even membrane staining when treated with this probe. We hypothesized that if PMB treatment were blocking LPS transport to the cell surface, there should be a change in the observed LPS localization. We treated *A. baumannii* cells with increasing concentrations of PMB and stained with the dansyl-PMB probe (all experiments performed by E. Moison). *A. baumannii* was used for these experiments because it was less sensitive to the probe, though the results are similar in *E. coli*. Imaging by epifluorescent microscopy revealed normal membrane staining at sub inhibitory concentrations of PMB (Figure 2.11). However, at higher concentrations, the membrane staining decreased and LPS appeared localized to puncta. The exact location of these puncta cannot be determined due to diffraction-limited resolution, but it is clear that the LPS is mislocalized. The phenotype is reminiscent of what is observed in cells where MsbA is inactivated.[16] In these cells, LPS builds up at the inner leaflet of the inner membrane since it cannot be flipped. If LPS were building up at the outer leaflet of the inner membrane, as our hypothesis would predict, we might expect to see LPS localization similar to that in the MsbA inactivated strain. While not conclusive on their own, these imaging experiments are consistent with our hypothesis and the *in vivo* data we have observed.

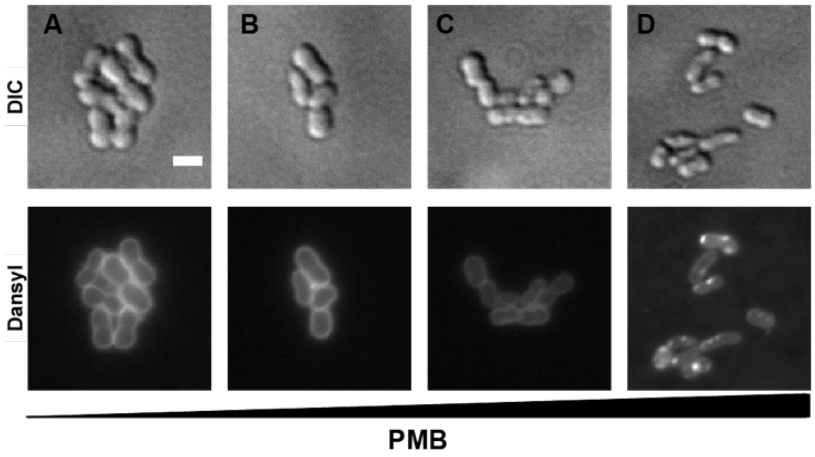

Figure 2.11 Treatment with PMB induces *A. baumannii* cells to mislocalize LPS. Cultures of AB19606 were treated with (A) 0, (B) 0.128x, (C) 1.28x, or (D) 12.8x MIC PMB and grown for 2 hours before staining with the LPS-specific probe dansyl-PMBN (12 μM). Cells were imaged by epifluorescence microscopy. Scale bars are 2 μm. DIC: Differential interference contrast.

2.4.3 Discussion

Early results from our lab led us to hypothesize that PMB might be interfering with LPS transport to the cell surface as part of its mechanism of action. We have used biochemical and imaging tools developed by the lab to explore this hypothesis. Using crosslinking experiments, both *in vitro* and *in vivo*, we have shown that PMB treatment inhibits LPS transport at a specific step and that inhibition is at concentrations relevant to the MIC. Imaging studies show LPS is mislocalized upon treatment with PMB in a manner that is phenotypically similar to and MsbA knock out, which causes LPS build up at the inner membrane. Taken together, these experiments have contributed to our current understanding of how PMB kills cells and led to the development of a new model of this mechanism, discussed further at the end of this chapter.

2.5 Recognition sites for LPS extraction

(Bertani, *et al*., A cluster of residues in the lipopolysaccharide exporter that selects substrate variants for transport to the outer membrane. (2018) *Mol Micro*)[19]

Our collaborators in the Ruiz lab (Ohio State University) identified positions in LptG important for LPS recognition and transport. The K34 residue, in particular, interacts with the negatively charged phosphates of LPS electrostatically, and mutations in this residue result in transport defects. Specifically, a K34D mutation that changes the charge profile of the residue from positive to negative results in poor growth. The negative charge would now be expected to repel the negatively charged phosphates of the LPS. This phenotype can be rescued by a mutation in BasSR, a two-component system regulating LPS modification. In these strains, phosphoethanolamine is added to the phosphates, thereby eliminating the charge conflict with the aspartic acid and restoring efficient transport. This residue, along with others in the same region appears to define an LPS binding site that can recognize different types of LPS.

The BasSR system is known to regulate the levels of phosphoethanolamine modification on LPS, and the mutation observed in the K34D strain constitutively activates the system. We wanted to verify that the LPS in these strains did contain a higher percentage of modification. We therefore optimized a method, using established protocols, to isolate LPS from wild type, K34D, and K34D with the BasSR suppressor strains. We then hydrolyzed the LPS to the lipid A core and analyzed the structure using MALDI mass spectrometry. Through our studies, we learned that the type of extraction method can affect the ratios of LPS present, as some methods (phenol chloroform extraction) seemed to extract modified LPS less efficiently. We settled on using a Bligh Dyer extraction method as it has been used by other labs to evaluate levels of LPS modification. Also, the medium in which the cells were grown had a substantial impact on the levels of modification. Cells grown in M63 minimal medium had far less modified LPS than those grown in LB, a rich medium. Because the genetics experiments were done with cells growing in

LB, we decided to use LB in our experiments for consistency. Analysis of the samples by MALDI showed that the LPS isolated from wild type cells had low levels of modifications, including phosphoethanolamine and aminoarabinose (Figure 2.12). The K34D stain without any suppressors also had fairly low levels of modifications, but a substantial amount of the LPS was heptacylated, whereas typical *E. coli* LPS is hexacylated. This extra acyl chain is the result of PagP activity in the outer membrane. In response to membrane stress, PagP cleaves an acyl chain from a phospholipid and attaches it to LPS. This phenotype, while unknown from the genetics experiments, agrees with the hypothesis that this strain is not transporting LPS efficiently and is thus experiencing membrane stress. Finally, the K34D strain with the BasSR suppressor showed high levels of modified LPS, as expected, and much reduced levels of heptacylation. All of these data were in strong agreement with results from genetics and biochemical experiments and supported the proposed hypothesis.

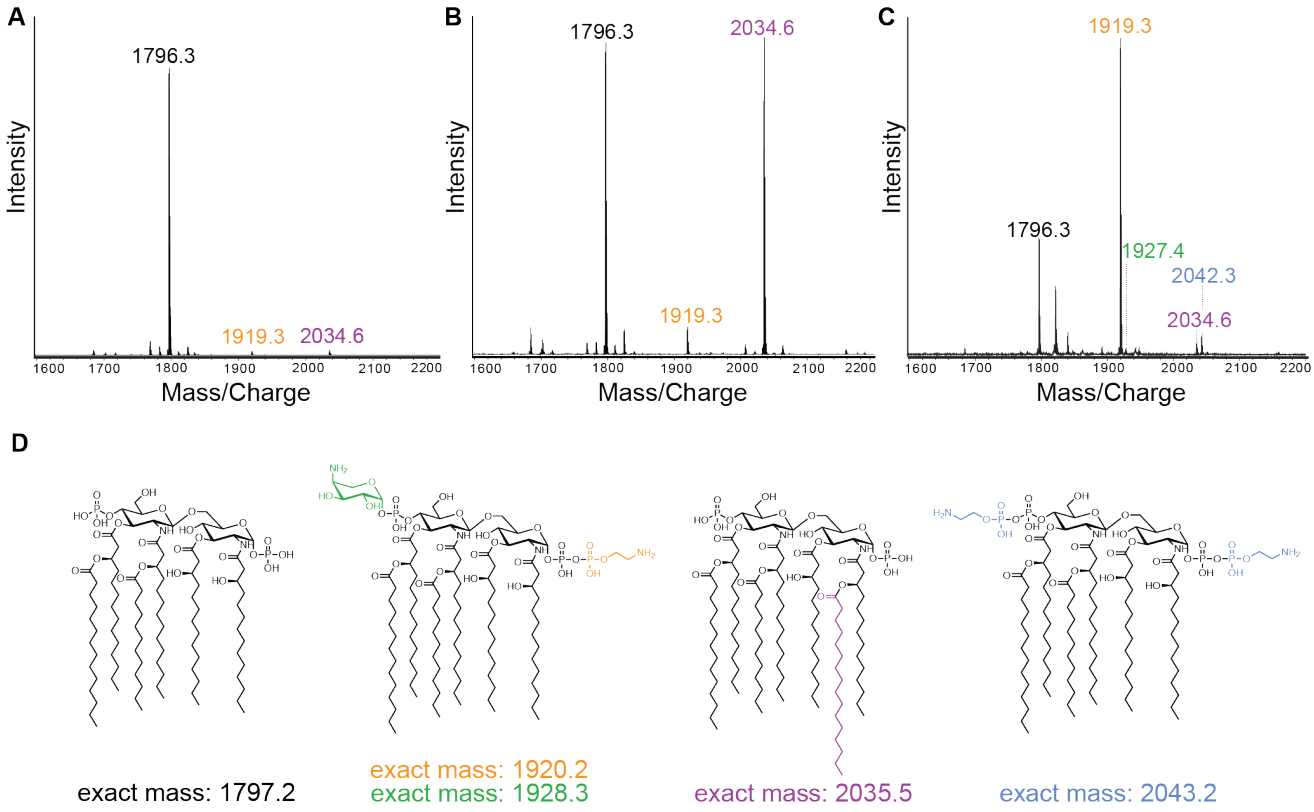

Figure 2.12 Analysis of lipid A structures by MALDI. Lipid A was isolated from three strains of NR 754 *E. coli* (A) Wild type. (B) LptG-K34D. (C) LptG-K34D, BasSL201Q using the Bligh Dyer extraction method. Samples were analyzed using MALDI mass spectrometry with a focus on structures with modifications to the phosphates.

2.6 Model of PMB's mechanism of action

Since this investigation into PMB's inhibition of LPS transport began, our understanding of the mechanics of LPS transport, especially at the inner membrane, has improved tremendously. A new crystal structure for the inner membrane complex combined with biochemical experiments has led our lab to a more specific mechanism of LPS entry into the complex, subsequent extraction from the membrane, and how that is coupled to ATP hydrolysis. The recent structures of $LptB_2FGC$ revealed that the transmembrane helix of LptC is positioned at the interface between helices of LptF and LptG, creating a gate for LPS entry into the cavity of LptFG.[18,20] LPS diffuses into the cavity at which point ATP hydrolysis by LptB causes the cavity to constrict,

extracting LPS from the membrane and transferring it into the β-jellyroll structure of LptC. If ATP hydrolysis is blocked by constructing an E163Q mutant in LptB, LPS cannot be extracted and builds-up at the M19 and G21 residues of the LptC transmembrane helix. This result implies that LPS diffuses passively into LptFG and distributes evenly between the residues pointing into and outside of the cavity. Recent work from the Ruiz lab (Ohio State University) also showed that residues at the gate helix of LptG are important for LPS recognition and subsequent efficient transport. The residues make electrostatic connections with moieties on LPS, and these interactions are important for entry into the cavity of LptFG. When blocked, LPS transport becomes less efficient and the cells are quite sick. This model of LPS transport suggests that LPS structure can play a role in its ability to be transported and shows that interference with ATP hydrolysis can block access of LPS to residues in LptC present in the β-jelly roll structure (T47). This indicates that entry into the machine (crosslinking at M19 and G21) is a separate step from extraction from the membrane (crosslinking to T47).

This greater understanding of LPS transport and our experiments exploring PMB's interaction with the transport components as well as other antibiotics have led us to develop a model of one way in which PMB treatment kills cells (Figure 2.13). Initially, PMB binds LPS on the surface of cells, permeablizing the membrane and promoting its own uptake into the periplasm. Once in the periplasm, rather than solely acting as an unspecific detergent at the cytoplasmic membrane, we propose that PMB is binding LPS that is sitting at the outer leaflet of the inner membrane, awaiting transport to the cell surface. To reach the cell surface, this complex would need to diffuse into LptFG, a process that requires recognition by residues in the helices of LptG and LptF. We believe that PMB interferes with proper recognition causing LPS to stall at the entry to LptFG.

PMB treatment eliminates crosslinking to the β-jellyroll portion of LptC (T47) showing that the PMB x LPS complex cannot be extracted from the membrane. Furthermore, treatment also causes a selective build-up at position M19 that points into the membrane, but not at G21 which points into the lumen of LptFG. If the PMB-LPS complex were simply stalled independently of the Lpt components or not able to be extracted from the membrane, we would expect to see build-up at both positions as we do when ATP hydrolysis is blocked. The fact that LPS only builds up in the membrane suggests that it is stalled specifically at the step for entry into the machine.

This mechanism is also consistent with the types of resistance PMB treatment generates. Most commonly, the cells add modifications to LPS that eliminate the negative charge on the phosphates. If PMB were preventing entry into the machine by interfering with LPS recognition, reestablishing the contacts by altering the LPS would be expected to restore transport. This is consistent with the work showing that mutations that change the charge of the recognition sites in LptG are fixed by altering the structure of LPS to restore those interactions. Additionally, LPS loss in *A. baumannii* would be expected to rescue cells since there is no flux of LPS through the transport pathway and thus no build-up at the inner membrane. The conditional essentiality of certain steps in LPS biosynthesis and transport in *A. baumannii* also suggests that if a drug were going to target LPS transport, it would have to target the intermediate steps to be lethal. Removal of LptD is tolerated in *A. baumannii* which implies that PMB can't simply be binding LPS on the outer membrane and affecting transport from there. The effect we observe seems to require a direct interaction with the inner membrane Lpt components.

PMB's strong interactions with drugs that target LPS flux through the Lpt pathway also provide supporting evidence that PMB interferes with transport to the cell surface. Significantly reducing

flux into the pathway with an LpxC inhibitor that blocks LPS synthesis rescues cells from killing by PMB. And treatment with novobiocin, which increases flux in the pathway, severely sensitizes the cells to the effects of PMB.[21] While the interaction with novobiocin is not yet fully understood, if PMB were acting solely as a detergent, there would not be an obvious reason for these types of drug interactions.

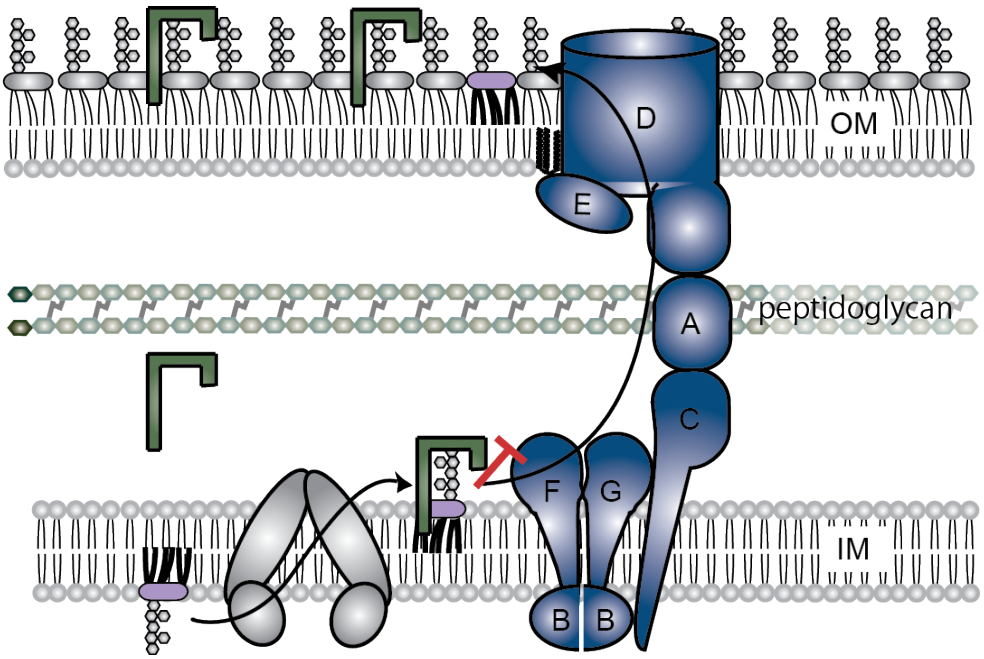

Figure 2.13 PMB prevents PS from entering LptFG at the inner membrane. PMB (green bracket) binds LPS at the cell surface promoting its uptake into the periplasm. There it binds LPS at the inner membrane and blocks entry into LptFG.

2.7 Discussion and future directions

Our model shows PMB interacting with a specific step of LPS transport to the cell surface; however, we do not yet have direct evidence of a specific interaction between PMB and $LptB_2FGC$. Efforts are currently underway to show such an interaction and investigate its location to better understand why PMB prevents entry into LptFG. Even though our current

understanding of how PMB kills cells is still incomplete, we have helped validate the Lpt pathway as a reasonable aim for antibiotic development. Considerable effort has been put into screening for small molecule inhibitors of Lpt components and the confirmation that a natural product does indeed target this pathway provides renewed confidence in this approach.

2.8 Materials and methods

2.8.1 Reagents

All chemical reagents were of analytical grade and used without further purification. Wang resin preloaded with Fmoc-Thr(tBu), chlorotrityl chloride resin, and *p*BPA were purchased from Bachem. Protected amino acids were purchased from Bachem, Santa Cruz Biotechnology, Novabiochem and AAPPTec. L-photo-leucine was purchased from ThermoFisher. PMB sulfate was purchased from Fluka. PMBN, PF-5081090, and 6-heptynoic acid were purchased from Sigma Aldrich. 6-methylheptanoic acid was purchased from Alfa Aesor.

For the proteoliposomes, *E coli* Polar Lipid Extract (100600P) was purchased from Avanti Polar Lipids Inc and Rough LPS from *E. coli* serotype EH100 (Ra mutant) was purchased from Sigma.

All cells were grown in LB Miller medium, purchased from BD at 37°C unless otherwise indicated.

For the western blots, Precision Plus Protein™ All Blue Prestained Protein Standards were purchased from Biorad. LPS was detected using an α-LPS core mouse monoclonal antibody purchased from Hycult Biotechnology. LptA and LptC were detected using α-LptC/A rabbit monoclonal antibodies reported previously.[22,23] All secondary antibodies were purchased from GE Amersham. Western blot bands were visualized using ECL™ Prime Western Blotting Detection Reagent from Amersham and imaged using an Azure c400 Imager (Azure Biosystems).

2.8.2 Fmoc protection of L-photo-leucine

L-photo-leucine (0.35 mmol) was dissolved in 2mL 10% (w/v) Na_2CO_3. Fmoc-OSu (0.385 mmol) was dissolved in 2 mL acetonitrile and then added to the flask with the L-photo-leucine. The reaction was stirred at room temperature overnight. The reaction was quenched by the addition of 1 N HCl (final pH ~ 3.0) and the mixture was extracted with EtOAc (3x). The organic layers were combined and dried with Na_2SO_4. The crude product was concentrated by rotary evaporation and purified via a silca gel column (95:5, DCM/MeOH). The product containing fractions were combined and concentrated to yield a yellow oil. The oil was dissolved in EtOAc and hexanes were added until the product crystallized, yielding a white powder (105 mg, 82%). Identity of the product was confirmed by mass spectrometry.

2.8.3 Synthesis of PMB probe

*2.8.3.1 Synthesis of PMB*1 and PMB*3 (without Click residue)*

Synthesis of the protected linear peptides was performed manually using Fmoc sold phase peptide chemistry and a Boc/Cbz protecting scheme. The process was started with Wang resin preloaded with the first amino acid, Fmoc-Thr(tBu)-OH (loading 0.58 mmol/g, 2 mmol scale). For each amino acid, three steps were carried out: Fmoc deprotection, amino acid coupling, and free amino coupling. Between each step, the resin was washed thoroughly with dimethylformamide (DMF). For Fmoc deprotection, the resin was incubated with a solution of 20% (v/v) piperidine in DMF (10 mL/g resin) for 30 minutes at room temperature. For the coupling reaction, a solution containing 2 molar equivalents of the Fmoc protected amino acid, 2 equivalents of 1-[Bis(dimethylamino)methylene]-1H-1,2,3-triazolo[4,5-b] pyridinium 3-oxid hexafluorophosphate (HATU), and 4 equivalents of diisopropylethylamine (DIPEA) in DMF (5 mL/g resin) was added to the resin. The mixture was incubated for 30 to 60 minutes at room temperature until

a Kaiser test revealed complete coupling. Finally, any remaining free amines were capped by the addition of 50 equivalents of acetic anhydride and 50 equivalents of pyridine in DMF (5 mL/g resin). Resin was incubated with this solution for 30 minutes at room temperature. Fmoc-L-photo-leucine was used instead of a Dab residue at the indicated position (replacing Dab ^{1} or Dab ^{3}). After the linear peptide was complete, 6-methylheptanoic acid was added using the same procedure.

The peptide was cleaved from the resin by addition of 95% (v/v) trifluoroacteric acid (TFA) on ice for 2 hours and the resin was then removed by filtration. The peptide was precipitated by dropwise addition to ice cold diethyl ether. Unfortunately, the peptides did not precipitate nicely, most likely due to the fatty acid, creating a gel-like substrate. That solution was centrifuged to remove as much of the ether as possible and then dried yielding an oily substance. To cyclize, the peptide was dissolved in DMF containing 4 equivalents of benzotriazol-1-yl-oxytripyrrolidinophosphonium hexafluorophosphate (PyBOP), 4 equivalents of hydroxybenzotriazole (HOBt) and 8 equivalents of DIPEA. Cyclization progress was monitored by mass spectrometry until complete, which took about 4 hours at room temperature. The reaction was concentrated by rotary evaporation and then washed with water to remove some of the excess PyBOP. The crude peptide product was then deprotected using excess (100 equivalents) of thioanisole in TFA for 6 hours. The reaction was concentrated to remove TFA via rotary evaporation.

Attempts were made to purify the peptide using HPLC, but the yield was extremely low. We believe this was due to the general stickiness of the peptide and its lack of a residue that could be readily detected. As a result, there was no defined peak coming off the HPLC. The peptide

was purified manually using a Strata C18-E solid phase extraction column (Phenomenex). The peptide eluted in a 95:5 (H_2O:ACN + 0.1% formic acid) mixture and purity was confirmed by mass spectrometry.

The formic acid salts of PMB are much less soluble in water than the purchased sulfate salts. In order to make the sulfate salt, the compound was dissolved in water and 1 M sodium hydroxide was added dropwise until the compound crashed out of solution as the free base. The solids were collected via centrifugation and then suspended in water. Concentrated sulfuric acid was added dropwise until the solids went back into solution. This sulfate salt could be dissolved in water to at least 50 mg/mL.

*2.8.3.2 Synthesis of PMB*3 with Click residue*[17]

For this synthesis, chorotrityl chloride resin was used, but it could not be purchased preloaded, so the first amino acid had to be attached before solid phase peptide synthesis could begin. Resin (1 g) was allowed to swell in dry DCM (10 mL). Fmoc-Thr(tBu) (1 mmol) was dissolved in dry DCM (4 mL) and added to the resin with DIPEA (5 equivalents). The resin was rocked for 1 hour at room temperature and then capped by the addition of MeOH (1 mL) for 15 minutes. The resin was thoroughly washed with DCM and then dried. Resin loading was measured by deprotecting a test amount of the resin (with 20% piperidine) and then measuring the A_{301} of the solution. The resin loading was determined to be 0.7 mmol/g, which was in agreement with the mass increase of the resin.

This synthesis utilized the same solid phase synthesis linking of amino acids but was based on a Boc/Alloc protecting strategy. Each amino acid was added through the same three steps as above: deprotection, coupling and capping. In this synthesis, the fatty acid was not added to the resin prior to cleavage. Before the linear peptide was cleaved from the resin, the Alloc protecting

group was removed from Dab[4]. To resin swelled in dry DCM (6 mL), $Pd(PPh_3)_4$ (1.1 equivalents) dissolved in dry DCM (2 mL) was added. A second aliquot of dry DCM (2 mL) containing Bu_3SnH (12 equivalents) and *p*-nitrophenol (2 equivalents) was added to the resin. The reaction was purged with N_2 and stirred for 1 hour. The resin was rinsed with dry DCM and a second aliquot of each reagent was added and the reaction was stirred for another hour. The solvent was removed, and the resin was rinsed with DCM + 0.5% sodium dithiodiethylcarbamate until there was no longer a yellow color (~40 mL). The resin was then rinsed with DMF, followed by DCM and dried completely. Successful removal of the Alloc was confirmed by the presence of a free amino as shown by a Kaiser test.

The peptide was cleaved from the resin by the addition of 0.8% (v/v) TFA in DCM for 90 minutes at room temperature. The reaction was quenched by the addition of DIPEA and the peptide was precipitated from DMF with water. The solid peptide was collected by centrifugation and lyophilized. To cyclize, the peptide was dissolved in DMF containing PyBOP (2 equivalents), HOBt (2 equivalents) and DIPEA (4 equivalents). Cyclization progress was monitored by mass spectrometry until complete which took about 2 hours at room temperature. The N-terminal Fmoc was removed by addition of 20% piperidine for 10 minutes. The peptide was precipitated from DMF by the addition of water, collected and lyophilized. 6-heptynoic acid (1.1 equivalents) was coupled to the peptide (1 equivalent) using the same reagents as the on resin coupling (HATU (3 equivalents), DIPEA (10 equivalents). The reaction was stirred for 1 hour and the DMF was removed by rotary evaporation. The crude peptide was dissolved in 5 mL of a mixture of TFA, triisopropylsilane (TIS) and water (5:2.5:2.5) and stirred for 40 minutes at 0°C to deprotect. The final product was precipitated by the addition of diethyl ether and was collected by

centrifugation. Purification was the same as for the other peptides though it did not work efficiently.

2.8.4 MIC measurements

MIC values were measured using the broth dilution method. Serial two-fold dilutions of the compound to be tested were prepared in LB medium and aliquoted into a 96-well plate. Overnight cultures of the test strains were diluted 1:100 into fresh LB and grown to early exponential phase (OD_{600} ~ 0.3). Cells were then added to each well at a final density of ~10^4 cells/mL. Plates were incubated at 37°C for 20 to 24 hours. OD_{600} was measured using a Tecan Sunrise™ plate reader. MIC was determined to be the lowest concentration at which there was no growth in the well.

Table 2.2 MIC values for *in vivo* photocrosslinking and imaging strains.

MIC	*A. baumannii* 19606	*E. coli* MC4100	*E. coli* BL21(λDE3)
PMBN	>40 μM	>40 μM	>40 μM
PMB	0.312 μM	0.29 μM	4.5 μM
Dansyl-PMBN	>40 μM	ND	ND

2.8.5 Silver staining and western blotting of LPS crosslinked to PMB*3

2.8.5.1 Silver stain protocol

Each sample (15 μL) consisted of varying ratios of LPS and PMB*3 dissolved in water. The amount of LPS (1.5 μg) was consistent across the samples, so the amount of PMB*3 varied depending on the required molar ratio. The sample was then irradiated with UV (365 nm) for 15 minutes and then added to 15 μL 2x SDS-PAGE loading buffer. Samples (10 μL each) were loaded

on a 20% SDS-PAGE gel with a 4% stacking gel and run until the 10 kDa ladder band was near the bottom of the gel (150 V for 2.5 hours).

For silver staining, the gel was incubated overnight in 200 mL wash buffer (40%ethanol/5% acetic acid). Periodic acid (0.7%) was added and the mixture was allowed to shake for 5 minutes. The gel was rinsed with 200 mL of water 3x over a period of 2 hours. The gel was soaked in 11 5mL of silver stain solution (0.86% silver nitrate, 0.13 M ammonium hydroxide, 24 mM sodium hydroxide) for 10 minutes. The gel was again washed with 200 mL of water 3x over a period of 45 minutes. Finally, the gel was soaked in 200 mL of developer solution (0.26 mM citric acid, 80 µL 37% formaldehyde, 37°C) until bands were visible. The development was stopped by soaking the gel in 200 mL 0.33% acetic acid for 1 hour.

2.8.5.2 Western blotting protocol

Sample prep was the same as above except only 5 µL of each sample was loaded onto the gel as to not oversaturate during imaging. After electrophoresis, the samples were transferred to a PVFG membrane at 10 V for 1 hour. The membrane was blocked in 1x casein in TBS-T for 1 hour. The membrane was treated with α-LPS primary antibody (1:20000) for 1 hour and then washed 3x15 minutes. Secondary antibody (1:10000) was added for 1 hour, followed by 3 final 15-minute washes. Bands were visualized using ECL Prime detection reagent and Biomax film.

2.8.6 Overexpression and purification of LptB$_2$FGC [22]

For overexpression of the LptB$_2$FGC complex, KRX cells containing pCDFDuetHis$_6$LptB-LptFG and pET22/42LptC were used. For the T47 crosslinking strain, a pET22/42LptC-T47Am plasmid was used instead and the cells also harbored pSup-BpaRS-6TRN for incorporation of the unnatural amino acid. Overnight cultures were diluted 100-fold intro fresh LB medium

supplemented with 50 µg/mL carbenicillin, 50 µg/mL spectinomycin, 30 µg/mL chloramphenicol (if T47Am) and 0.5 mM *p*BPA (in 1 M NaOH) (if T47Am) and grown at 37°C to OD 1.0. Expression was induced with 0.02% L-rhamnose (w/v) and cells were grown for an additional 3 hours. Cells were harvested by centrifugation (5200g, 15 min, 4°C) and resuspended in 50 mM Tris-HCl (pH 7.4) supplemented with 1 mM phenylmethylsulfonyl fluoride (PMSF), 100 µg/mL lysozyme and 100 µg/mL DNase I. Cells were lysed by 3 passages through an Emusiflex C3 homogenizer (Avestin) at 15,000 psi. Cell debris and unbroken cells were removed by centrifugation (5000g, 10 min, 4°C) before membranes were pelleted by ultracentrifugation (100,000g, 1 hour, 4°C, Beckman 45Ti rotor). Membranes were resuspended in solublization buffer (20 mM Tris-HCl pH 7.4, 5 mM $MgCl_2$, 300 mM NaCl, 10% (v/v) glycerol). The suspension was homogenized using an IKA T18 basic UltraTurrax and 1% n-dodecyl β-D-maltoside (w/v) (DDM) and 2 mM adenosine 3'triphosphate (ATP) were added before being rocked for 1 hour at 4°C. Debris was removed by centrifugation (100000g, 30 min, 4°C) and the supernatant was washed over TALON metal affinity resin 3x. The resin was washed with 20 cv of wash buffer (20 mM Tris-HCl pH 7.4, 300 mM NaCl, 0.05% DDM, 10% (v/v) glycerol and 5 mM imidazole) and the protein eluted with 3 cv elution buffer (20 mM Tris-HCL pH 7.5, 300 mM NaCl, 0.5% DDM, 10% (v/v) glycerol, 25 mM imidazole). The eluate was concentrated using an Amicon 100-kDa molecular weight cutoff centrifugation filter (EMD Millipore) and then applied to a Superdex 200 Increase 10/300 gel filtration column (GE Healthcare) equilibrated in 20 mM Tris-HCl pH 7.4, 300 mM NaCl, 0.05% DDM and 10% (v/v) glycerol. Peak fractions were pooled and concentrated to ~10 mg/mL. Complexes were analyzed by SDS-PAGE to assess purity and then flash frozen at -80°C.

2.8.7 Overexpression and purification of LptA [6]

LptA was overexpressed in the periplasm and purified using spheroplasts from Bl21(λDE3) cells harboring pET22b-LptA-I36Am-His_6 and pSup-BpaRS-6TRN. Overnight cultures were diluted 100-fold in LB supplemented with 50 µg/mL carbenicillin, 30 µg/mL chloramphenicol and 0.8 mM *p*BPA and grown at 37°C. When the cultures reached OD_{600} ~ 0.5, expression was induced with the addition of 50 µM isopropyl-β-D-1-thiogalactopyranoside (IPTG) for 2 hours at 37°C. Cells were harvested by centrifugation (5200g, 20 min, 4°C) and converted to spheroplasts. To do this, cells were resuspended in 10 mL sucrose buffer (50 mM Tris-HCl pH 8.0, 500 mM sucrose) supplemented with 300 µg/mL lysozyme and 100 µg/mL DNase I and kept on ice for 2 minutes. 10 mL of buffer 2 (50 mM Tris-HCl pH 8.0, 3 mM EDTA) was added and mixed quickly and the tubes were left on ice for 20 minutes. Cell debris was removed by centrifugation (6000g, 15 min 4°C) and then the samples were ultracentrifuged (100000g, 30 min, 4°C). The supernatant was passed over equilibrated Ni-NTA resin 3x and then the resin was washed with column buffer (20 mM Tris-HCl pH 8.0, 300 mM NaCl, 20 mM imidazole). The protein was eluted with elution buffer (20 mM Tris-HCl pH 8.0, 150 mM NaCl, 200 mM imidazole) and concentrated using an Amicon 10kDa molecular weight cutoff centrifugation filter. Glycerol was added to a final concentration of 10% (v/v) and purity was assessed by SDS-PAGE. Aliquots (~2 mg/mL) were flash frozen and stored at -80°C.

2.8.8 Preparation of $LptB_2FGC$ proteoliposomes [6]

Proteoliposomes were prepared using the detergent dilution method as previously reported.[24,25] Stocks of polar lipids and LPS were prepared prior to use in the liposomes. For the polar lipids, *E. coli* polar lipid extract was suspended in water at a concentration of 20 mg/mL and sonicated in ice water until the suspension was relatively clear. For LPS, Ra LPS from *E. coli* was

suspended in water at 2 mg/mL and also sonicated in ice water until dissolved. Stocks were flash frozen in aliquots and stored at -80°C. Immediately before use, aliquots were thawed on ice and briefly sonicated to fully homogenize the solution. To prepare the proteolipsomes containing $LptB_2FGC$, the following mixture was prepared: TBS buffer (20 mM Tris-HCl pH 8.0, 150 mM NaCl), 7.5 mg/mL polar lipid stock, 0.5 mg/mL LPS, 0.25% DDM, and 0.86 µM purified inner membrane complex. The order of assembly matters greatly. First, the polar lipids, with the TBS buffer, were mixed with DDM to destabilize the liposososmes and then, LPS was added to the mixture and incubated on ice for 10 minutes. The protein complex was then added, and the mixture was kept on ice for an additional 20 minutes. The solution was transferred to an ultracentrifuge tube (100 µL mixture/tube) and diluted 100-fold with cold TBS buffer. After another 30-minute incubation on ice, the proteoliposomes were pelleted by ultracentrifugation (300000g, 2 hours, 4°C, Beckman 70.1Ti rotor). The supernatant was carefully removed, and the pellet resuspended in 200 µL cold TBS. After resuspension, the mixture was again diluted 100-fold in cold TBS and the centrifugation step was repeated. This time the proteoliposomes were resuspended in 250 µL cold buffer (20 mM Tris-HCL pH 8.0, 150 mM NaCl, 10% (v/v) glycerol) and sonicated on ice until the solution was homogenous. The proteoliposomes were aliquoted and flash frozen for storage at -80°C.

2.8.9 *In vitro* reconstitution of LPS transport to LptC

The reconstitution of LPS transport to LptC was performed using established protocols that were previously reported. [6] Each assay was done in a buffer containing 50 mM Tris-HCl pH 8.0, 500 mM NaCl and 10% (v/v) glycerol (final concentrations in assay). Each reaction consisted of 60% (by volume) proteoliposomes containing $LptB_2FGC$-T47*p*BPA in the above buffer. The

transport reaction was initiated by the addition of ATP/$MgCl_2$ (5 mM ATP, 2 mM $MgCl_2$) and transfer of the tube to 30°C. Only $MgCl_2$ was added to control reactions. At each time point, a 30 µL aliquot of the reaction was removed and added to a 384-well plate. The plate was then irradiated with UV light (365 nm) on ice to for minutes using a B-100AP lamp (UVP). The sample (25 µL) was then transferred to a tube and 220 µL of cold buffer (20 mM Tris-HCl pH 8.0, 150 mM NaCl, 0.2% DDM) was added. The proteins were then precipitated by the addition of 250 µL 20% (v/v) trichloroacetic acid (TCA) and incubation on ice. After precipitation, the proteins were pelleted (20000g, 15 min, 4°C) and washed with cold acetone. Following a second spin, the pellets were resuspended in 30 µL 2x SDS-PAGE sample loading buffer with 5% B-mercaptoethanol (BME). Samples were briefly sonicated and then boiled for 10 minutes before analysis by SDS-PAGE and immunoblotting. For PMB or PMBN treatment, the process was the same; however, the appropriate concentration of drug was added after the reactions were assembled, but before addition of ATP. The reactions were incubated with the drug for 15 minutes and then ATP/$MgCl_2$ was added to initiate transport. All subsequent steps were the same.

2.8.10 *In vitro* reconstitution of LPS transport to LptA

The reconstitution of LPS release from LptC to LptA was similar to the reconstitution described above. Assay preparation was the same; however, LptA-I36*p*BPA-His_6 was added to the reaction mixture at a final concentration of 2 µM before transport initiation. At specified time points, 25 µL aliquots were removed and irradiated. The samples were transferred to tubes and 225 µL of cold buffer (20 mM Tris-HCl pH 8.0, 150 mM NaCl, 0.2% DDM) was added. Proteins were

precipitated and prepared for immunoblotting in the same way as above. Treatment with PMB or PMBN also followed the same protocol was with LptC crosslinking.

2.8.11 *In vivo* photocrosslinking with overexpression [7]

Overnight cultures of BL21(DE3) cells harboring pSup-BpaRS-6TRN, pCDFLptBFG, and pBAD-HisA-His-LptC-T47Am were diluted 100-fold into LB (5 mL) supplemented with 30 μg/mL chloramphenicol, 50 μg/mL spectinomycin, 50 μg/mL carbenicillin and 0.8 mM *p*BPA and grown at 37°C. Once the cells reached OD_{600} ~ 1.0, 0.02% (w/v) L-arabinose and 10 μM IPTG were added to induce protein expression. Thirty minutes after induction, PMB or PMBN were added if necessary, and cells were grown for an additional 90 minutes (2 hours total after induction). 2 mL of each culture was transferred to a 6-well plate and irradiated with UV light (365 nm) for 5 minutes. Cells were then harvested by centrifugation (4000g, 5 min) and pellets were stored at -80°C. For each sample, 2 mL of culture was also centrifuged and stored without irradiation as no-UV controls. Final OD_{600} measurements for each sample were also taken at this time, so that samples could be normalized to cell density when loaded onto a gel.

To prepare samples for analysis, cell pellets were thawed and resuspended in 2 mL lysis buffer (20 mM Tris-HCl pH 8.0, 300 mM NaCl, 20 mM imidazole, 5 mM $MgCl_2$, 1 mM phenylmethylsulfonyl fluoride, 50 μg/mL DNase I, 100 μg/mL lysozyme) and lysed with 2 freeze/thaw cycles. 1% (w/v) Anzergent 3-14 was added and each sample was incubated on ice for 30 minutes before insoluble cell debris was removed by centrifugation (15000g, 15 min, 4°C). The soluble lysate was then incubated with Ni-NTA resin, pre-equilibrated with column buffer (20 mM Tris-HCl pH 8.0, 300 mM NaCl, 20 mM imidazole, 0.02% Anzergent 3-14), for 45 minutes. The resin was then washed 3x with 20 cv column buffer and eluted with 900uL elution buffer (20

mM Tris-HCl pH 8.0, 150 mM NaCl, 200 mM imidazole, 0.02% Anzergent 3-14). Proteins were precipitated by the addition of TCA (10% final concentration) and incubation on ice. The pellets were collected by centrifugation (20000g, 15 min, 4°C) and resuspended in 25 µL of 1 M Tris-HCl pH 8.0 and 25 µL 2x SDS-PAGE sample loading buffer with 5% BME. Samples were stored at -20°C until analysis by immunoblotting.

2.8.12 *In vivo* photocrosslinking with leaky expression [7]

For the leaky expression experiments, overnight cultures of MC4100 harboring pSup-BpaRS-6TRN and pET23/42-His-LptC-T47Am were diluted 100-fold in LB (50 mL) supplemented with 30 µg/mL chloramphenicol, 50 µg/mL carbenicillin and 0.8 mM *p*BPA and grown at 37°C. When cultures reached OD_{600} ~ 0.6, PMB or PMBN was added, as appropriate, and cells were grown for an additional 90 minutes. 23 mL of each culture were transferred to a 1-well plate and irradiated with UV light (365 nm) for 5 minutes. Cells were then harvested by centrifugation (4000g, 5 min). 23 mL of culture that was not irradiated was also collected as no-UV controls. Final OD_{600} measurements for each sample were also taken at this time, so that samples could be normalized to cell density when loaded onto a gel. All pellets were frozen at -80°C.

For analysis, pellets were resuspended in 4.5 mL lysis buffer (20 mM Tris-HCl pH 8.0, 300 mM NaCl, 20 mM imidazole, 5 mM $MgCl_2$, 1 mM PMSF, 50 µg/mL DNase I, 100 µg/mL lysozyme, 1% Anzergent 3-14) and incubated on ice for 10 minutes before disruption by sonication (1 min, 27%). Cell debris was removed by centrifugation (15000g, 15 min, 4°C) and then samples were prepped following the same protocol as above.

2.8.13 SDS-PAGE and immunoblotting for *in vitro* and *in vivo* experiments

For immunoblotting, samples in SDS-PAGE loading buffer were boiled for 5 minutes and then sonicated before loading onto a Tris-HCl 4-20% polyacrylamide gradient gel. For *in vivo* experiments, sample loading was normalized to the final OD_{600} of the original culture. A Tris-glycine running buffer was used for all experiments and gels were run for 48 minutes at 200 V. Proteins were then transferred onto Immun-Blot PVDF membrane (Biorad) for 20 minutes at 1.3 A using a Thermo Scientific Pierce Power Blotter. Blots were blocked for 1 hour using 1x casein in TBS-T. Blots were incubated with primary antibodies for LPS (1:20000 dilution), LptC (1:10000 dilution), or LptA (1:10000 dilution) for 1 hour. After 3x 15 minute washes with TBS-T, blots were incubated with either a sheep α-mouse horseradish peroxidase (HRP) secondary antibody (LPS) or a donkey α-rabbit HRP secondary (Lpt proteins) for 1 hour. The blot was washed again with 3x15 minute washes with TBS-T before imaging. Bands were visualized using ECL Prime detection reagent and an Azur imager.

2.8.14 Imaging using dansyl-PMBN probe

Imaging was carried out as described by Eileen Moison. Microscopy was carried out on a Nikon Ti fluorescence microscope. The microscope was equipped with a Prior Proscan III linear-encoded motorized stage. Images were obtained using a 1.5 x tube lens and a Plan Apo 100 x 1.4NA objective with a polarizer, DIC H condenser and DIC prism in the light path. A Prior LumenPro fluorescence light source was used for fluorescence imaging. The microscope had excitation and attenuation wheels, which were used to set λ_{ex}= 405/15 nm and λ_{em}=535/50 nm (dansyl channel). MetaMorph image acquisition software controlling a Hamamatsu ORCA-R2 cooled CCD camera was used to acquire images. Images were processed in ImageJ by adjusting contrast identically for compared image sets.

A. baumannii ATCC 19606 was seeded at a density of 10^6 cells/ml from stationary phase cultures directly into LB containing 0, 0.04, 0.4, or 4 µM PMB (0, 0.128, 1.28 or 12.8×MIC, respectively) and were cultured for 2 hours at 37℃ (225 rpm). Cells were then treated with 12 µM Dansyl-PMBN at room temperature for 30 minutes before being immobilized on a 2% agarose/PBS pad for fluorescence microscopy (dansyl channel, λ_{ex} = 405/15 nm, λ_{em} = 535/50 nm).

2.8.15 LPS isolation and mass spectrometry analysis
(as reported in Bertani, *et al*. 2018) [19]

Cultures of each strain were grown in LB medium (200 mL) at 37°C. Cells were harvested when they reached OD_{600} ~ 1.0 and then washed with 25 mL phosphate buffered saline, pH 7.4. Lipid A was isolated from each sample using the Bligh-Dyer extraction method and acid hydrolysis.[26] Briefly, pellets were resuspended in 95 mL of a single-phase Bligh-Dyer mixture (chloroform:methanol:PBS (pH 7.4); 1.0:2.0:0.8 (v/v)). The mixture was allowed to sit at room temperature for 30 minutes for lysis. The sample was centrifuged at 2000g for 20 minutes and then the pellet was washed with an additional 25 mL of single phase Bligh-Dyer mixture. After centrifugation, the pellet was suspended in 2.4 mL hydrolysis buffer (50mL sodium acetate, pH 4.5, 1% SDS) and boiled for 30 minutes. Lipid A was harvested by extractions in two-phase Bligh-Dyer mixture (chloroform/methanol/water, 2:2:1.8 (v/v)). After extraction, the combined chloroform layers were dried by rotary evaporation and the sample was transferred using a 4:1 chloroform:methanol mixture. The dried sample was washed 1 x with acidified ethanol (2% HCl in EtOH) and 2 x with ethanol to ensure complete removal of SDS.[27] Samples were then lyophilized and stored at -20°C.

Samples were analyzed using a Bruker Ultraflextreme MALDI-TOF/TOF mass spectrometer. An ATT matrix was used, and it was prepared as follows. A saturated solution of 6-aza-2-thiothymine (ATT) in 50% acetonitrile and a saturated solution of tribasic ammonium citrate were combined (20:1, (v/v)). Lipid A samples were dissolved in chloroform:methanol (4:1). The matrix (0.5 µL) was deposited on the sample plate and allowed to dry and then an equal volume of sample was added on top of the matrix. Each spectrum represents the average of ~50 laser shots. Data were acquired in negative-ion mode with a reflectron analyzer and delayed extraction.

Table 2.3 Strains used in this chapter

Strain	Genotype	Source
A. baumannii ATCC 19606	Wild type	ATCC
E. coli KRX	[F', *tra*D36, Δ*omp*P, *pro*A+B+, *lac*Iq, Δ(*lac*Z)M15] Δ*omp*T, *end*A1, *rec*A1, *gyr*A96, *thi*-1, *hsd*R17 (rK–, mK+), e14– (McrA–), *rel*A1, *sup*E44, Δ(*lac-pro*AB), Δ(*rha*BAD)::T7 gene 1	Promega
E. coli BL21 (λDE3)	F– *omp*T *gal dcm hsd*SB(r_B-, m_B-) λ(DE3)	Novagen
E. coli MC4100	F– *araD139 Δ(argF-lac)169 λ⁻ rpsL150 relA1 rbsR22 flhD5301 Δ(fruK-yeiR)725(fruA25) Δ(fimB-fimE)632(::IS1) deoC1*	Novagen
E. coli NR754	MC4100 *ara*$^+$	Ruiz laboratory (Ohio State University)

Table 2.4 Plasmids used in this chapter

Plasmid	Source
pCDFLptBFG	Okuda *et al* (2012)[7]
pBAD-HisA-His-LptC-T47Am	Okuda *et al* (2012)[7]
pSup-BpaRS-6TRN	Ryu *et al* (2006)[28]
pCDFDuet-His6LptBFG	Sherman *et al* (2014)[22]
pET22/42-LptC-T47Am	Sherman *et al* (2018)[6]
pET22/42-LptC	Sherman *et al* (2014)[22]
pET22b-LptA-I36Am-His6	Okuda *et al* (2012)[7]
pBAD-HisA-His-LptC-M19Am	This work
pBAD-HisA-His-LptC-G21Am	This work

2.9 References

1 Falagas, M. E. & Kasiakou, S. K. Colistin: the revival of polymyxins for the management of multidrug-resistant gram-negative bacterial infections. *Clin Infect Dis* **40**, 1333-1341, doi:10.1086/429323 (2005).

2 Li, J. *et al.* Colistin: the re-emerging antibiotic for multidrug-resistant Gram-negative bacterial infections. *Lancet Infect Dis* **6**, 589-601, doi:10.1016/S1473-3099(06)70580-1 (2006).

3 Brogden, K. A. Antimicrobial peptides: pore formers or metabolic inhibitors in bacteria? *Nat Rev Microbiol* **3**, 238-250, doi:10.1038/nrmicro1098 (2005).

4 Zhang, G. *et al.* Cell-based screen for discovering lipopolysaccharide biogenesis inhibitors. *Proc Natl Acad Sci U S A* **115**, 6834-6839, doi:10.1073/pnas.1804670115 (2018).

5 Montgomery, J. I. *et al.* Pyridone methylsulfone hydroxamate LpxC inhibitors for the treatment of serious gram-negative infections. *J Med Chem* **55**, 1662-1670, doi:10.1021/jm2014875 (2012).

6 Sherman, D. J. *et al.* Lipopolysaccharide is transported to the cell surface by a membrane-to-membrane protein bridge. *Science* **359**, 798-801, doi:10.1126/science.aar1886 (2018).

7 Okuda, S., Freinkman, E. & Kahne, D. Cytoplasmic ATP hydrolysis powers transport of lipopolysaccharide across the periplasm in E. coli. *Science* **338**, 1214-1217, doi:10.1126/science.1228984 (2012).

8 Vaara, M. & Vaara, T. Sensitization of Gram-negative bacteria to antibiotics and complement by a nontoxic oligopeptide. *Nature* **303**, 526-528 (1983).

9 Vaara, M. & Viljanen, P. Binding of polymyxin B nonapeptide to gram-negative bacteria. *Antimicrob Agents Chemother* **27**, 548-554 (1985).

10 Ruiz, N., Gronenberg, L. S., Kahne, D. & Silhavy, T. J. Identification of two inner-membrane proteins required for the transport of lipopolysaccharide to the outer membrane of Escherichia coli. *Proc Natl Acad Sci U S A* **105**, 5537-5542, doi:10.1073/pnas.0801196105 (2008).

11 Sperandeo, P. *et al.* Functional analysis of the protein machinery required for transport of lipopolysaccharide to the outer membrane of Escherichia coli. *J Bacteriol* **190**, 4460-4469, doi:10.1128/JB.00270-08 (2008).

12 Richie, D. L. *et al.* Toxic Accumulation of LPS Pathway Intermediates Underlies the Requirement of LpxH for Growth of Acinetobacter baumannii ATCC 19606. *PLoS One* **11**, e0160918, doi:10.1371/journal.pone.0160918 (2016).

13 Wei, J. R. *et al.* LpxK Is Essential for Growth of Acinetobacter baumannii ATCC 19606: Relationship to Toxic Accumulation of Lipid A Pathway Intermediates. *mSphere* **2**, doi:10.1128/mSphere.00199-17 (2017).

14 Velkov, T., Thompson, P. E., Nation, R. L. & Li, J. Structure--activity relationships of polymyxin antibiotics. *J Med Chem* **53**, 1898-1916, doi:10.1021/jm900999h (2010).

15 Tsubery, H., Ofek, I., Cohen, S. & Fridkin, M. Structure-function studies of polymyxin B nonapeptide: implications to sensitization of gram-negative bacteria. *J Med Chem* **43**, 3085-3092 (2000).

16 Moison, E. *et al.* A Fluorescent Probe Distinguishes between Inhibition of Early and Late Steps of Lipopolysaccharide Biogenesis in Whole Cells. *ACS Chem Biol* **12**, 928-932, doi:10.1021/acschembio.7b00159 (2017).

17 van der Meijden, B. & Robinson, J. A. Synthesis of a polymyxin derivative for photolabeling studies in the gram-negative bacterium Escherichia coli. *J Pept Sci* **21**, 231-235, doi:10.1002/psc.2736 (2015).

18 Owens, T. W. *et al.* Structural basis of unidirectional export of lipopolysaccharide to the cell surface. *Nature* **567**, 550-553, doi:10.1038/s41586-019-1039-0 (2019).

19 Bertani, B. R., Taylor, R. J., Nagy, E., Kahne, D. & Ruiz, N. A cluster of residues in the lipopolysaccharide exporter that selects substrate variants for transport to the outer membrane. *Mol Microbiol* **109**, 541-554, doi:10.1111/mmi.14059 (2018).

20 Li, Y., Orlando, B. J. & Liao, M. Structural basis of lipopolysaccharide extraction by the LptB2FGC complex. *Nature* **567**, 486-490, doi:10.1038/s41586-019-1025-6 (2019).

21 Mandler, M. D. *et al.* Novobiocin Enhances Polymyxin Activity by Stimulating Lipopolysaccharide Transport. *J Am Chem Soc* **140**, 6749-6753, doi:10.1021/jacs.8b02283 (2018).

22 Sherman, D. J. *et al.* Decoupling catalytic activity from biological function of the ATPase that powers lipopolysaccharide transport. *Proc Natl Acad Sci U S A* **111**, 4982-4987, doi:10.1073/pnas.1323516111 (2014).

23 Chng, S. S., Gronenberg, L. S. & Kahne, D. Proteins required for lipopolysaccharide assembly in Escherichia coli form a transenvelope complex. *Biochemistry* **49**, 4565-4567, doi:10.1021/bi100493e (2010).

24 Brundage, L., Hendrick, J. P., Schiebel, E., Driessen, A. J. & Wickner, W. The purified E. coli integral membrane protein SecY/E is sufficient for reconstitution of SecA-dependent precursor protein translocation. *Cell* **62**, 649-657 (1990).

25 Yakushi, T., Masuda, K., Narita, S., Matsuyama, S. & Tokuda, H. A new ABC transporter mediating the detachment of lipid-modified proteins from membranes. *Nat Cell Biol* **2**, 212-218, doi:10.1038/35008635 (2000).

26 Henderson, J. C., O'Brien, J. P., Brodbelt, J. S. & Trent, M. S. Isolation and chemical characterization of lipid A from gram-negative bacteria. *J Vis Exp*, e50623, doi:10.3791/50623 (2013).

27 Caroff, M., Tacken, A. & Szabo, L. Detergent-accelerated hydrolysis of bacterial endotoxins and determination of the anomeric configuration of the glycosyl phosphate present in the "isolated lipid A" fragment of the Bordetella pertussis endotoxin. *Carbohydr Res* **175**, 273-282 (1988).

28 Ryu, Y. & Schultz, P. G. Efficient incorporation of unnatural amino acids into proteins in Escherichia coli. *Nat Methods* **3**, 263-265, doi:10.1038/nmeth864 (2006).

Chapter 3

Survival Without Lipopolysaccharide in *Acinetobacter baumannii* Depends on the Rate of Outer Membrane Biogenesis

---

Some of the work in this chapter is reproduced from:

Nagy, E *et al*. Robust suppression of lipopolysaccharide deficiency in *Acinetobacter baumannii* by growth in minimal medium. *in preparation*

3.1 Abstract

In this chapter we present our efforts to understand why LPS is seemingly essential in so many Gram-negative species but can be dispensable in a few others. We more fully characterize the phenotypes associated with LPS loss in *A. baumannii* and define conditions in which growth and morphological deviations are minimal. We describe suppressor mutations that improve growth in LPS deficient strains and utilize detailed growth analysis to show that the improvement is only modest. We propose a model for how an outer membrane can be built without LPS and explain why we believe this to be rate limiting for growth. We also examine how blocking LPS synthesis at different steps can change the observed phenotypes. We present efforts to understand why a later stage block of synthesis (*lpxD*) is more severe than a block at or before the committed step (*lpxC* or *lpxA*). We conclude by foreshadowing efforts to apply what we've learned in an attempt to remove LPS in *E. coli.*

3.2 Background

Acinetobacter baumannii is one of a small number of Gram-negative species that can survive without lipopolysaccharide (LPS) in the outer membrane.[1-3] Early investigations revealed that strains of *Neisseria meningitidis* lacking LPS still create an outer membrane, presumably filled with phospholipids.[2,4] Transmission electron microscopy (TEM) images obtained in our lab, and others, confirmed that *A. baumannii* also has a second membrane though it is quite heterogeneous in morphology and poorly defined in places (Figure 3.1, data from Ge Zhang). As expected, since LPS creates a barrier to entry of many compounds, these cells are leaky and sensitive to a wide variety of antibiotics. They also exhibit growth phenotypes and have heterogeneous cellular morphology.[5,6] Beyond the physical changes in the outer membrane, it is not well understood what other pathways and process LPS loss might affect.[7,8] We wanted to better characterize the phenotypes to try to understand why LPS is highly conserved in so many Gram-negative species, yet is dispensable in *A. baumannii*. We show here the progress we've made at dissecting the growth phenotypes across different conditions as well as a search for suppressors. We've synthesized these results into a model for how LPS loss affects cells and why it could be lethal in certain species. We also describe efforts into understanding the differences in phenotypes resulting from LPS loss when blocked at different points in the biosynthetic pathway.

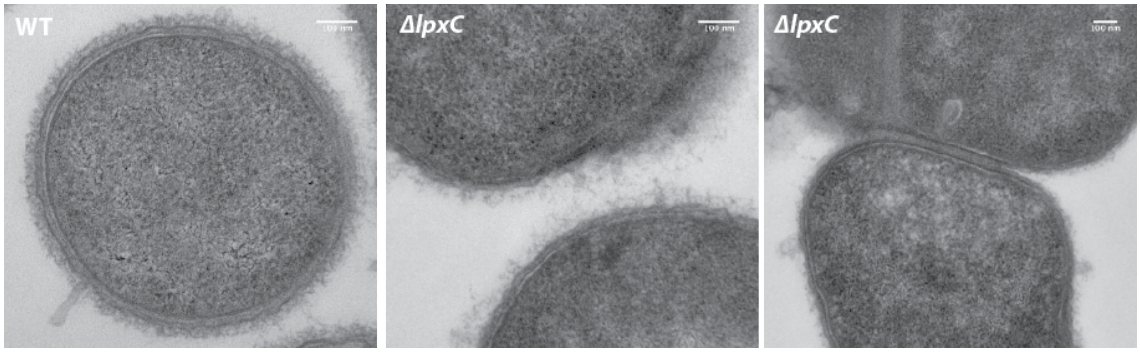

Figure 3.1 *A. baumannii* cells lacking LPS have an outer membrane with heterogeneous morphology**.** *A. baumannii* 19606 cells (wild type and *ΔlpxC)* were imaged using transmission electron microscopy. Scale bars are 100 nm.

3.3 Growth without LPS is dependent on conditions

3.3.1 Introduction

Previous studies showing the reduced fitness and growth rate of *A. baumannii* cells lacking LPS were all done with cells grown in rich medium (LB). These strains have a deletion in *lpxC*, the first committed step in LPS biosynthesis, meaning they produce no LPS or intermediates. We were curious as to what effect growth conditions would have on both the growth and morphology phenotypes observed in LB at 37°C.

3.3.2 Results

We verified that our strain showed the same phenotypes as had been seen before in rich medium (LB). When grown at 37°C, a strain lacking *lpxC* grew significantly more slowly than the wild-type (Figure 3.2 A). When viewed by light microscopy, cells showed a variety of morphological phenotypes. While some cells looked indistinguishable from wild-type, many were much more rounded and aggregated into small clumps and others were elongated (Figure 3.2 B,C). Most striking was the significant heterogeneity in the morphology with no one cell type predominating.

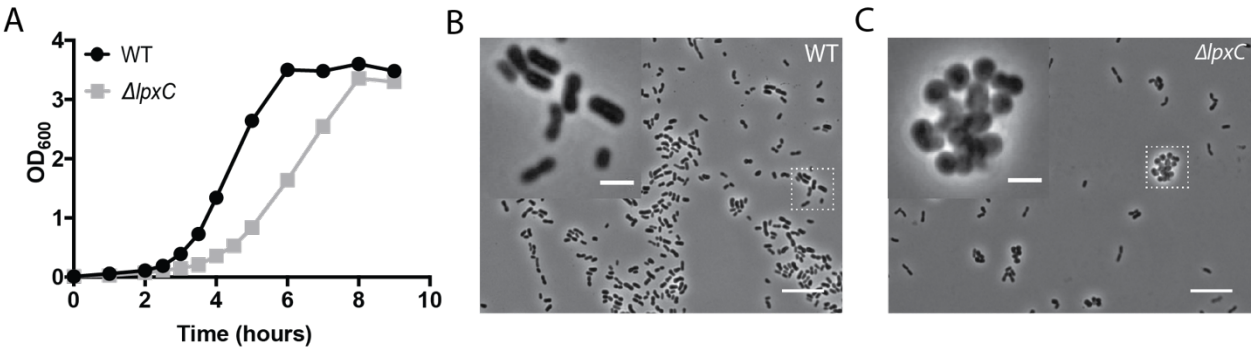

Figure 3.2 LPS deficient cells have defects in rich medium. A) Strains of wild type or *ΔlpxC A. baumannii* were grown in LB medium at 37°C and OD_{600} measurements were taken regularly. B-C) Phase microscopy with a 100 x objective of cells grown in the same conditions. Insets are a 4 x magnification of the white boxes in the larger images. Inset in (C_ is representative of the aggregation, not of all visible cell types. Scale bars are 10 µm for the larger images and 2 µm for the insets.

Since membrane composition and hydrophobicity are known to change with decreasing temperature, we wondered how growth at lower temperature would affect the observed phenotypes.[9] Growth in LB at 25°C exacerbated of the phenotypes seen at 37°C. The cells grew substantially more slowly than did the wild type and the final OD_{600} of saturated cultures was low (Figure 3.3 A). Imaging of these cells revealed that there was no longer obvious heterogeneity in the cell shapes as almost all cells existed in clumps (Figure 3.3 B,C). While some aggregation was observed at 37°C, at 25°C it was difficult to find single, separated cells in any field of view. This clumping explained the growth defects, as growth measurements depend on $OD_{600,}$ which is a measure of the number and size of particles in solution. Clumping would significantly affect the particle size and number, making OD_{600} a poor readout of the number of cells. While we don't know what is causing the clumping, we hypothesize that it is a result of the altered lipid and protein composition of the outer membrane. Other studies have shown that the outer

membrane of *A. baumannii* without LPS contains large amounts of small lipoproteins.[10] These lipoproteins may be prone to aggregation at lower temperatures due to changes in hydrophobicity. In any event, we did not see any new phenotypes at the lower temperature other than an exacerbation of what was observed at 37°C.

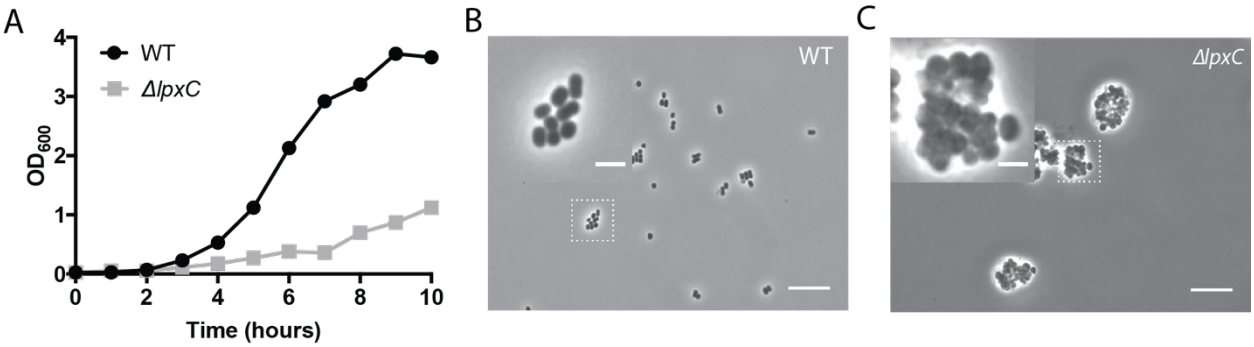

Figure 3.3 LPS deficient cells aggregate when grown at low temperature. A) Strains of wild type or *ΔlpxC A. baumannii* were grown in LB medium at 25°C and OD_{600} measurements were taken regularly. B-C) Phase microscopy with a 100 x objective of cells grown in the same conditions. Insets are a 4 x magnification of the white boxes in the larger images. Scale bars are 10 µm for the larger images and 2 µm for the insets.

We also characterized growth in a minimal medium, rather than the typical rich medium, LB. Surprisingly, the LPS deficient cells grew at the same rate as the wildtype in minimal medium (Figure 3.4 A). Cellular morphology was also largely indistinguishable from wild-type (Figure 3.4 B,C). The lack of phenotypes showed that LPS deficient cells could grow normally without genetic suppressors in certain conditions.

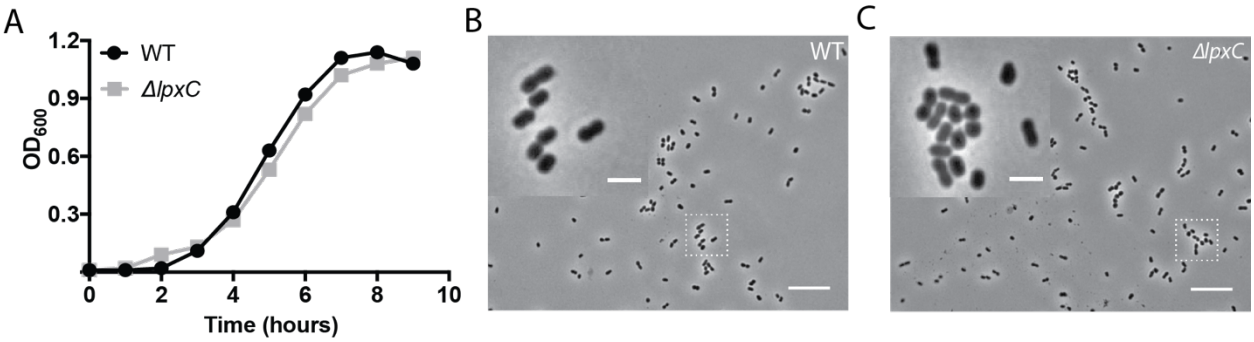

Figure 3.4 Growth of LPS deficient cells is normal in minimal medium. A) Strains of wild type or *ΔlpxC A. baumannii* were grown in M9+ medium at 37°C and OD_{600} measurements were taken regularly. B-C) Phase microscopy with a 100 x objective of cells grown in the same conditions. Insets are a 4 x magnification of the white boxes in the larger images. Scale bars are 10 µm for the larger images and 2 µm for the insets.

3.3.3 Discussion

We have shown that the severity of the growth phenotypes that LPS deficient *A. baumannii* exhibits is dependent on the growth conditions. When growing in rich medium, the mutant cells exhibited obvious growth and morphological defects that were exacerbated at lower temperatures. However, in minimal medium, the cells appeared and similar to the wildtype, both in morphology and growth rate. There are many possible reasons minimal medium might be more favorable to the LPS deficient cells. The nutrients are more limited, so growth tends to be slower and cells are smaller. Metabolism might also be different as the carbon source shifts from peptides in LB to succinate in minimal medium. One approach we took to understand the poor growth in LB was to look for suppressors of the growth phenotype.

3.4 Suppressor screen yielded genes in pathways for lipid recycling

3.4.1 Introduction

One way to understand a pathway and its effects is to perturb it and then look at the genetic modifications the cell makes to improve its fitness. Analysis of the modifications should then

provide insight into the nature of the problem they were selected to fix. For our system, the perturbation is LPS removal. We hoped that serial passaging of the cells, which selects for a faster growing population, would generate suppressors that would be informative about the pathways involved in surviving without LPS.

3.4.2 Results

In designing the experiment, we chose conditions, namely growth in LB at 25°C, that would maximize the difference in growth between the wildtype and LPS deficient cells. We separately grew several independent clones of *ΔlpxC* mutant cells and diluted each culture 100-fold every 24 hours into fresh LB medium (Figure 3.5 A). We monitored growth using a plate reader. Over the course of a week, each lineage showed substantial growth improvement (Figure 3.5 B). To minimize the impact on our analysis of random unrelated mutations, samples of each culture were saved after every noticeable growth improvement. In addition to potentially simplifying analysis, this also allowed for a determination of the order of acquisition if there were multiple mutations of interest. Sequencing data was then obtained for each stored lineage at multiple time points.

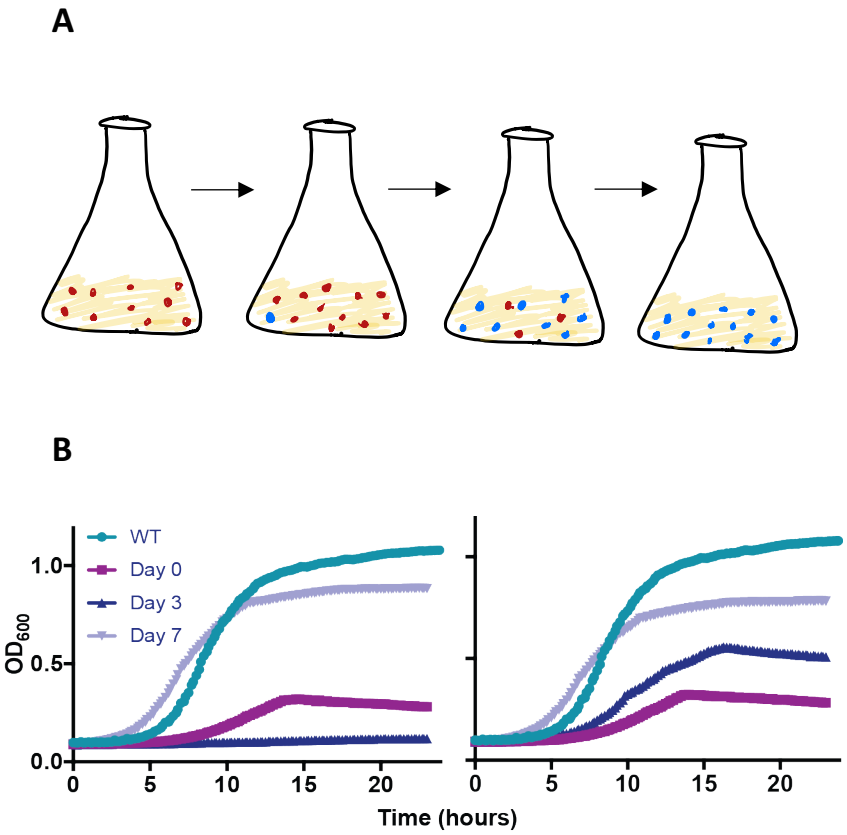

Figure 3.5 Suppressor screen yielded LPS deficient strains with improved growth. A) Multiple replicates of *ΔlpxC* were inoculated in LB and grown at 25°C. Every 24 hours, each replicate of *ΔlpxC* was diluted 100-fold into fresh LB medium. This process was repeated until growth, which was monitored using a plate reader, improved to wild type levels. B) Representative growth curves for two different replicates of *ΔlpxC* at each measured time point. Plates were incubated at 25°C with shaking in a Tecan plate reader for 20 hours and OD_{600} readings were taken every 10 minutes. Growth is compared to wild type *A. baumannii*.

To simplify our analysis, we sequenced the starting lineage for each replicate as well as the wild type, so that we could eliminate mutations already present before the passaging. The basal mutation rate in the strains was quite low and each replicate generally had three or fewer distinct genetic differences. A large number of the mutations were the result of insertions in the genome

from mobile elements resulting in loss of function disruptions rather than specific base-pair changes within a gene. A table with all assigned mutations can be found in the methods section.

Analysis of the sequencing data revealed a clear pattern. Almost all of the replicates were double mutants with loss of function mutations in bith *pldA* and *mlaA*, or another component of the *mla* pathway (Table 3.1). As was discussed in detail in Chapter 1, both of these genes are components of phospholipid recycling pathways that maintain normal outer membrane asymmetry. When phospholipids diffuse into the outer leaflet of the membrane, they disrupt the packing of the LPS creating a leaky barrier. To counteract this process, cells have dedicated systems to remove the phospholipids. PldA is a phospholipase in the outer membrane that is activated by dimerization in the presence of phospholipids.[11] Once active, it cleaves the fatty acyl tails from the phospholipids. *mla* is a six-protein pathway that spans the inner and outer membranes.[12] MlaA, an outer membrane lipoprotein, removes phospholipids and sends them back to the inner membrane through the rest of the pathway components. In *E. coli*, removal of any component results in failure of the pathway.[12] Recent work in *A. baumannii* has indicated the pathway functions in the same way, and our work is in agreement.[13] We never saw a mutation of more than one gene in the pathway in the same lineage, suggesting that removal of any component results in the same phenotype.

Table 3.1 Mutations in *pldA* and *mla* pathway are prevalent and occur together. *ΔlpxC* replicates (15 total) were passaged for 7 days while the *ΔmlaA ΔlpxC* replicates were passaged for 3 days. Whole genome sequencing of single colonies revealed loss of function mutations in both the *mla* pathway (mostly *mlaA*) and either *pldA* or the immediate upstream gene, DJ41_RS17650.

	Loss of Function Mutations		
Strain	***pldA***	***DJ41_RS17650***	***Mla* pathway**
Δ*lpxC*	6/15	9/15	13/15
Δ*mlaA* Δ*lpxC*	7/12	5/12	___

The majority of the observed mutations were in *pld*A itself; however, an insertion sequence into the gene immediately upstream of *pldA* was also commonly observed. We interpreted the effect of this insertion to be due to polar effects on the expression of the downstream *pldA* gene. We based this interpretation on the fact that we never observed a *pldA* mutation in the same strain as this upstream insertion, suggesting that disruption of either gene resulted in the same phenotype. Also, the upstream gene was always disrupted with an unspecific insertion, whereas we saw both insertions and point mutations in *pldA*.

In addition to the *pldA* and *mla* mutations, only one gene (DJ41_RS10590) was disrupted more than twice. This gene encodes a protein with unknown function in *A. baumannii* and searches of the BLAST database revealed no similar annotated sequences. A search for structural predictions using the PHYRE database yielded several potential matches, all of which were outer membrane β-barrel proteins.[14,15] Interestingly, this gene was only disrupted in strains that did not have a

mutation in the *mla* pathway, and all replicates had either an *mla* mutation or a mutation in this gene. This evidence suggests that the gene might be involved with the function of the *mla* pathway, especially since it appears likely to be located in the outer membrane. Investigations into the possible function of this gene are ongoing.

3.4.3 Discussion

When we designed this passaging experiment, we believed we would be able to evolve strains that grew more quickly than the parent *ΔlpxC* strain. We did not know, however, if the mutational analysis would reveal any striking patterns that would be easy to interpret. Each replicate we sequenced had accumulated only a small number of overall genetic differences, allowing for easier interpretation. The natural evolution of the populations also showed that two loss of function mutations in particular, *pldA* and *mla*, were the most efficient and consistent ways to improve growth. That these two pathways are both involved in lipid recycling led to a reasonable hypothesis of how they might be affecting growth in cells lacking LPS. When cells are trying to build a membrane from phospholipids, systems that actively remove those phospholipids from the outer leaflet would be detrimental. The small number of potential mutations also made it much easier for us to follow up on each one to verify which were causative.

3.5 Removal of phospholipid recycling systems improves growth in cells lacking LPS

3.5.1 Introduction

While we were fairly confident from the sequencing results that *pldA* and *mla* were in fact the causative mutations for the improved growth we were observing, we needed to confirm that was the case by constructing double mutants with null mutations in the genes of the two pathways.

We also always observed the two mutations in conjunction and it was therefore necessary to test whether both were in fact required for growth improvement. There was also interest in the effects of the mutations on the morphology phenotypes we observed. To address these questions, we constructed *ΔlpxC* strains with single and double deletions in *pldA* and *mlaA* since we predominately observed loss of function mutations in these genes in the screen.

3.5.2 Results

For each of the constructed strains, we compared their growth profiles at both 37°C and 25°C (Figure 3.6 A). Only the strain harboring mutations in both *pldA* and *mlaA* in addition to *lpxC* showed growth near wild type levels at both temperatures. Single deletions of either gene in conjunction with *ΔlpxC* had no effect. This result was consistent with the sequencing results in which every replicate had mutations in both pathways. Also, since the two mutations in conjunction have a growth profile similar to what we observed with the passaged strains, we were confident they were the causative mutations.

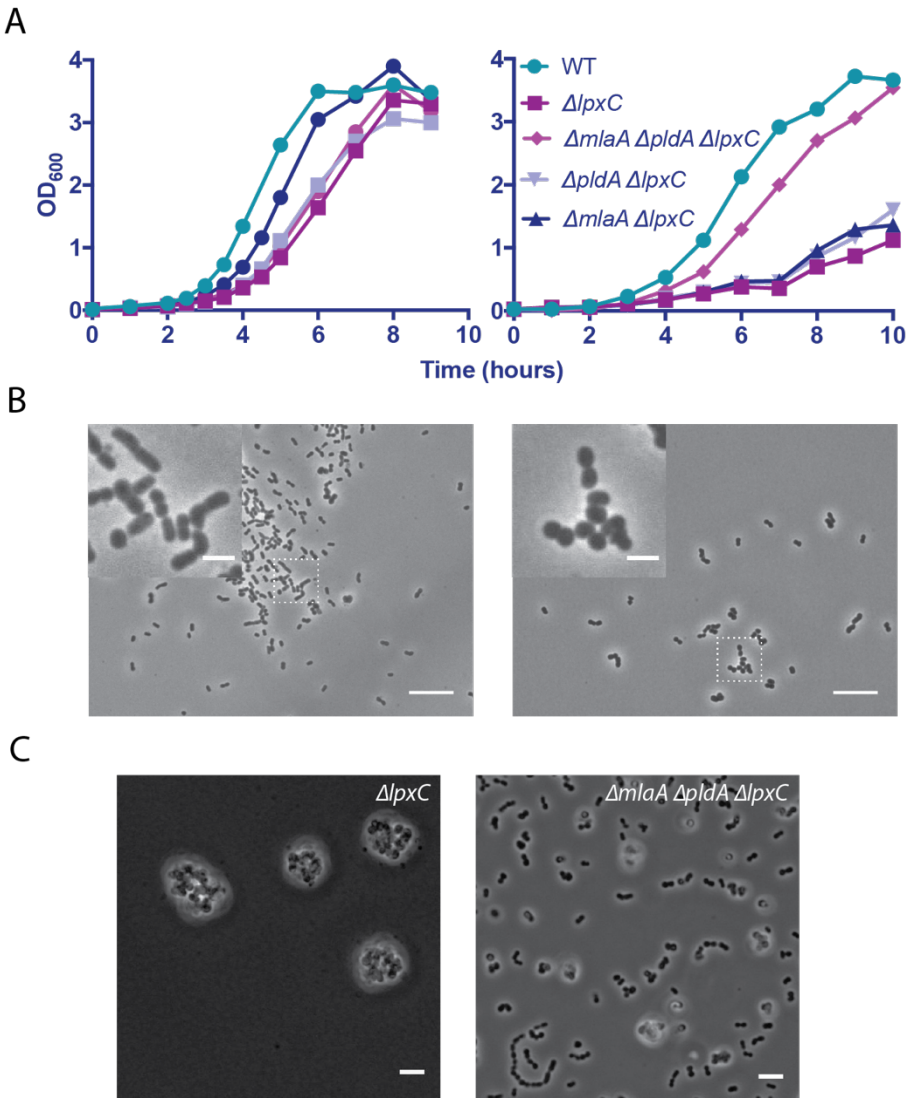

Figure 3.6 *ΔmlaA* and *ΔpldA* partially suppress phenotypes of LPS deficiency. A) Growth of LPS deficient strains with either single or double mutations in *mlaA* and *pldA* in LB. Left panel shows growth at 37°C and right panel at 25°C. B) Phase microscopy with a 100 x objective of *ΔmlaA ΔpldA ΔlpxC* strain grown in the same conditions. Insets are a 4 x magnification of the larger images. Scale bars are 10 µm for the larger images and 2 µm for the insets. C) Phase microscopy with a 60 x objective of either *ΔlpxC* or *ΔmlaA ΔpldA ΔlpxC* cells grown in LB at 25°C. Scale bars are 10 µm.

Imaging of each strain showed that the suppressors also largely eliminated the clumping phenotype we observed at 25°C for *ΔlpxC* (Figure 3.6 B). While the morphology of *ΔmlaA ΔpldA ΔlpxC* (MPC) was still distinguishable from wild-type, the cells were less heterogeneous and more

consistently rod shaped. To quantify the level of clumping in some way, we measured colony forming units (CFU/mL) at stationary phase of each strain by plating and then counting cells. The suppressed strain MPC had colony counts similar to wild-type at both temperatures where the *ΔlpxC* strain had significantly fewer colonies at low temperature (Figure 3.7). This confirmed the change in clumping phenotype that we were observing by microscopy.

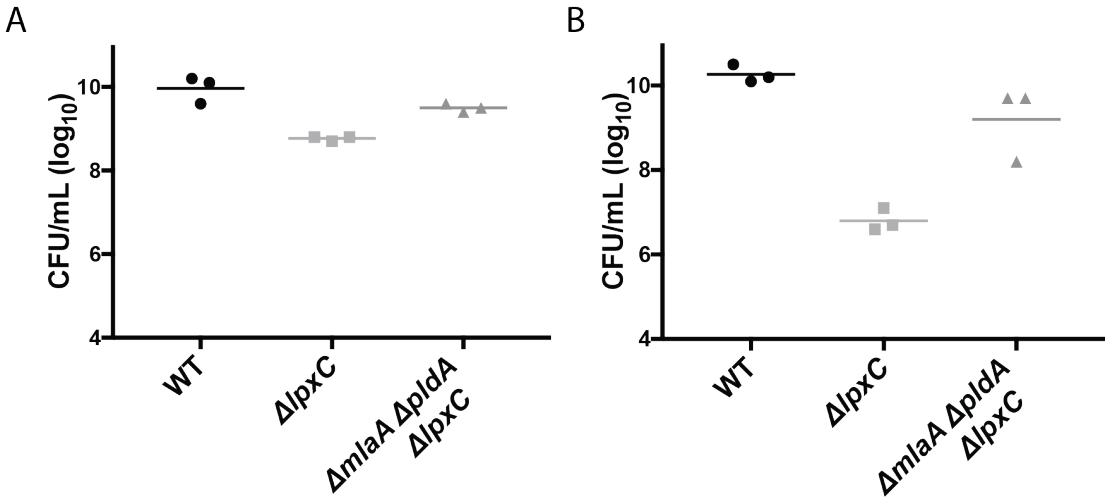

Figure 3.7 Suppressor mutations significantly reduce cellular aggregation. A) Strains were grown to saturation in LB at 37°C and then serially diluted. 5 µL of each dilution was plated on LB agarose plates in duplicate. Plates were incubated for 24 hours at 37°C and the number of individual colonies at each dilution were counted. Values shown represent $\log_{10}$ of the calculated CFU/mL. All data is a compilation of 3 biological replicates B) Conditions were same as in (A) except cells were grown to saturation at 25°C before plating.

3.5.3 Discussion

The constructed strains confirmed our hypothesis that the *pldA* and *mla* mutations from the passaged strains were responsible for the improved growth profiles we observed. Importantly, the suppressor strain also did not aggregate, especially at lower temperatures. This observation raised the question of whether the improved growth profile was due to a faster doubling time or

a result of less clumping. To attempt to distinguish between these two possibilities, we did a closer analysis of the early exponential growth rates of the different strains.

3.6 Early phase growth analysis reveals LPS deficient growth is independent of nutrients

3.6.1 Introduction

Comparing the shape of growth curves of different strains can provide information about the overall phases of growth. It makes it easy to compare features like duration of lag phase or cell density at the time of saturation. When the growth profiles of even the same strain are significantly different between conditions, as with minimal and rich medium, it becomes difficult to realize useful comparisons by just overlaying growth curves. For this type of information, calculating growth constants (or doubling time) for a particular period of growth becomes a useful quantitative tool for comparing strains across conditions.[16]

3.6.2 Results

We calculated growth constants for each of the strains (wild type, *ΔlpxC*, MPC) in every condition we had investigated (LB at 37°C, LB at 25°C and minimal medium at 37°C). To do this, we chose the early exponential growth period (OD_{600} ~ 0.1 – 0.5) where doubling time should be at a minimum. This period was also conducive for this type of analysis because the doubling rate is almost constant, and linearization yields consistent data. To compensate for the clumping phenotype at 25°C, we calculated growth constants from both OD_{600} data and cellular ATP levels at each time point. The OD_{600} would be impacted by clumping, but ATP levels should be the same whether or not cells are aggregating. Comparison of these growth constants revealed two important facts that had not been obvious from just looking at growth curves (Figure 3.8).

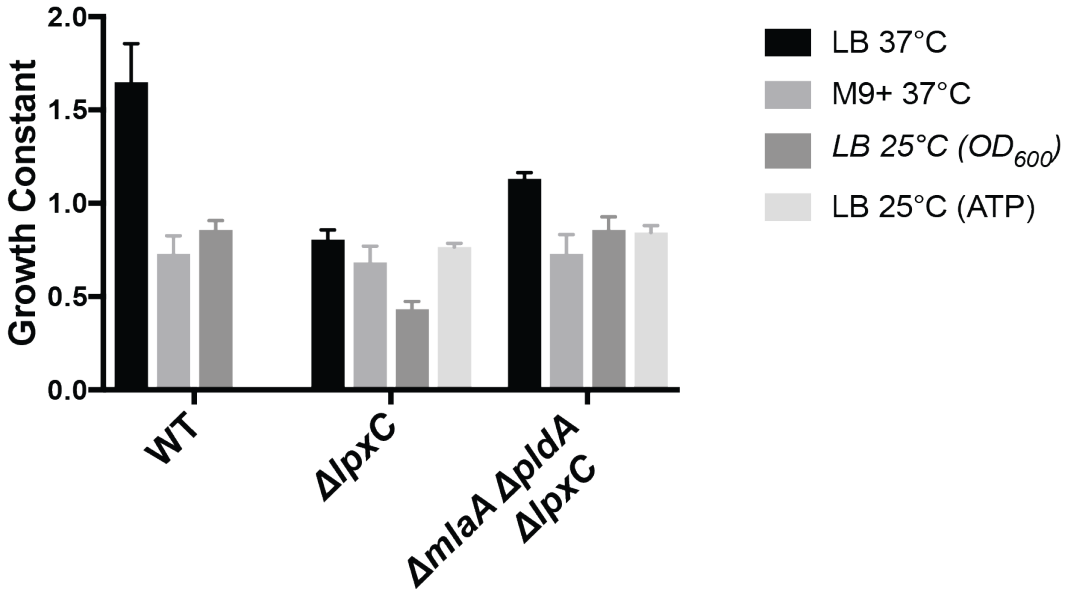

Figure 3.8 *ΔlpxC* cells do not change their growth rate in response to nutrient levels or temperature. Growth constants were calculated for each condition by linearizing growth data from $OD_{600!}$ ~ 0.15-0.5 and determining the slope of the regression line. *ΔlpxC* cells aggregate extensively at 25°C, so growth was also calculating using total ATP levels.

First, the suppressors did not restore growth to wild-type levels in LB at 37°C when cells were growing the most quickly. In fact, the growth improvement over *ΔlpxC* was modest. This result suggests that much of the growth improvement we saw in the growth curve might actually be a result of a reduction in clumping. The fact that these mutations were the only ones we found in our suppressor screen suggests that fixing whatever is causing the reduced doubling time is not simple.

The second striking result was that the LPS deficient strain had the same growth rate in all conditions. Wild-type cells double more quickly in LB than in minimal medium due to the greater nutrient availability. The *ΔlpxC* cells, however, did not respond to the change in nutrients, maintaining the same growth rate. Wild-type cells also slowed their growth when the temperature decreased, but the *ΔlpxC* cells did not, if that growth was measured by ATP levels

to reduce the impact of the aggregation. Under normal conditions, wild-type cells adjust their growth rates based on whatever is rate limiting in that condition, often nutrients. The LPS deficient cells, however, appeared to have the same rate determining step (and thus growth rate) regardless of condition.

3.6.3 Discussion

This detailed growth analysis revealed important differences between the strains that had not been obvious by simply overlaying growth curves. Contrary to our initial impression, the suppressors do not fully fix the growth defect caused by LPS loss. And perhaps most intriguingly, the LPS deficient strains seemed to be rate limited for growth by a process different from the wild-type cells. These two points were very important for the development of our model for growth without LPS described in detail in the next section.

3.7 Model for growth without LPS

A mutation in the biosynthetic pathway for LPS impairs the cell's ability to produce an outer membrane. LPS deficient cells must presumably rely on phospholipids for both the inner and outer leaflets of the outer membrane. Since cells can only grow as quickly as they can produce a membrane bilayer, growth of LPS deficient cells would be limited by their ability to incorporate these phospholipids. We propose that removal of LPS results in membrane synthesis becoming rate limiting for growth and that this is responsible for the phenotypes we have characterized.

To build this new membrane, cells must synthesize sufficient phospholipids, transport them across the periplasm and then insert and flip them into the outer leaflet. While any of these particular steps could be rate limiting, we predict that the most likely slow step is flipping the

phospholipids into the outer leaflet. While it is certainly possible that cells have difficulty synthesizing enough phospholipids due to regulatory changes in fatty acid biosynthesis, there should be sufficient supplies of fatty acid precursors due to the lack of LPS synthesis competing for resources. While the method of transporting phospholipids to the outer membrane is unknown, it is reasonable to expect that the rate of transport could be modulated at least to some extent. There is no reason to presume, however, that cells have an enzymatic mechanism for flipping phospholipids into the outer leaflet because it normally only contains LPS, which has an energy-driven pathway dedicated to transport and insertion. Therefore, to put phospholipids into the outer leaflet would be challenging because the energetic barrier for flipping would be expected to be high.

This model is consistent with the phenotypes we have worked to characterize. When growing quickly in LB, the cells cannot synthesize membrane fast enough to support wild-type levels of growth. As a result, they grow significantly more slowly than wild-type. In minimal medium, cells are growing slowly and are typically smaller, which reduces the surface area of the cell and hence the amount of membrane needed to surround it.[17-19] This combination of factors reduces the demand on membrane synthesis to the point where it is no longer rate limiting and thus cells grow as quickly as wild type without morphological anomalies. Lowering the temperature, which reduces the growth rate without limiting nutrients or reducing cell size, also slows growth sufficiently to allow the LPS deficient cells to double at wild type levels. Cell size is still large though, so more membrane is needed per division, which we believe is a possible explanation for the observed clumping defects. It has been noted that Δ*lpxC* cells have more small lipoproteins in their outer membrane. We propose that the cell is filling empty space in the bilayer with these

lipoproteins in an attempt to produce a complete membrane more quickly. These lipoproteins might be expected to clump more at lower temperatures due to changes in hydrophobicity. The suppressors bring lipoprotein levels back to wild type which might explain why those cells do not clump and have better morphology (data not shown).

Our hypothesis also helps to explain how the *mla* and *pldA* suppressors we found only partially restored growth in LB medium and had no effect in minimal medium. Simply put, they do not fix the barrier to phospholipid flipping. Rather, by eliminating the pathways responsible for removing phospholipids from the outer leaflet, cells can somewhat increase the rate at which they build the outer leaflet of the membrane, thus modestly improving their growth rate. We would expect that finding a way to increase the rate of flipping would be difficult for the cell and thus those types of mutations would be rare. This would explain why we were unable to find any suppressors that substantially improved growth rate.

3.8 Investigations into the role of Pbp1a

Early in our investigations, a paper from the Trent lab appeared that that survival in the absence of LPS is connected to cell wall synthesis.[10] They showed that certain strains of *A. baumannii* could only lose LPS if they had a concurrent loss of *ponA*, the gene encoding Pbp1a. This result generated a great deal of interest because people have long sought the regulatory connection between outer membrane and cell wall synthesis.

We were curious about this result as we had not seen any mutations in *ponA* in our suppressor screen. Our particular strain, ATCC19606, happened to be one of the strains that the paper showed had naturally low levels of *ponA* expression and thus did not require a deletion. We have another strain, ATCC17978, however that did require a *ponA* mutation to lose LPS. Ge Zhang in

our lab had constructed a *ΔlpxC* derivative of the 17978 strain. So we asked if that strain also had a mutation in *ponA* as the paper suggested was necessary. Sequencing of the *ponA* gene showed no mutations in the coding or regulatory regions.

Since the paper asserted that 19606 has low levels of *ponA* transcripts despite having an identical promoter sequence to 17978, we wondered if our 17978 strain also had unexplained low expression levels. To investigate this possibility, we determined expression levels in our 19606 and 17978 strains, both with and without LPS, using reverse transcription quantitative PCR (RT-qPCR). Initially, we used the same primers targeting *ponA* that were reported in the publication; however, early control experiments showed the primers had poor efficiency in 19606. We determined that there was a single basepair mismatch in the reverse primer sequence between the two strains. So only 19/20 base pairs matched the target sequence in 19606. We switched the sequence such that the mismatch was now in 17978 and observed that the efficiency switched as well. With the new probe, 19606 had satisfactory efficiency and 17978 did not. Since we could not be confident that any differences observed would not be a result of efficiency differences between these two primer pairs, we decided to screen for a primer set that had good efficiency in both strains (Table 3.2).

Table 3.2 Primer efficiency varies depending on basepair mismatch. Efficiency values were determined for each set of primers used in the RT-qPCR experiment. If no value is listed, the data was too poor to get a good correlation. PT = published primers, PE = published primers flipped to match 19606, PN = newly designed primers

	Primers			
Strain	**16S**	**PT**	**PE**	**PN**
19606	107	No value	116	100
17978	99	105	No value	106

We then took these three primer sets and analyzed the *ponA* transcript levels in each of our strains. While we could not replicate the 80-fold difference in levels they observed between 17978 and 19606, we could see higher expression in 17978 using their primers (Figure 3.9). Surprisingly though the levels remained high in the *ΔlpxC* 17978 strain suggesting that the high levels did not preclude LPS removal. When using the primers that matched 19606 rather than 17978, we could reverse the difference, seeing higher levels in 19606. This result made us believe that some of the observed effect was in fact a result of poor primer matching. Finally, we tested the primers we designed that controls suggested functioned well in both strains. In this case, we could see almost no difference between the two strains (Figure 3.9). From this data, we concluded that *ponA* removal was not necessary for LPS removal in either of our strains. We are not sure why we have this discrepancy with their data, though it is possible our wild type 17978, or theirs, has another mutation we are unaware of. Also, we made clean deletions of *lpxC* while they selected for LPS loss on polymyxin. It is possible the cell wall phenotype is a byproduct of their selection method.

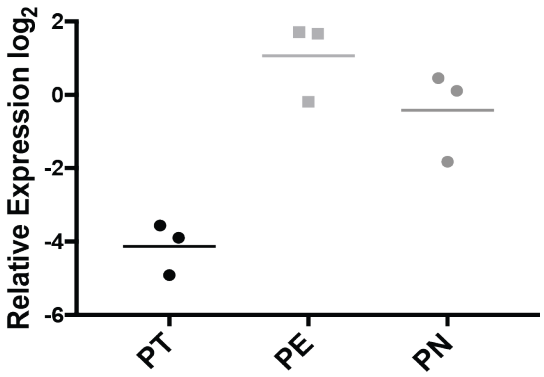

Figure 3.9 Differences in *ponA* expression levels depend on primer pair. RT-qPCR data was normalized to 16S expression levels for each strain. Data shown is relative expression levels of 17978 compared to 19606, where 19606 is normalized to 0. Horizontal bars indicate the average for each set and the experiment represents three biological replicates.

Very recently, the Trent lab released another paper identifying the *pldA* and *mla* suppressors as important for growth restoration in LPS deficient *A. baumannii*.[13] Much of what they showed is consistent with what we've seen, though they again identified the *ponA* mutation in their suppressor screen. They argued that the mutations restore growth to wild-type, a difference we believe is simply the result of growth curve analysis rather than looking at the growth constants. They suggested that the morphological phenotypes are a result of problems with cell wall synthesis. While we cannot be sure, we believe our model offers a more reasonable alternative explanation.

3.9 Blocking LPS synthesis at different steps in the pathway

3.9.1 Introduction

In *A. baumannii*, any one of the first three steps of LPS biosynthesis can be removed and the cells are still viable. Removal of subsequent steps is lethal, presumably due to a build-up of toxic intermediates.[20,21] Most of the work in the literature to characterize and understand LPS loss has been done using a *ΔlpxC* strain. We were curious if there would be differences in the observed

phenotypes for a *ΔlpxA* or *ΔlpxD* strain and what effect the suppressors would have. We predicted that the *ΔlpxA* strain should look much like a *ΔlpxC* strain since LpxC catalyzes the first committed step in the pathway. An *lpxD* deletion, however, results in build-up of an acylated sugar intermediate (the product of LpxC) and therefore might have more severe phenotypes than *ΔlpxC*. Understanding these differences could provide additional insight into the problems caused by LPS loss.

3.9.2 Results

We constructed strains with deletions in either *lpxA* or *lpxD* and then characterized their growth in LB at both 37°C and 25°C (Figure 3.10). As predicted, an *lpxA* deletion phenocopied the *ΔlpxC* mutant at both temperatures. Removal of *lpxD*, however, resulted in more severe growth phenotypes, especially at lower temperatures where the cells barely grew, only reaching and OD_{600} of ~0.5. While the *ΔlpxD* cells also clump, we do not believe that was the sole cause of the growth defect since the *ΔlpxC* cells are also extensively clumped yet grow to a higher OD_{600}. We concluded that some aspect of *lpxD* removal is more detrimental to cells than removal of *lpxC*.

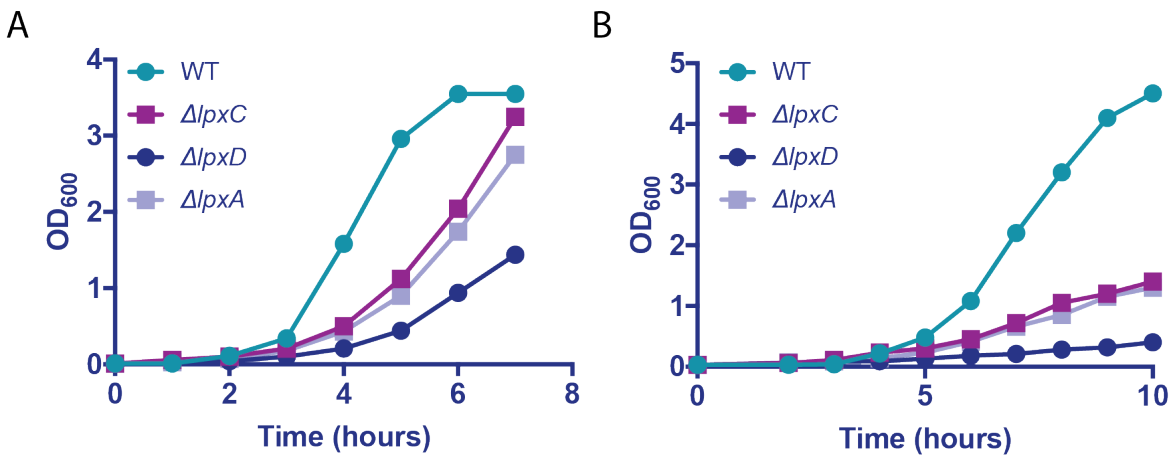

Figure 3.10 The step at which LPS synthesis is blocked matters. A) Strains of *A. baumannii* were grown in LB medium at 37°C and OD_{600} measurements were taken regularly. B) Same as above but strains were grown in LB at 25°C.

We also investigated the effect of the suppressors on *ΔlpxA* and *ΔlpxD* strains (Figure 3.11). The suppressors appeared to have a similar effect in both strains, with growth improving modestly in each case (Figure 3.11 A). As with the single deletions, strains with *ΔlpxC* or *ΔlpxA* grew similarly. Analysis of the growth constants for the *ΔlpxD* strains showed that the suppressors improved growth by an amount proportional to the increase in *ΔlpxC* (Figure 3.11 B). This suggests that the effect of the suppressors is downstream and independent of whatever is causing the toxicity in *ΔlpxD*. The basal rate of membrane formation, as it specifically relates to phospholipid flipping, and thus the effect of the suppressors would not be expected to be affected by toxicity earlier in the pathway.

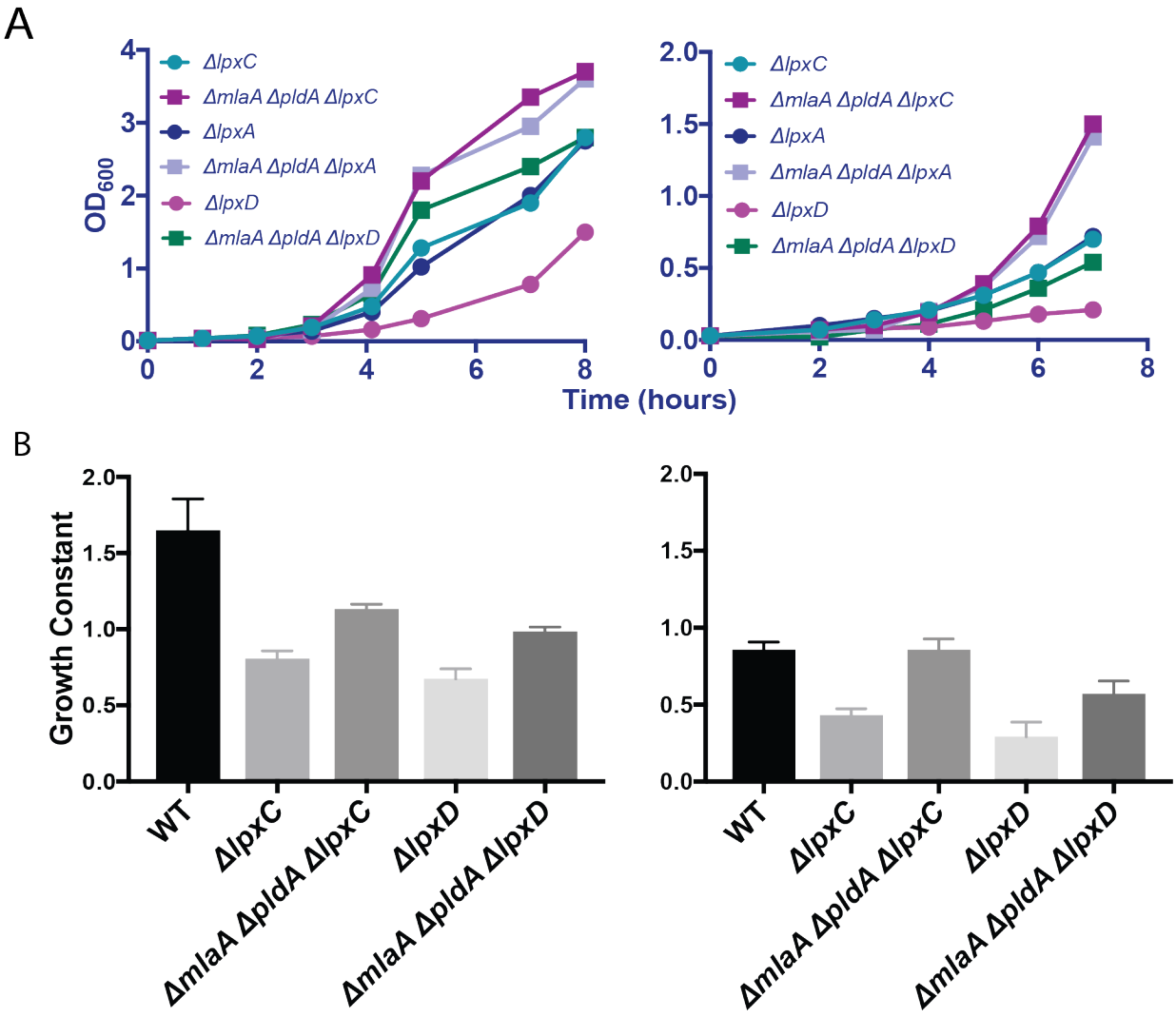

Figure 3.11 Suppressors have a similar effect regardless of biosynthetic step. A) Strains of *A. baumannii* were grown in LB medium at 3°7C (left panel) or 25°C (right panel) and OD_{600} measurements were taken regularly. B) Growth constants for the early log-stage were calculated for the same conditions as above.

Finally, as a confirmation that the toxicity of LpxD removal is related to the formation of the LPS intermediate, we constructed strains with deletions in either *lpxA* or *lpxC* in addition to *lpxD*. Both of these stains grew like a *ΔlpxC* mutant, confirming the mutations are epistatic to the *lpxD* mutation (Figure 3.12). Active flux of precursors into the pathway is required for the phenotypes observed in *ΔlpxD*.

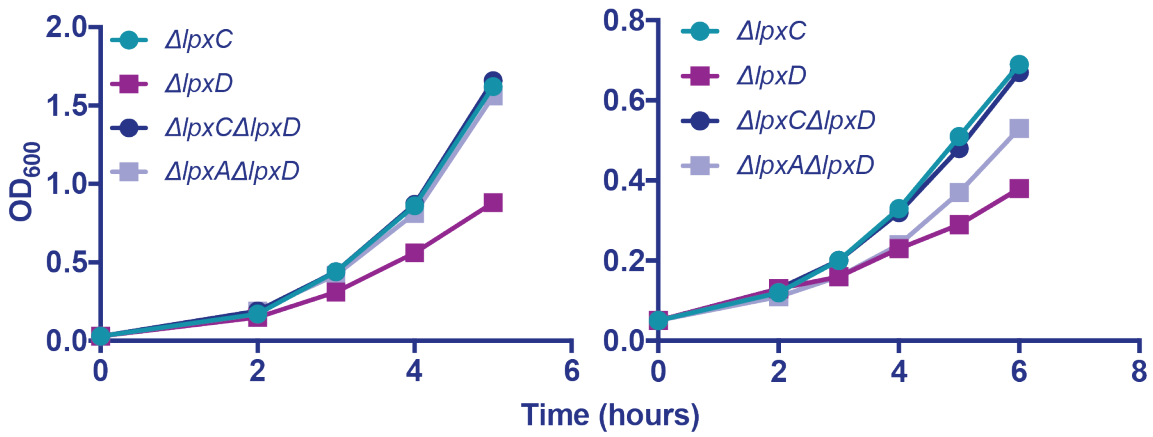

Figure 3.12 *ΔlpxD* phenotype is a result of flux into the biosynthesis pathway. Strains of *A. baumannii* were grown in LB medium at 37C (left panel) or 25C (right panel) and OD_{600} measurements were taken regularly.

3.9.3 Discussion

As predicted removal of LPS at an earlier step in the pathway (*lpxA*) was less detrimental to cells than removal at a later step (*lpxD*). While the most obvious difference between these two steps is the presence of an intermediate formed by LpxC, it is not entirely clear what effect that intermediate might be having. It is possible that the presence of large amounts of a lipidated sugar in the cytoplasm is toxic on its own. However, it is also possible that the toxicity could be related to regulation of the pathway and the balance between phospholipid and LPS synthesis. Normally, LPS synthesis is regulated by specific proteolysis of LpxC by FtsH, but what triggers the proteolysis is unknown.[22] It seems reasonable that the point of sensing and regulation would be at LpxC as it is the first committed step in the pathway. Because intermediate build-up is toxic, the cell needs to know if it has committed to making an LPS molecule to ensure that enough precursors, specifically fatty acids, are available. In *E. coli*, LPS depletion causes LpxC to stabilize, thus increasing the synthesis rate.[23] In an *lpxD* strain, there is no LPS at the cell surface, so if LpxC

is stabilized, we would predict large amounts of toxic intermediates would be produced. This could deplete or change the ratio of available fatty acid precursors, making it difficult for the cell to synthesize sufficient phospholipids.

While we predicted that communication between the LPS and phospholipid synthesis pathways would occur at the LpxC catalyzed step, we were not sure if the signal would be LpxC itself or its product. The experiments with double mutants of *lpxA/lpxC* and *lpxD* suggest that the presence of the LpxC protein alone is not sufficient for toxicity. With the *lpxAlpxD* mutant, LpxC is still present, though not active, yet the *lpxA* mutation rescues the toxic effects of *lpxD* removal. Investigations are ongoing to determine if it is the catalytically active form of LpxC or the lipidated product that is so toxic to the cells.

3.10 Efforts to understand the phenotypes of *ΔlpxD*

3.10.1 Introduction

Since fatty acid synthesis is so tightly regulated in cells, we predicted that changes in that system could be causing the phenotypes observed in *ΔlpxD*.[24] In LPS, all of the attached acyl chains are saturated, but in phospholipids there is often a 1:1 ratio of saturated to unsaturated fatty acids. This ratio can change in response to environmental conditions, especially lowered temperature.[9,25,26] Since the *ΔlpxD* strain is particularly sensitive to growth at lower temperatures, we wondered if this was a result of an imbalance in fatty acid synthesis. Perhaps, with LPS no longer being made, there were too many saturated fatty acids available which could be affecting phospholipid synthesis. Efforts to test this hypothesis were unsuccessful.

3.10.2 Results

Since fatty acids might be limiting in these cells, we supplemented cultures exogenously with varying concentrations of the most commonly incorporated saturated (palmitic acid 16:0) and unsaturated (oleic 18:1) fatty acids (Figure 3.13). We predicted that if levels of one type were too low, supplementation might rescue cell growth. Due to technical reasons, the results were difficult to interpret. *A. baumannii* cells without LPS are quite permeable and known to be sensitive to detergents. Even low concentrations of the added fatty acids were toxic to the cells. Concentrations at which the cells would grow were significantly below the normal level for supplementation experiments, so the lack of change in growth might simply be because there was not enough fatty acid to make a difference.

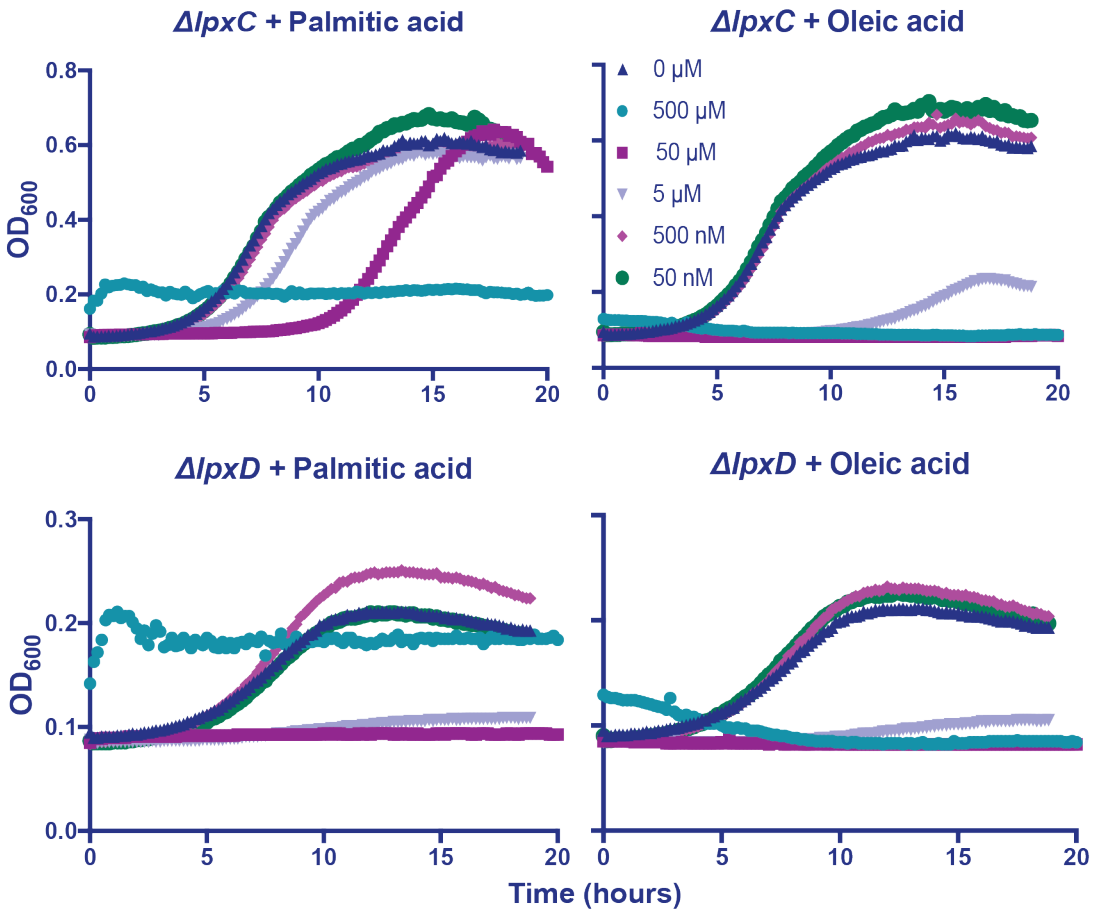

Figure 3.13 Exogenous fatty acid supplementation inhibits growth. Strains of *ΔlpxC* or *ΔlpxD A. baumannii* were diluted 100-fold into LB in a 96-well plate. The wells were supplemented with (Continued) varying concentrations of palmitic acid (saturated) or oleic acid (unsaturated). Plates were incubated at 37°C with shaking in a Tecan plate reader for 20 hours and OD_{600} readings were taken every 10 minutes.

We wondered if the acyl chain composition of phospholipids in the membrane might reveal differences between the strains, suggesting a change in fatty acid availability or regulation. We grew cells to mid-log stage and then submitted the cell pellets for analysis by GC-FAME. While the results showed differences, mostly between the wild-type and LPS deficient mutants, there was too much variation between replicates to draw significant conclusions (Table 3.3). Also, there did not appear to be any obvious, significant differences between the *ΔlpxC* and *ΔlpxD* strains.

Table 3.3 GC-FAME analysis of phospholipids shows no significant differences between LPS deficient strains. The indicated strains of *A. baumannii* were grown at either 37°C or 25°C to OD_{600} 0.6. Cell pellets were submitted for analysis by GC-FAME. Percentages of the significant lipid species (>5% of total) are shown below with the standard deviation between two biological replicates.

Lipid Species	Strain				
37°C	**WT**	***ΔlpxC***	**MPC**	***ΔlpxD***	**MPD**
16:0	26.07±2.31	36.06±1.07	32.64±1.19	32.12±2.57	30.62±3.00
16:1 w7c	6.59±0.59	6.84±1.51	5.94±1.22	8.44±2.35	6.0±1.56
18:1 w9c	44.77±0.38	49.52±0.11	51.21±1.55	51.68±0.46	53.57±0.47
25°C					
16:0	15.72±0.54	19.67±1.18	17.53±0.33	19.73±0.53	15.79±0.87
16:1 w7c	16.25±0.64	14.9±1.69	18.02±1.44	14.4±0.57	15.7±1.55
18:1 w9c	49.3±0.19	52.93±1.87	53.17±0.09	53.24±0.94	54.03±0.88

If *ΔlpxD* cells cannot produce enough fatty acid precursors, one would predict that they would be hypersensitive to drugs targeting fatty acid biosynthesis. Triclosan is an antibiotic that kills cells by inhibiting FabI, an enzyme in the fatty acid biosynthesis pathway.[27] Unfortunately, we had the same problem as with fatty acid supplementation: all LPS deficient strains were extremely sensitive to triclosan treatment due to permeability changes (data not shown).

Finally, we decided to use the same approach that had been successful with the *ΔlpxC* strain and screen for suppressors of the growth phenotype. Using the same experimental setup, we were able to evolve *ΔlpxD* strains that grew more quickly, but not as robustly as what we had

found with *ΔlpxC*. Sequencing analysis was inconclusive with most of the strains having a mutation in *pldA* (7/9) and some having either *mla* (2/9) or DJ41_RS10490 (2/9). It was perhaps not unexpected that *ΔpldA* and *Δmla* were not quite as prevalent as they do not have as great of an effect on growth in *ΔlpxD*. Most of the other mutations involved transcriptional regulators or ribosomal proteins, presumably having a wide spread metabolic effect. We were surprised that we did not see mutations in *lpxC* or *lpxA* since we have shown that they are epistatic and thus improve growth, especially in conjunction with *pldA* and *mla* mutations. We do not know if we did not passage the strains long enough to evolve that specific combination or if something more specific was going on that we do not understand.

3.10.3 Discussion

Several different approaches have been used to attempt to discern the role of fatty acid synthesis in the toxicity associated with LpxD loss. We have been unable to show that fatty acid regulation plays a role, but we also do not have any evidence that it does not. Many of the experiments were inconclusive due to technical difficulties related to working with these strains. Further attempts to understand the *ΔlpxD* phenotypes are ongoing.

3.11 Future directions

We used a variety of approaches to better understand the challenges cells face when removing LPS from the outer membrane. It began with more fully characterizing the types of phenotypes LPS deficiency causes including slowed growth and changes in morphology. These investigations led us to the discovery that LPS-deficient cells grow normally in minimal medium without the need for additional genetic suppressors. We believe that cells grow slowly enough in this condition to have sufficient time to properly build an outer membrane composed of

phospholipids. When growing quickly, the cells cannot flip phospholipids into the outer leaflet quickly enough and thus are limited in their maximum growth rate. Suppressors found to date are in lipid recycling systems, which addresses the problem only superficially by reducing the phospholipids actively removed from the outer membrane.

Searches for other suppressors that can more fully restore growth to the LPS deficient strains are ongoing. We predict that they will be rare as the cell will have to gain a functionality, phospholipid flipping, it does not normally possess. Towards this effort, we are working to engineer a strain that has this additional functionality to test our hypothesis further. There is a gain of function mutation in MlaA in *E. coli* (MlaA*) that actively flips phospholipids into the outer membrane. We are attempting to construct an *A. baumannii* strain harboring an *mlaA** allele from *E. coli* to see if the functionality is the same. If it is, we would predict that the mutation should improve growth rate by increasing the amount of phospholipid in the outer leaflet. We imagine this type of mutation would be difficult to find via an evolution experiment as losing *mla* pathway functionality is easier since the necessary mutations are loss of function rather than a specific gain of function in MlaA, and removing the pathway has its own beneficial effect on growth.

One of our goals when beginning this project was to learn enough about LPS loss in *Acinetobacter* to understand why so many other Gram-negative species, like *E. coli*, cannot seem to survive without it. While we certainly do not have all of the answers, we do believe that growth needs to be slow enough to allow sufficient time for membrane construction. We also suspect that the cells need to be flexible enough to not activate extreme stress responses when the membrane is incomplete. *Acinetobacter* seems to be particularly able to adjust to a lack of

phospholipids by adding other components such as lipoproteins to the membrane. It is possible that faster growing species like *E. coli* are not able to make these changes quickly enough and are overwhelmed by stress responses. We plan to try to remove LPS in *E. coli* while it is growing very slowly. We have a variety of ways including minimal medium, lowered temperature and protein synthesis inhibition in which we can slow the growth rate. We hope to find a condition in which *E. coli* will survive LPS loss as a foothold that we can use to evolve a strain better equipped to live without LPS.

3.12 Materials and methods

3.12.1 Bacterial strains, growth conditions and reagents

All strains and plasmids used in this chapter are described in Tables 3.5 and 3.6. The growth media used were LB Miller (BD) and M9 formulated for *Acinetobacter* (6.78 g/L Na_2HPO_4, 3 g/L KH_2PO_4, 0.5 g/L NaCl, 1 g/L NH_4Cl, 0.4% sodium succinate, 2 mM $MgSO_4$, 0.1 mM $CaCl_2$). M9+ was a formulation of M9 with 2.5% LB added. When preparing cells from glycerol stocks, all LPS deficient strains were streaked on LB plates containing 1.2% agarose instead of agar to compensate for a plating defect. All other strains were streaked on LB agar (1.2%) and all plates were incubated at 37°C. When appropriate, media was supplemented with antibiotics at the following concentrations: kanamycin (40 μg/mL), apramycin (150 μg/mL), carbenicillin (100 μg/mL).

Ambion PureLink™ RNA Mini, DNA-*free*™ DNA Removal and PureLink™ *Pro* 96 Genomic DNA kits were purchased from Thermo Fisher. QuantiTect Reverse Transcription, QIAprep Spin Miniprep and QIAquick PCR purification kits were purchased from Qiagen. Kapa SYBR® Fast qPCR

kit was purchased directly from Kapa. Nextera DNA Sample Preparation and Nextera Index kits were purchased from Illumina. BacTiter-Glo™ Microbial Cell Viability Assay was purchased from Promega. All oligonucleotides were purchased from IDT. Palmitic acid and oleic acid were purchased from Sigma Aldrich.

3.12.2 Growth curves

3.12.2.1 Manual OD_{600} Measurements

To increase consistency, all strains were freshly streaked from glycerol stocks the day before starting the growth curves and were never refrigerated. Also, it was noticed that good aeration was essential for the growth of the LPS deficient mutants. Starter cultures (2 mL) of LB were inoculated from the plates and grown O/N (<16hrs.) to saturation at 37°C. Cells were then diluted 1:10 into fresh media (2 mL), LB or M9+ depending on the experiment, and grown for 90 minutes at 37°C. These cultures were diluted again into 20 mL of the appropriate media in 125 mL flasks, normalizing to OD_{600} 0.01 (LB) or 0.03 (M9+). The cultures were grown at the indicated temperature with vigorous shaking (220 rpm) and OD_{600} measurements were taken every 30 minutes to 1 hour. Each experiment was repeated at least 3 times and a representative curve is shown. All growth curves were generated using GraphPad Prism.

3.12.2.2 Growth in a plate reader

Due to the number of replicates, growth was monitored during the passaging experiment using a plate reader. Briefly, 150 µL of each of the newly passaged replicates (1:100 dilution of O/N culture) was transferred to a 96-well plate. The plate was transferred to a Tecan Sunrise plate reader and incubated with shaking at 25°C or 30°C, depending on the replicate set. OD_{600} measurements were taken every 10 minutes for 24 hours. We believe the exacerbated growth defect observed for the mutants is a result of the poor aeration in the plate. Data from the plate

reader was processed using Microsoft Excel and all growth curves were generated using GraphPad Prism.

3.12.2.3 Growth using total ATP levels

The same cultures that were used to measure OD_{600} over a period of time were also tested for total ATP levels using the BacTiter-Glo™ Microbial Cell Viability Assay. At each time period, 100 µL of cell culture was added, in duplicate, to a 96-well plate. Reagents were added according to the manufacturer instructions. Samples were incubated together for 5 minutes and luminescence was measured.

3.12.3 Microscopy

All images were of overnight cultures grown to saturation in the indicated medium at either 37°C or 25°C. The cells were immobilized on 2% agarose pads made with phosphate-buffered saline. Cells were imaged using an Olympus BX-61 upright microscopy with either a 100 x objective. Images using a 60 x objective were obtained on a Nikon Eclipse *Ti* inverted microscope. Image*s* were processed using Fiji and all compared image sets were adjusted identically.

3.12.4 Suppressor screen

We started with 16 replicates of each of two strains, *ΔlpxC* and *ΔmlaA ΔlpxC*, half of which were grown at 25°C and half at 30°C. To initiate the experiment, each strain was streaked onto LB agarose plates and grown at 37°C. Single colonies (16 each) were inoculated into 2mL of LB and were grown O/N at 37°C. Glycerol stocks of these starting populations were saved and sequenced as Day 0. The set up for the two temperatures differed slightly, but the 16 replicates at each temperature originated from the same 16 starting populations. For the 25°C populations, 5mL cultures of LB were inoculated with 50 µL of the O/N started cultures and allowed to grow in a roller drum at 25°C. For the 30°C populations, 150 µL of the starter cultures was added to

15 mL LB in 50 mL Falcon tubes and grown at 30°C (220 rpm). The populations were then passaged into fresh LB (1:100 dilution) every 24 hours. Initially some of the 25°C replicates were clear after 24 hours and were not passaged until there was visible growth (in 24 hours increments). Growth was monitored via a plate reader at days 3 and 7 and glycerol stocks were saved at the same time. After 7 days, all replicates were showing growth profiles that matched wild type and thus the passaging was ended so as not to accumulate additional mutations. The protocol for the *ΔlpxD* strains was nearly identical. 9 replicates were started in 2 mL LB and diluted (1:100) every 24 hours into 15 mL of fresh LB. Cultures were grown at 25°C (220 rpm).

3.12.5 Next generation sequencing

DNA was isolated from single colonies of each replicate using the PureLink™ *Pro* 96 Genomic DNA kit according to the manufacturer instructions. Samples were barcoded and prepped for sequencing using a Nextera DNA Sample Preparation kit following Illumina's protocols. Sequencing was done at the Bauer Core using an Illumina HiSeq 2500 instrument. Reads were aligned and mapped to the *A. baumannii* ATCC19606 published genome using Breseq software in consensus mode.[28] Variants were also identified using Breseq and aligned reads were visualized using the Integrated Genomics Viewed (Broad Institute).[29]

Table 3.4 List of mutations found in suppressor screen for *ΔlpxC.* The first set of replicates were *ΔlpxC* at the start of the screen and the second set listed below were *ΔmlaA ΔlpxC.* Only assigned mutations are listed, with a few exceptions. The references for the genes listed are as follows: *pldA* (DJ41_RS17655), *mlaA* (DJ41_RS06905), *mlaD* (DJ41RS_11945), *mlaF* (DJ41_RS11935), *adeJ* (DJ41_RS13520), *adeR* (DJ41_RS18535).

Replicate	Gene/Reference	Mutation	Position	Result
1	*pldA*	Insertion with target site duplication (5bp)	1091	Disruption
	mlaA	Deletion (Δ708bp)	*	Disruption
2	*pldA*	$(A)_{7\rightarrow 6}$	238	Truncation
	mlaA	Deletion (Δ693bp)	*	Disruption
3	DJ41_RS17650	Insertion with target site duplication (4bp)	2937	Disruption
	DJ41_RS10490	Insertion with target site duplication (5bp)	453	Disruption
4	DJ41_RS17650	Insertion with target site duplication (5bp)	386	Disruption
	mlaA	Insertion with target site duplication (4bp)	448	Disruption
5	*pldA*	G→A	1022	W341*
	mlaA	Deletion (Δ709bp)	*	Disruption
6	DJ41_RS17650	Insertion with target site duplication (4bp)	278	Disruption
	mlaA	T→G	457	N152K
7	*pldA*	Deletion (Δ3bp)	1023	ΔW341 A342C
	mlaA	Deletion (Δ730bp)	*	Disruption
8	DJ41_RS17650	Deletion (Δ92bp)	5	Disruption
	mlaD	Insertion with target site duplication (5bp)	296	Disruption
9	DJ41_RS17650	Insertion with target site duplication (5bp)	1757	Disruption
	mlaA	Deletion (Δ1770bp)	*	Disruption
10	DJ41_RS17650	Insertion with target site duplication (4bp)	2932	Disruption
	mlaA	Insertion with target site duplication (4bp)	451	Disruption

Table 3.4 (Continued)

11	DJ41_RS17650	Deletion (Δ2193bp)	548	Disruption
	mlaA	Deletion (Δ2820)	*	Disruption
12	DJ41_RS17650	Insertion with target site duplication (5bp)	1730	Disruption
	mlaA	Insertion with target site duplication (5bp)	454	Disruption
13	*pldA*	$(A)_{7\rightarrow 6}$	238	Truncation
	DJ41_RS10490	Insertion with target site duplication (4bp)	452	Disruption
14	DJ41_RS17650	Insertion with target site duplication (4bp) (Unassigned)	2937	Disruption
	mlaF	New junction with repeat region (Unassigned)	87	Disruption
15	*pldA*	Deletion (Δ19bp)	1078	Truncation
	mlaA	Deletion (Δ1529bp)	*	Disruption

Replicate	**Gene/Reference**	**Mutation**	**Position**	**Result**
1	*pldA*	Deletion (Δ1bp)	895	Truncation
2	*pldA*	Insertion with target site duplication (4bp)	340	Disruption
3	DJ41_RS17650	T→A	140	L47*
4	*pldA*	$(A)_{7\rightarrow 6}$	238	Truncation
5	*pldA*	Deletion (Δ3bp)	1023	ΔW341 A342C
6	*pldA*	Insertion with target site duplication (5bp)	536	Disruption
7	DJ41_RS17650	Insertion with target site duplication (4bp)	2815	DJ41_RS17650
	adeJ	Insertion with target site duplication (4bp)	2385	Disruption
8	DJ41_RS17650	Insertion with target site duplication (4bp)	294	Disruption
	DJ41_RS13530	Insertion with target site duplication (5bp)	600	Disruption
9	DJ41_RS17650	Insertion with target site duplication (4bp)	2926	Disruption

Table 3.4 (Continued)

10	*pldA*	New junction with repeat region (Unassigned)	400/887	Disruption
	adeR	Insertion with target site duplication (5bp) (Unassigned)	423	Disruption
11	*pldA*	Insertion with target site duplication (5bp)	524	Disruption
	adeR	Insertion with target site duplication (4bp) (Unassigned)	186	Disruption
12	DJ41_RS17650	Insertion with target site duplication (4bp)	646	Disruption
	adeJ	Deletion (Δ13bp)	1961	Truncation

3.12.6 Strain construction

All oligonucleotide primer sequences are given in Table 3.7

3.12.6.1 Marked Deletions

Mutants were constructed by allelic exchange through double crossover homologous recombination as reported previously with some minor changes.[30] Briefly, the linear constructs containing either a KanR (amplified from pIM1440) or AprR (amplified from pSET152) resistance marker were constructed as follows. Upstream and downstream regions (~500 bp) of the target gene were amplified with primers designed to create overlap with the resistance marker on the 3' end of the upstream region and 5' end of the downstream region. The flanking regions and resistance cassette were subsequently assembled into a linear cassette using Gibson Assembly master mix (NEB). The linear cassette was then amplified by PCR to obtain sufficient quantities for transformation. To construct the deletion strains, 20 mL of the recipient strain was grown in LB at 37°C to an OD_{600} of approximately 0.8. The cells were pelleted and washed 2x with 2mL chilled water. A final wash with chilled 10% (v/v) glycerol was performed and the cells were

resuspended in 150 µL 10% glycerol. The cell suspension was mixed with ~8 µg of the linear DNA cassette and transferred to a chilled electroporation cuvette (2 mm gap). It was then pulsed with an Eppendorf Eporator (2.5 kV). 1 mL of LB was quickly added and the cells were transferred to a culture tube and incubated at 37°C (220 rpm) for 90 minutes. The entire transformation was plated on LB plates with kanamycin or apramycin and incubated at 37°C for 24 hours. All isolated colonies were tested by colony PCR for insertion of the resistance cassette. In cases of strains with multiple mutations, the removal of LPS (*lpxA, lpxC*, or *lpxD*) was always done last. In the case of the *ΔlpxC ΔlpxD* strain, the *ΔlpxD* deletion was constructed first and *lpxC* was removed in that background since we predicted that mutation should make the strain more fit.

3.12.6.2 Markerless Deletions

The *pldA* markerless deletion was introduced by biparental conjugation following a known protocol (3) with modifications. Briefly, the upstream and downstream regions of *pldA* (~1 kb) were amplified with overlap to the pEX18ApGW plasmid as well as overlap to one another. The plasmid was also amplified by PCR with primers originating at the HindIII and KpnI restriction sites. The final plasmid (pEX18ApGW-*pldA*) was constructed by assembling the three fragments using Gibson Assembly and then transformed into *E. coli* strain pRK2013 via electroporation. The transformants were plated on LB agar with kanamycin and carbenicillin (50 µg/mL) and grown at 30°C for 24 hours. The recipient *Acinetobacter baumanni mlaA*::kanR strain was streaked at the same time. The two plates were gently scraped and cells were resuspended in LB to an OD_{600} of ~1.0. Equal amounts (100 µL) of the two suspensions were added to 600µL LB and subsequently collected by centrifugation (7000g, 2 min). Cells were washed 2x by resuspending gently in 600µL LB. After the final spin, the pellet was resuspended in 50 µL LB, spotted in the center of a dried

LB plate and incubated O/N at 30°C. To select against *E. coli*, the entire spot was resuspended in 1mL LB and then 100 µL was plated on a large plate with Simmons citrate agar (BD) containing carbenicillin. After two days of incubation at 37°C, the plate contained *Acinetobacter* colonies that had integrated the plasmid which could be confirmed by colony PCR. Several colonies were inoculated into LB and grown O/N at 37°C to cure the plasmid. 10-fold dilutions of the cultures were then plated on LB plates with 10% (v/v) sucrose. Surviving colonies were expected to have flipped out the plasmid. Several colonies were checked by PCR to distinguish the mutants from those that had resolved to wild type.

3.12.7 CFU plating

All colony counts were obtained from saturated cultures grown overnight. Cultures were serially diluted in LB and then 5uL of each dilution was plated on an LB agarose plate in duplicate. Plates were incubated at 37C for 24 hours and then the colonies in each were counted. The number of colony forming units (CFU)/mL was calculated based on the average number of colonies per dilution. All experiments were performed in biological triplicate and graphs were generated using GraphPad Prism.

3.12.8 Growth constants

To calculate growth constants, the growth curve data from the OD_{600} range ~0.15-0.5 was linearized on a semi-log plot. The range varied slightly from sample to sample depending on the OD_{600} at the time tested and the quality of the linear regression. Only data with $R^2 > 0.99$ were used. The slope of the linear regression line was calculated which determined the growth constant. Doubling times can be obtained from the growth constant by calculating ln (2) divided

by the growth constant. All shown growth constants are the average of at least 3 separate experiments.

3.12.9 RT-qPCR

Stationary phase cultures were diluted into 2 mL LB and grown to OD_{600} 0.6. Cells were harvested and normalized to the equivalent of collecting 1 mL of cells at OD_{600} 0.6. RNA was isolated from cell pellets using an Ambion PureLink™ RNA Mini kit according to manufacturer instructions. gDNA contamination was removed by using the DNA-*free*™ DNA removal kit. RNA concentration was determined using a NanoDrop and samples were normalized for conversion to cDNA using the QuantiTect Reverse Transcription kit. RT-qPCR analysis was performed using the Kapa SYBR Fast kit and 25 µL reaction volume for each sample. Each primer pair was tested on 3 reference genes: 16S, *secA* and *rpoB* since quality reference genes aren't well defined in *A. baumannii*.[31] Control reactions without reverse transcription or without template were also run for each primer pair. RT-qPCR methods were set up following the instructions in the Kapa kit on a BioRad CFX-96-Real-Time PCR Detection System. Each sample was tested with a minimum of 3 biological replicates, each in technical triplicate. Results were analyzed by normalizing C_T values to the reference genes C_T values (ΔC_T). Differential expression was calculated using the $\Delta\Delta C_T$ method.

3.12.10 Fatty acid supplementation

Fatty acid stocks were made in 80% ethanol. A 96-well plate was set up with 100-fold dilutions of saturated cultures in 150 µL LB. 1.5 µL of a 100x stock of the appropriate fatty acid was added to each well. All strains were also tested with 1.5 µL of 80% ethanol as a control. The plate was analyzed in a Tecan Sunrise plate reader following the protocol described above.

3.12.11 GC-FAME analysis

Strains were grown overnight to saturation at 37°C in LB. Cultures were diluted 100-fold into 3 mL of fresh LB and grown at either 37°C or 25°C to OD_{600} ~ 1.0. Cells were harvested by centrifugation and washed 2x with 1 mL phosphate buffered saline (PBS). Pellets were resuspended in 250 µL PBS, flash frozen and lyophilized overnight. Pellets were sent to Microbial ID for analysis.

Table 3.5 Strains used in this chapter

Strain or Plasmid	Genotype	Source
A. baumannii ATCC 19606	Wild type	ATCC
A. baumannii ATCC 17978	Wild type	ATCC
A. baumannii lpxC mutant	*ΔlpxC*::kan	Moison et al., 2016
A. baumannii mlaA lpxC mutant	*ΔlpxC::*apr *ΔmlaA::*kan	This work
A. baumannii pldA lpxC mutant	*ΔlpxC::*apr *ΔpldA::*kan	This work
A. baumannii mlaA pldA lpxC mutant	*ΔpldA ΔlpxC::*apr *ΔmlaA::*kan	This work
A. baumannii lpxD mutant	*ΔlpxD*::apr	This work
A. baumannii lpxA mutant	*ΔlpxA*::apr	This work
A. baumannii mlaA pldA lpxD mutant	*ΔpldA ΔlpxD::*apr *ΔmlaA::*kan	This work
A. baumannii mlaA pldA lpxD mutant	*ΔpldA ΔlpxA::*apr *ΔmlaA::*kan	This work
A. baumannii lpxC lpxD mutant	*ΔlpxD::*apr *ΔlpxC::*kan	This work
A. baumannii lpxA lpxD mutant	*ΔlpxD::*apr *ΔlpxA::*kan	This work
A. baumannii mlaA pldA mutant	*ΔpldA ΔmlaA::*kan	This work

Table 3.6 Plasmids used in this chapter

Plasmid	Source
pEX18ApGW	Hoang *et al*. 1998[32]
pEX18ApGW-*pldA*	This work

Table 3.7 Primers used in this chapter

Primer	Sequence (5' - 3')	Application
Strain Construction		
*mlaA*_up_F	GGTGCCAATTCTGGCTCATCAATTAC	Amplification of upstream and downstream regions of *mlaA* for *mlaA*-kanR linear construct
*mlaA*_up_R	CGAATTCGCGGCCGCTTCTA TCCGAACTAGCGGCAGATTCTT	
*mlaA*_down_F	GAGCTCGCTTGGACTCCTGT GCGTTCCAGATTGCCGAGAA	
*mlaA*_down_R	GTACCAGTCGCCTGATAAATAGGCA	
*mlaA*_seq_F	GTAGGTCTTTACACCTCAGCCC	Verification of *mlaA* gene knock out
*mlaA*_seq_R	CTTCTGGTACATCTTCAGATTCGTCATC	
*lpxC*_up_F	CATTACTGGTGGCGATGACATCAC	Amplification of upstream and downstream regions of *lpxC* for *lpxC*-aprR linear construct
*lpxC*_up_R	GCGTAATCTGCTGCTTGCAA CTCCATCCACGGTATGTGGAATG	
*lpxC*_down_F	GCGGAGAACGAGATGACGTT CAGCTATTACGCAATGTTCAAAGCGA	
*lpxC*_down_R	AGGAAACCTTACGTTTCTAACAACGC	
*lpxC*_seq_F	CACACTCACGTATGGAATTGGACAG	Verification of *lpxC* gene knock out
*lpxC*_seq_R	AGCGAGTGGAATAGGTCTTCATAGC	
*pldA*_up_F	GGTATTGGCAGCTTACTTGCGTAATG	Amplification of upstream and downstream regions of *pldA* for *pldA*-kanR linear construct
*pldA*_up_R	CGAATTCGCGGCCGCTTCTA GGCTAAGGTGTCGGCATATGC	

Table 3.7 (Continued)

*pldA*_down_F	GAGCTCGCTTGGACTCCTGT CTGCGCGGACACTTCCAATTAT	
*pldA*_down_R	GATGCTACTCATGTTCATCGGTGG	
*pldA*_seq_F	TTTACAGCTAAGTATGGGAACCCTG	Verification of *pldA* gene knock out
*pldA*_seq_R	CCGGCATAAGTTGCACGATG	
*lpxD*_up_F	TGTTAGGGTTAGGCCTGACAGTAG	
*lpxD*_up_R	GCGTAATCTGCTGCTTGCAA ACCTCTGCATTTTCCAAACTCGC	Amplification of upstream and downstream regions of *lpxD* for *lpxD*-aprR linear construct
*lpxD*_down_F	GCGGAGAACGAGATGACG GCGACAATTAGCAGATGTGCCA	
*lpxD*_down_R	AGATGGATCAATAATGGCGGTAGAATGG	
*lpxD*_seq_F	GGTGAGCTAATTGGTGAAGGTAGTCTTC	Verification of *lpxD* gene knock out
*lpxD*_seq_R	GTATATGATCAAGTCGTTTAGTGATTTGGGTC	
*lpxA*_up_F	CCGAGTCTACTACACCTAAATTTGCCA	
*lpxA*_up_R	GAGATCCTTTTTTTCTGCGCGTAATCTGCTGCTTGCAA CAGCACCAATAGTCACTTGGGG	Amplification of upstream and downstream regions of *lpxA* for *lpxA*-aprR linear construct
*lpxA*_down_F	GAGCTCATGAGCGGAGAACGAGATGACGTT CTGGATTAACTTCTGTTCAAGCTATTGACC	
*lpxA*_down_R	AGCAGCCTAGCGCACTAACA	
*lpxA*_seq_F	CCGCCATTATTGATCCATCTGCAG	Verification of *lpxA* gene knock out
*lpxA*_seq_R	CAATCAAGAGTTGAGCTTCTGGAACTG	
*lpxC*_up_kan_R	GACGTCGAATTCGCGGCCGCTTCTA CTCCATCCACGGTATGTGGAATG	Amplification of upstream and downstream regions of *lpxC* for *lpxC*-kanR linear construct
*lpxC*_down_kan_F	AGTACCGAGCTCGCTTGGACTCCTGTC AGCTATTACGCAATGTTCAAAGCGA	
*lpxA*_up_kan_R	TATGATAGAATTTGACGTCGAATTCGCGGCCGCTTCTA CAGCACCAATAGTCACTTGGGG	Amplification of upstream and downstream regions of *lpxA* for *lpxC*-kanR linear construct
*lpxA*_down_kan_F	TTTTAGTACCGAGCTCGCTTGGACTCCTGT CTGGATTAACTTCTGTTCAAGCTATTGACC	

Table 3.7 (Continued)

Kan_F	TAGAAGCGGCCGCGAATTCG	Amplification of KanR cassette
Kan_R	ACAGGAGTCCAAGCGAGCTC	
Apr_F	TTGCAAGCAGCAGATTACGC	Amplification of AprR cassette
Apr_R	AACGTCATCTCGTTCTCCGC	
*pldA*_up_pEX_F	TTCCCAGTCACGACGTTGTAAAACGACGGCCAGTGCCA GCAGCAACGTAAGACACGCT	Amplification of upstream region of *pldA* with 5' overlap to pEX18ApGW and 3' overlap to the downstream region of *pldA*
*pldA*_up_pEX_R	CATAACCATTAAATAATTGGAAGTGTCCGCGCAG GGCTAAGGTGTCGGCATATGC	
*pldA*_down_pEX_F	ATGTGCGTCGGTGGCATATGCCGACACCTTAGCC CTGCGCGGACACTTCCAATTAT	Amplification of downstream region of *pldA* with 5' overlap to the upstream region of *pldA* and 3' overlap to pEX18ApGW
*pldA*_down_pEX_R	AGGAAACAGCTATGACCATGATTACGAATTCGAGCTCG TATGGCTTTGCTCGGGGACT	
pEX_*pldA*_F	CGAGCTCGAATTCGTAATCATGGTCA	Amplification of pEX18ApGW
pEX_*pldA*_R	TGGCACTGGCCGTCGTTTTA	
*pldA*_pEX_seq_F	GGGTGCTTCGTTACGCAGTAAG	To verify pEX18ApGW integration at *pldA* site
*pldA*_pEX_seq_R	GGCCTTAAACAGCAAATGATGGCT	
RT-qPCR		
16S_F	CTTTAGCTCGCTTGGTTGCC	Forward and reverse primers for 16S transcript amplification
16S_R	TTGGGTCGACTCCTGCTTTC	
rpoB_F	AATTCGTACGTATGCCGCCT	Forward and reverse primers for *rpoB* transcript amplification
rpoB_R	TGCCTGACGTTGCATGTTTG	
secA_F	GGCAACGATTGAAGCCAGTG	Forward and reverse primers for *secA* transcript amplification
secA_R	TGTCTGCTTCACGCTCATGT	
PT_F/PE_F	ACCGCTTTTAAAACCATTGC	Published forward and reverse primers for *ponA* transcript amplification (matches 17978)
PT_R	TGCCAGGAATGCATGAATAA	

Table 3.7 (Continued)

PE_R	TGCTAGGAATGCATGAATAA	Reverse for published *ponA* (matches 19606)
P2_F	GAAAAAGCTGTGCAGGACGG	Forward and reverse primers for *ponA* transcript amplification
P2_R	CTTGCGCCGGATAAGTGTTG	

3.13 References

1 Peng, D., Hong, W., Choudhury, B. P., Carlson, R. W. & Gu, X. X. Moraxella catarrhalis bacterium without endotoxin, a potential vaccine candidate. *Infect Immun* **73**, 7569-7577, doi:10.1128/IAI.73.11.7569-7577.2005 (2005).

2 Steeghs, L. *et al.* Meningitis bacterium is viable without endotoxin. *Nature* **392**, 449-450, doi:10.1038/33046 (1998).

3 Moffatt, J. H. *et al.* Colistin resistance in Acinetobacter baumannii is mediated by complete loss of lipopolysaccharide production. *Antimicrob Agents Chemother* **54**, 4971-4977, doi:10.1128/AAC.00834-10 (2010).

4 Steeghs, L. *et al.* Outer membrane composition of a lipopolysaccharide-deficient Neisseria meningitidis mutant. *EMBO J* **20**, 6937-6945, doi:10.1093/emboj/20.24.6937 (2001).

5 Mu, X. *et al.* The Effect of Colistin Resistance-Associated Mutations on the Fitness of Acinetobacter baumannii. *Front Microbiol* **7**, 1715, doi:10.3389/fmicb.2016.01715 (2016).

6 Bojkovic, J. *et al.* Characterization of an Acinetobacter baumannii lptD Deletion Strain: Permeability Defects and Response to Inhibition of Lipopolysaccharide and Fatty Acid Biosynthesis. *J Bacteriol* **198**, 731-741, doi:10.1128/JB.00639-15 (2015).

7 Moffatt, J. H. *et al.* Lipopolysaccharide-deficient Acinetobacter baumannii shows altered signaling through host Toll-like receptors and increased susceptibility to the host antimicrobial peptide LL-37. *Infect Immun* **81**, 684-689, doi:10.1128/IAI.01362-12 (2013).

8 Henry, R. *et al.* Colistin-resistant, lipopolysaccharide-deficient Acinetobacter baumannii responds to lipopolysaccharide loss through increased expression of genes involved in the synthesis and transport of lipoproteins, phospholipids, and poly-beta-1,6-N-acetylglucosamine. *Antimicrob Agents Chemother* **56**, 59-69, doi:10.1128/AAC.05191-11 (2012).

9 Marr, A. G. & Ingraham, J. L. Effect of Temperature on the Composition of Fatty Acids in Escherichia Coli. *J Bacteriol* **84**, 1260-1267 (1962).

10 Boll, J. M. *et al.* A penicillin-binding protein inhibits selection of colistin-resistant, lipooligosaccharide-deficient Acinetobacter baumannii. *Proc Natl Acad Sci U S A* **113**, E6228-E6237, doi:10.1073/pnas.1611594113 (2016).

11 Dekker, N. Outer-membrane phospholipase A: known structure, unknown biological function. *Mol Microbiol* **35**, 711-717 (2000).

12 Malinverni, J. C. & Silhavy, T. J. An ABC transport system that maintains lipid asymmetry in the gram-negative outer membrane. *Proc Natl Acad Sci U S A* **106**, 8009-8014, doi:10.1073/pnas.0903229106 (2009).

13 Powers, M. J. & Trent, M. S. Phospholipid retention in the absence of asymmetry strengthens the outer membrane permeability barrier to last-resort antibiotics. *Proc Natl Acad Sci U S A* **115**, E8518-E8527, doi:10.1073/pnas.1806714115 (2018).

14 van den Berg, B., Bhamidimarri, S. P. & Winterhalter, M. Crystal structure of a COG4313 outer membrane channel. *Sci Rep* **5**, 11927, doi:10.1038/srep11927 (2015).

15 Kelley, L. A., Mezulis, S., Yates, C. M., Wass, M. N. & Sternberg, M. J. The Phyre2 web portal for protein modeling, prediction and analysis. *Nat Protoc* **10**, 845-858, doi:10.1038/nprot.2015.053 (2015).

16 Monod, J. THE GROWTH OF BACTERIAL CULTURES. *Annual Review of Microbiology* **3**, 371-394, doi:10.1146/annurev.mi.03.100149.002103 (1949).

17 Yao, Z., Davis, R. M., Kishony, R., Kahne, D. & Ruiz, N. Regulation of cell size in response to nutrient availability by fatty acid biosynthesis in Escherichia coli. *Proc Natl Acad Sci U S A* **109**, E2561-2568, doi:10.1073/pnas.1209742109 (2012).

18 Schaechter, M., Maaloe, O. & Kjeldgaard, N. O. Dependency on medium and temperature of cell size and chemical composition during balanced grown of Salmonella typhimurium. *J Gen Microbiol* **19**, 592-606, doi:10.1099/00221287-19-3-592 (1958).

19 Vadia, S. *et al.* Fatty Acid Availability Sets Cell Envelope Capacity and Dictates Microbial Cell Size. *Curr Biol* **27**, 1757-1767 e1755, doi:10.1016/j.cub.2017.05.076 (2017).

20 Richie, D. L. *et al.* Toxic Accumulation of LPS Pathway Intermediates Underlies the Requirement of LpxH for Growth of Acinetobacter baumannii ATCC 19606. *PLoS One* **11**, e0160918, doi:10.1371/journal.pone.0160918 (2016).

21 Wei, J. R. *et al.* LpxK Is Essential for Growth of Acinetobacter baumannii ATCC 19606: Relationship to Toxic Accumulation of Lipid A Pathway Intermediates. *mSphere* **2**, doi:10.1128/mSphere.00199-17 (2017).

22 Ogura, T. *et al.* Balanced biosynthesis of major membrane components through regulated degradation of the committed enzyme of lipid A biosynthesis by the AAA protease FtsH (HflB) in Escherichia coli. *Mol Microbiol* **31**, 833-844 (1999).

23 Sutterlin, H. A. *et al.* Disruption of lipid homeostasis in the Gram-negative cell envelope activates a novel cell death pathway. *Proc Natl Acad Sci U S A* **113**, E1565-1574, doi:10.1073/pnas.1601375113 (2016).

24 Zhang, Y. M. & Rock, C. O. Membrane lipid homeostasis in bacteria. *Nat Rev Microbiol* **6**, 222-233, doi:10.1038/nrmicro1839 (2008).

25 Gill, C. O. & Suisted, J. R. The effects of temperature and growth rate on the proportion of unsaturated fatty acids in bacterial lipids. *J Gen Microbiol* **104**, 31-36, doi:10.1099/00221287-104-1-31 (1978).

26 Kropinski, A. M., Lewis, V. & Berry, D. Effect of growth temperature on the lipids, outer membrane proteins, and lipopolysaccharides of Pseudomonas aeruginosa PAO. *J Bacteriol* **169**, 1960-1966 (1987).

27 Heath, R. J. *et al.* Mechanism of triclosan inhibition of bacterial fatty acid synthesis. *J Biol Chem* **274**, 11110-11114 (1999).

28 Deatherage, D. E. & Barrick, J. E. Identification of mutations in laboratory-evolved microbes from next-generation sequencing data using breseq. *Methods in molecular biology (Clifton, N.J.)* **1151**, 165-188, doi:10.1007/978-1-4939-0554-6_12 (2014).

29 Robinson, J. T. *et al.* Integrative genomics viewer. *Nature biotechnology* **29**, 24-26, doi:10.1038/nbt.1754 (2011).

30 Aranda, J. *et al.* A rapid and simple method for constructing stable mutants of Acinetobacter baumannii. *BMC Microbiol* **10**, 279, doi:10.1186/1471-2180-10-279 (2010).

31 Rocha, D. J., Santos, C. S. & Pacheco, L. G. Bacterial reference genes for gene expression studies by RT-qPCR: survey and analysis. *Antonie Van Leeuwenhoek* **108**, 685-693, doi:10.1007/s10482-015-0524-1 (2015).

32 Hoang, T. T., Karkhoff-Schweizer, R. R., Kutchma, A. J. & Schweizer, H. P. A broad-host-range Flp-FRT recombination system for site-specific excision of chromosomally-located DNA sequences: application for isolation of unmarked Pseudomonas aeruginosa mutants. *Gene* **212**, 77-86 (1998).